NATIONAL COOPERATIVE HIGHWAY RESEARCH PROGRAM
REPORT 101

EFFECT OF STRESS ON FREEZE-THAW DURABILITY OF CONCRETE BRIDGE DECKS

HIGHWAY RESEARCH BOARD
NATIONAL RESEARCH COUNCIL
NATIONAL ACADEMY OF SCIENCES—NATIONAL ACADEMY OF ENGINEERING

NATIONAL COOPERATIVE HIGHWAY RESEARCH PROGRAM
REPORT 101

EFFECT OF STRESS ON FREEZE-THAW DURABILITY OF CONCRETE BRIDGE DECKS

JOSEPH P. CALLAHAN, CHESTER P. SIESS,
CLYDE E. KESLER
UNIVERSITY OF ILLINOIS
URBANA, ILLINOIS

RESEARCH SPONSORED BY THE AMERICAN ASSOCIATION
OF STATE HIGHWAY OFFICIALS IN COOPERATION
WITH THE BUREAU OF PUBLIC ROADS

SUBJECT CLASSIFICATIONS
BRIDGE DESIGN
CEMENT AND CONCRETE
CONSTRUCTION

HIGHWAY RESEARCH BOARD
DIVISION OF ENGINEERING NATIONAL RESEARCH COUNCIL
NATIONAL ACADEMY OF SCIENCES—NATIONAL ACADEMY OF ENGINEERING 1970

NATIONAL COOPERATIVE HIGHWAY RESEARCH PROGRAM

Systematic, well-designed research provides the most effective approach to the solution of many problems facing highway administrators and engineers. Often, highway problems are of local interest and can best be studied by highway departments individually or in cooperation with their state universities and others. However, the accelerating growth of highway transportation develops increasingly complex problems of wide interest to highway authorities. These problems are best studied through a coordinated program of cooperative research.

In recognition of these needs, the highway administrators of the American Association of State Highway Officials initiated in 1962 an objective national highway research program employing modern scientific techniques. This program is supported on a continuing basis by funds from participating member states of the Association and it receives the full cooperation and support of the Bureau of Public Roads, United States Department of Transportation.

The Highway Research Board of the National Academy of Sciences-National Research Council was requested by the Association to administer the research program because of the Board's recognized objectivity and understanding of modern research practices. The Board is uniquely suited for this purpose as: it maintains an extensive committee structure from which authorities on any highway transportation subject may be drawn; it possesses avenues of communications and cooperation with federal, state, and local governmental agencies, universities, and industry; its relationship to its parent organization, the National Academy of Sciences, a private, nonprofit institution, is an insurance of objectivity, it maintains a full-time research correlation staff of specialists in highway transportation matters to bring the findings of research directly to those who are in a position to use them.

The program is developed on the basis of research needs identified by chief administrators of the highway departments and by committees of AASHO. Each year, specific areas of research needs to be included in the program are proposed to the Academy and the Board by the American Association of State Highway Officials. Research projects to fulfill these needs are defined by the Board, and qualified research agencies are selected from those that have submitted proposals. Administration and surveillance of research contracts are responsibilities of the Academy and its Highway Research Board.

The needs for highway research are many, and the National Cooperative Highway Research Program can make significant contributions to the solution of highway transportation problems of mutual concern to many responsible groups. The program, however, is intended to complement rather than to substitute for or duplicate other highway research programs.

NCHRP Report 101

Project 6-9 FY '64
ISBN 0-309-01889-7
L. C. Card No 78-607598

Price: $3.60

Published reports of the

NATIONAL COOPERATIVE HIGHWAY RESEARCH PROGRAM

are available from:

Highway Research Board
National Academy of Sciences
2101 Constitution Avenue
Washington, D.C. 20418

(See last pages for list of published titles and prices)

FOREWORD

By Staff

Highway Research Board

This report is recommended to bridge design engineers, construction engineers, concrete researchers, and others concerned with concrete bridge deck deterioration. It reports the results of investigations primarily concerned with answering the question—what are the effects of stress on concrete durability? The question is not answered conclusively, but certain findings should be valuable to designers and construction engineers interested in trying new approaches. Other findings, including two theories of mechanisms causing deterioration, will interest concrete researchers.

During the period from 1920 to 1950, total road and street mileage in the United States remained relatively constant at about 3.3 million miles. Construction during this period was primarily for the purpose of upgrading existing roads. About 1950, the construction of new roads in the United States began an upturn. The construction of the National System of Interstate and Defense Highways, following the Federal funding authorization of 1956, has contributed to the steadily increasing highway mileage growth through the 1960's. New mileage, recently constructed, has been designed to high standards of performance necessitating more bridges and structures per mile of road than ever before. At this time, with about 64 percent of the planned Interstate System completed, it has become obvious that maintenance crews and funds are feeling the consequences of design and construction decisions made a few years ago. Far more maintenance effort has been required on relatively new highways than anyone predicted, and forecasts for the future are indeed dismal. Researchers have been attempting to find ways of alleviating the built-in maintenance problems that will require extensive corrective action over long design lives.

Not the least of the built-in maintenance problems is the deterioration of concrete bridge decks, often within a few years after placing the bridges in service. In certain sections of the country this mode of failure has become excessively prevalent. The cost of correcting deficiencies, when they have been cast in concrete and steel, is usually far greater than the initial construction cost. The potential savings in alleviating the problem of bridge deck deterioration alone is astronomical.

The University of Illinois has attacked this complex and serious problem, first in NCHRP Project 6-5 (findings published as *NCHRP Report 27,* "Physical Factors Influencing Resistance of Concrete to Deicing Agents," 1966) and now in Project 6-9 (findings reported herein). An indication of the complexity of the problem of concrete bridge deck deterioration is realized by considering some of the variables—material properties, additives, air-entrainment, handling, finishing, curing, stress, environment, etc. Field investigations also help to confuse the issue when one discovers that of two concrete bridge decks, apparently constructed as alike as humanly possible, one deteriorates rapidly and the other remains sound.

The University of Illinois research reported in this document does not con-

clusively solve the problem of concrete bridge deck scaling and spalling. It does, however, shed light on the effects of stress in accelerating distress. It offers to the discerning reader additional evidence concerning air entrainment, thermal characteristics, and the failure mode of corroded reinforcing steel, as well as clues as to what might be tried in design and construction to produce more durable concrete bridge decks. This report is an important contribution toward the solution of concrete bridge deck deterioration because of its broad scope of investigation.

CONTENTS

ACKNOWLEDGMENTS

The research reported herein was conducted by the Department of Theoretical and Applied Mechanics under the auspices of the Engineering Experiment Station, University of Illinois. The Project Administrator was T. J. Dolan, Head, Department of Theoretical and Applied Mechanics, and the Project Director was Clyde E. Kesler, Professor of Theoretical and Applied Mechanics and Civil Engineering. Chester P. Siess, Professor of Civil Engineering, rendered considerable assistance as Project Consultant. The Project Investigator was Joseph P. Callahan, Research Associate, Department of Theoretical and Applied Mechanics. The principal project personnel were G. K. Beall, A. C. Edwards, D. M. Fischer, D. A. Haines, H M. Rejali, and R. J. Colver. In addition to these individuals the authors wish to acknowledge the cooperation and assistance of the many students and nonacademic personnel who contributed to the success of the project.

The assistances rendered by members of the Division of Highways, State of Illinois, by members of the Portland Cement Association Research Laboratories, and by Ellis Danner, Professor of Highway Engineering and Director of the Illinois Cooperative Highway Research Program, are gratefully acknowledged.

EFFECT OF STRESS ON FREEZE-THAW DURABILITY OF CONCRETE BRIDGE DECKS

SUMMARY

This report contains the findings of research conducted to determine if stresses resulting from the action of traffic, differential settlement, warping of slabs, and volume changes in the concrete will initiate or accelerate deterioration during freezing and thawing of concrete exposed to a deicing solution. For those readers interested primarily in the significance of the results and possible practical applications, Chapters Five and Six should be consulted.

The stress study was divided into two parts—a stressed surface study and a simulated bridge deck study.

The stressed surface study consisted of investigations of the effects of uniaxial, flexural, and biaxial static stresses on freeze-thaw durability of concrete composed of either a river gravel or crushed limestone coarse aggregate. Both 3- by 3- by 15-in. and 3- by 8- by 8-in. specimens were used to study uniaxial static stress effects. The flexural and biaxial stress studies consisted of 3- by 8- by 22-in. specimens. Both cracked and uncracked conditions were investigated in the flexural stress study.

The specimens used in the simulated bridge deck study were replicas of portions of actual bridge deck slabs cast from ready-mixed air-entrained concrete containing crushed limestone coarse aggregate. The effects of both static and cyclic flexural loading producing either tension or compression on the slab surface exposed to a saline solution were studied. The laboratory investigation consisted of slabs 6 in. deep and 3 ft wide that were divided into pairs composed of one 8-ft stressed slab and one 6-ft unstressed companion slab. One set, consisting of one unstressed and two stressed slabs, was subjected to three winters of natural outdoor exposure.

The combined results of these two studies indicated that stress does affect freeze-thaw durability; however, its effect is not dominant. Surfaces subjected to static tensile stress deteriorated at a slightly faster rate than did unstressed surfaces. On the other hand, surfaces subjected to static compression or biaxial stress due to torsion scaled at a reduced rate. Relatively low or high cyclic tensile stresses had little influence on the rate of surface scaling. Also, tensile slabs with different flexibility when subjected to the same cyclic loading exhibited little difference with respect to either rate of scaling or severity of cracking. The slabs subjected to cyclic compression scaled faster than their unstressed companions, and one set of these slabs containing a construction joint showed no significant distress along the joint. Scaling was never observed to occur in a stressed specimen without it also occurring in the unstressed companion specimen, nor was scaling completely prevented by stressing when it was observed on the unstressed specimens. Although feathering of cracks was caused by the mechanical action of cyclic loading, spalling was not observed.

Available bridge deck survey data and first-hand observations revealed the importance of transverse cracking and spalling of concrete on bridge deck durability; therefore, a study was conducted for the purpose of examining the effects of crack

width and concrete cover depth on reinforcement corrosion. Reinforcement was wrapped with helical strips of copper for the purpose of accelerating corrosion. The results of this study were inconclusive because of the inability to develop significant corrosion during the allotted period of time. A study was also made of the internal pressures necessary to produce spalling of various amounts of concrete cover above reinforcement and the nature of the resulting failures. Slotted galvanized pipes were cast into the concrete in place of conventional upper reinforcement and were subjected to hydraulic pressures after curing. Three types of failures occurred. Trench-type failures were observed for cover of 1 in. or less. For covers of 1¼ to 1½ in. failure generally occurred by propagation of horizontal cracks between adjacent pipes. These modes of failure were comparable to those observed in the field. Covers greater than 1½ in. led to failures either by horizontal cracking or by vertical cracks extending along a plane through the pipe centerline. It was found that for concrete covers of 4¼ in. the pressure needed to produce horizontal failure was much lower than the pressure needed to inhibit corrosion and it was not appreciably above the values for 1½-in. cover. The failure pressure depended primarily on the pipe spacing; therefore, for typical bar spacings used in bridge decks additional concrete cover will have little effect in preventing spalling if corrosive elements can reach the reinforcement. During the pressure study, two basic types of cracks resulting from shrinkage and consolidation of plastic concrete were observed. Vertical cracks were frequently seen directly above the top reinforcement; less frequently, horizontal cracks were located below the reinforcement.

Although stress had a discernible influence on the rate of scaling of surface mortar, it was of secondary importance. Significant differences in freeze-thaw durability were seen for specimens cast from different batches of concretes made using the same basic mix with similar air contents. A comparison of the measured properties of the concretes and their air void systems failed to disclose the reason for this inconsistent behavior. A microscopic examination of cross-sections of the freeze-thaw test specimens indicated that significant differences in the composition of the fine aggregate existed. Observations made by the ready-mix plant operator confirmed the possibility that, although the sand was obtained from a single source, periodic variations in composition had been detected. These variations in sand composition could result in surface mortar layers having appreciably different thermal length change coefficients than the remainder of the concrete containing the crushed limestone. Subsequent measurement of thermal length change differentials between mortar and concrete specimens confirmed this possibility.

Studies were also conducted to determine the effect of cyclic wetting and drying on concrete durability. It was shown that specimens subjected to periodic wetting and drying during early stages of freezing and thawing had improved durability. On the other hand, for specimens previously subjected to over 150 freeze-thaw cycles, subsequent cyclic wetting and drying proved to have a detrimental effect on freeze-thaw durability. Cyclic wetting and drying of a simulated bridge deck study slab previously subjected to over 100 freeze-thaw cycles revealed that scaling of surface mortar could be produced on a slab which showed no sign of scaling during prior freeze-thaw testing.

Based on the literature survey, results of published bridge deck surveys, field trips, and laboratory studies, two mechanisms of deterioration are postulated. The incompatibility mechanism offers an explanation of scaling of surface mortar, and the structural cracking mechanism explains deterioration associated with transverse cracking of bridge decks and reinforcement corrosion. It is believed that these mechanisms do not contradict any of the existing accepted theories but merely ex-

plain observed deterioration of air-entrained concrete bridge decks made from durable cement and aggregates.

A substantial decrease in the paste air content at the finished surface of four simulated bridge deck slabs indicated that there is a consistent depletion of surface air caused by normal finishing procedures. Microscopic examinations also revealed that, for concretes having high air contents, the air voids accumulated at the paste-aggregate interfaces, which could cause a decrease in durability by weakening the paste-aggregate bond. From these results, it is apparent that distribution of the entrained air rather than the gross air content is an imporant consideration.

CHAPTER ONE

INTRODUCTION AND RESEARCH APPROACH

STATEMENT OF THE PROBLEM

The motoring public is now realizing the benefits of the Interstate Highway System. Once heralded as the greatest public works project in history, this system is now having a pronounced effect on state highway department maintenance budgets.

Strict alignment and grade requirements of the Interstate program have resulted in the use of vast numbers of structures having reinforced concrete bridge decks. As a result, bridge deck durability is an even more important consideration now than it was in the past. This is especially true in urban areas having high traffic densities and in the more severe climatic regions where high frequencies of deicer application are necessary. Failures of recently constructed concrete bridge decks have in fact already become the topic of considerable discussion (*1, 2*).

Current procedures for repairing bridge decks are expensive and cause public inconvenience. The cost of replacement of bridge deck concrete can be as high as $1,000 per cubic yard, compared to the original construction cost of $60 per cubic yard. Therefore, there should be little doubt of the value of an economical preventative for bridge deck deterioration. But before a preventative can be prescribed the causes of the problem must first be understood.

Because the distress observed in concrete bridge decks is of several basic types which are not confined to structures of one locality, it can be assumed that they are caused by one or more of the following practices:

1. The employment of unsound ingredients in the concrete mix.
2. Inconsistent reinforcement placement.
3. Improper concrete handling, placing, finishing, or curing.
4. Inadequate air drying.
5. Faulty structural design.

Current specifications require that bridge decks be constructed with adequately air-entrained concrete composed of sound ingredients. There have been instances that indicate that these specifications might not have been followed; but, for the most part, it is probably reasonable to assume that they are now being met.

There is ample evidence to indicate that the placement of reinforcement during bridge deck construction was inadequately controlled, and frequently less than the prescribed minimum concrete cover resulted. Much of this problem can probably be attributed to a lack of understanding of construction practices by design personnel. The state highway departments have already taken steps to ensure that the desired minimum cover will be obtained. This has been accomplished by increasing the specified depth of cover and by requiring construction personnel to follow more stringent rules during placement of reinforcement and casting of bridge decks.

Under the category of improper handling, placing, finishing or curing of concrete, the most common violations are over-finishing, over-vibrating, and addition of water before or during finishing. Field observations indicate that these malpractices could produce harmful effects (*3*). Laboratory research, however, has failed to produce convincing evidence that the durability of air-entrained concrete is overly sensitive to moderate violations (*4, 5*). Also, increasing vigilance of responsible federal and state authorities has minimized the possibility that chronic violations exist.

It is a strong possibility that research currently being conducted will develop new insight into the role of retarders and curing techniques in minimizing cracking and producing durable concrete. Until that time, however, transverse cracking of bridge decks and subsequent corrosion of reinforcement will continue to be a serious problem.

The importance of air drying before concrete is subjected

to cycles of freezing and thawing has been demonstrated conclusively in the laboratory (*6*). To insure that air drying occurs, some states do not permit concreting after a specified date in the fall. Linseed oil treatments are also being used to prevent, at least temporarily, resaturation of concrete. It is well known that if water can be prevented from entering concrete, there will be no durability problem associated with freezing and thawing.

If it can be assumed that most of the concrete used is of satisfactory composition, it has been suggested that the basic structural design may be at fault This would also lead one to suspect that if this were true, concrete durability must be affected either by the states of stress present or by deflections, distortions, cracking, etc. If one stands on a bridge having reasonably long spans at the instant a heavy vehicle passes, the resulting deflection and vibration are impressive

Probably the most generally accepted explanation of the destruction of concrete during freezing and thawing involves the generation of pressures by the solution contained in saturated voids at the instant of freezing (*7*). The expansion as the ice crystals nucleate forces excess solution into the adjacent porous material. The frictional resistance of this material to the flow produces a hydraulic pressure which, in turn, induces a stress in the mortar of the concrete.

To explain observed increases in severity of deterioration attributed to the use of deicing chemicals on bridge decks, the "osmotic pressure theory" was postulated (*8*). This phenomenon is said to occur when relatively pure water freezes in capillary pores and causes increased salt concentration in the remaining liquid. Frequently separated from capillary pores by cement gel are the small gel pores. Owing to size restrictions the gel water freezes at a lower temperature than the capillary water. The higher concentration of the remaining unfrozen capillary solution induces a flow through the semi-permeable cement gel to correct the concentration imbalance. Because expansion of water during freezing initiates a flow out of the capillaries, the oppositely directed osmotic flow will reinforce the resulting pressure development

Because a bridge deck is continually subjected to flexural stresses approaching the design value during the passage of heavy vehicles, a portion of its surface could be so stressed at the instant of freezing. The combination of the loading stress and freezing stress could then exceed the strength of the mortar and scaling would result. This theory could contribute another explanation of why bridge deck concrete has frequently been found to be less durable than adjacent pavement slabs made with the same mix.

Many additional stress and distortion conditions can be produced through expansion, contraction, and differential settlement that would also contribute to scaling of bridge decks.

OBJECT AND SCOPE

This research was undertaken to determine if the durability of air-entrained concrete bridge decks under assimilated environmental conditions is significantly affected by externally applied forces. This investigation sought a relationship between reinforced concrete performance, as indicated by surface deterioration and cracking, and externally applied loading of either a static or cyclic nature.

Two predominant types of deterioration have been reported from the field: scaling of surface mortar, and deep-seated disruptions resulting from weakened plane formation. During this study, an attempt was made to investigate both these basic types of deterioration and to determine what effect, if any, external loading will have on the rate and magnitude of the deterioration.

RESEARCH APPROACH

Throughout this investigation considerable attempts were made to keep the research focused on bridge deck durability by maintaining a close contact with both field construction procedures and observations of bridge deck deterioration.

The results of first-hand observations of bridge deck deterioration were combined with published bridge deck survey data from the various states in order to determine basic mechanisms for the two predominant types of deterioration (*9-18*).

Laboratory studies were then designed for the purposes of developing these two major types of deterioration, based on their predicted causes, and to determine the effects of external forces on this deterioration.

To examine as many aspects of the problem as possible, a two-fold approach to the research was adopted.

The stressed surface study included specimens 3 by 3 by 15 in , 3 by 8 by 8 in , and 3 by 8 by 22 in. in size. The purpose of this study was to examine material behavior; therefore, no attempt was made to relate these specimens to bridge slab structure other than to ensure that adequate cover reinforcement was provided. This program was used to investigate the effects of uniaxial, biaxial, and flexural static stress states on freeze-thaw durability in the presence of a deicing agent Two types of coarse aggregates were employed. a crushed limestone free of deleterious particles, and a river gravel containing a small amount of chert. The gravel was used to determine if the frequency of occurrence of "pop-outs" was influenced by the presence of external forces.

The simulated bridge deck study consisted of slabs 3 ft wide, 6 in. deep, and either 6 or 8 ft long, depending on the loading condition employed. This study was used to investigate the behavior of replicas of portions of actual bridge deck slabs subjected to design loading while in an environment simulating field conditions of freezing and thawing in the presence of a deicing agent. Ready-mixed concrete was used throughout the simulated bridge deck study to ensure that the concrete in the slabs would be the same as that available for field construction.

Three of these slabs were installed in an outdoor area adjacent to the laboratory where they remained under static flexural loading for the duration of the project. A continu-

ous temperature history of the slabs was kept to permit comparisons of deterioration accruing during three consecutive winters of freezing and thawing with the results of equivalent laboratory freeze-thaw tests.

Each test conducted in the simulated bridge deck study required the use of considerable testing space and time; therefore, the stressed surface study was used as a guide in order to make more effective use of the simulated bridge deck program. Simulated bridge deck slabs were subjected to flexural loads of either a static or cyclic nature with either positive or negative moment regions, whereas companion slabs remained unstressed.

To provide insight into physical properties that might influence freeze-thaw durability, the following tests were conducted:

1. Cylinder test for compressive strength (ASTM C30-61).
2. Split cylinder test for tensile strength (ASTM C496-66).
3. Beam test for flexural strength (ASTM C78-59).
4. Pull-off test for surface mortar strength (Chap. Three of this report).
5. Modified point count for air void parameters (ASTM C457-66T; Chap. Three of this report).
6. Pressure test for air content (ASTM C457-66T).

In addition to the two primary studies, two secondary investigations were conducted.

Relative thermal length changes of mortar and concrete were measured using 3- by 3- by 15-in. specimens to obtain supplementary information necessary to prescribe a mechanism of scaling for concrete surface mortar.

Scaling of concrete owing to disruptions attributed to weakened plane formation was the objective of the second study. One portion of the investigation consisted of an experimental study of modes of failure of concrete owing to pressures induced by reinforcement corrosion, including an examination of weakened planes and vertical cracks produced by settlement of fresh concrete. The other portion of the research consisted of a laboratory study of the effects of crack size and depth on corrosion. The attempt was made to reproduce spalling attributed to reinforcement corrosion which is commonly seen in the field. Specimens 4 by 8 by 22 in. in size were cast using deformed bars which were wrapped with copper strips to accelerate corrosion.

Certain specimens from both of the primary studies were subjected to cycles of wetting and drying, in addition to freezing and thawing, to determine the effect of cyclic wetting and drying on durability.

OUTLINE OF THE REPORT

Chapter Two contains a review and summary of results of previously reported research concerning the effects of stress on freeze-thaw durability of concrete, and bridge deck survey information available from the literature.

Chapter Three consists of a description of the laboratory procedures used in preparing and testing specimens for the following studies:

1. Stressed surface study of effects of uniaxial, biaxial, and flexural static stresses.
2. Simulated bridge deck study of both static and cyclic flexural loading effects.
3. Study of thermal length change differentials of mortars and concrete.
4 Reinforcement corrosion study, divided into a study of modes of failure by simulated spalling and an accelerated corrosion study.
5. The influence of cyclic wetting and drying on concrete durability

In Chapter Four, the results of all experimental studies are presented in the following order:

1. The basic concrete properties and their relationship to concrete durability.
2. Stress study results presented according to the type of stresses employed.
3. The thermal length change study.
4. Reinforcement corrosion study.
5. The measurement of air void parameters in concrete cores from simulated bridge deck study slabs.
6. The study of cyclic wetting and drying of specimens from both the stressed surface and simulated bridge deck studies.

The first four chapters of this report include detailed discussions of the designated topics, however, for a discussion of the significance of the results and of possible practical application, see Chapters Five and Six.

Two mechanisms of deterioration of air-entrained reinforced concrete appear in Chapter Five. The first two sections contain discussions of the incompatability mechanism and the structural cracking mechanism, respectively. Included in that chapter are discussions of laboratory results and field observations pertaining to these mechanisms.

The conclusions drawn from the results of these studies, with suggestions of possible application to engineering practice, appear in Chapter Six.

Chapter Seven contains recommendations for further study of freeze-thaw durability of concrete bridge decks.

Appendix A gives the results of a study conducted to measure experimentally the nature of the strains produced on stressed surface study specimens by the various loading systems employed.

CHAPTER TWO

REVIEW OF RELATED RESEARCH

The research reviewed in this chapter includes the results of bridge deck surveys and that research relating directly to the effects of stress on freeze-thaw durability. For a more general discussion of freeze-thaw durability see Malisch (*6*), Kennedy (*8*), and Cordon (*19*).

BRIDGE DECK SURVEYS

Although none of the reports of bridge deck surveys reviewed could definitely state the causes of observed deterioration, most agreed on the major types of deterioration and possible causes. One exception is the 1930 "Progress Report of the Committee on Curing of Concrete Pavement Slabs" (*14*) which indicated that scaling appeared frequently to be associated with increases in silt content of fine aggregate of non-air-entrained concrete.

The three major types of deterioration indicated by the surveys were scaling of surface mortar, cracking in the transverse direction, and surface spalling (potholes) Many of the surveys indicated that the predominant problem was scaling (*9, 10, 16, 17, 18*), whereas others felt that transverse cracking was of paramount concern (*11, 13*). Three surveys concluded that although scaling was the predominant type of deterioration, it was not a very serious problem (*15, 16, 17*).

The Kansas, Michigan, and California cooperative surveys presented the most thorough analysis of bridge deck survey data (*11, 12, 13*). Similar types of deterioration were reported in all three surveys. Scaling was found to be associated with freeze-thaw action and the use of deicing agents The predominant form of cracking was in the transverse direction and was located over the primary reinforcement.

Most of the reports agreed that scaling followed no particular pattern. Illinois observed that the severity of scaling was as great in the relatively warm southern portions of the state as in the north (*16*). Wisconsin reported little correlation between scaling of structures on major arteries and those on secondary routes (*18*), whereas Maine found that routes having more traffic showed higher percentages of curb deterioration (*15*).

It was generally concluded that scaling of surface mortar can probably be attributed to one or more of the following:

1. Excessive and/or late finishing.
2 General hand-finishing practices.
3. Batch-to-batch differences in air content and/or slump.
4. "Washing out" of air due to excessive bleeding and/or additions of water during finishing and placement.
5. Insufficient dispersion of entrained air during mixing.
6. Poor drainage of bridge decks.
7. Excessive use of deicers.

Transverse cracking was considered to have been caused by one or more of the following:

1. Plastic and/or drying shrinkage.
2. Poor consolidation of concrete.
3. Improper placement of steel.
4. Excessive drying by heaters during winter concreting (*17*).
5. Long-time volume changes, including temperature effects.
6. Resistance to subsidence of concrete during the bleeding period by the rigidly held top reinforcement.
7 Vehicle loading.
8 Stresses resulting from the removal of falsework from continuous reinforced concrete bridges.

Surface spalling was attributed to the following:

1. Subsidence of plastic concrete resulting in "weakened plane" formation
2. Corrosion of reinforcement, primarily at transverse cracks.
3. Development of "shallow pockets" (*18*).
4. Traffic action combined with inadequate drainage of bridge decks.
5. Early drying shrinkage.

Results of the three cooperative surveys indicated that surface spalling and cracking do not appear to be influenced by air content. Owing to the small amount of longitudinal cracking observed, it was concluded that the slabs were adequately designed for live loading.

STRESS INVESTIGATIONS

The major portions of the related studies of other investigators were concerned with durability of prestressed concrete; however, in two studies flexural and tensile stress effects were considered.

One of the earliest studies was reported by Kennedy in 1955 (*20*). Tests were conducted by the U.S. Army Corps of Engineers with specimens at half-tide elevation on the New England coast. Reinforced concrete beams 8 to 10 in. wide, 14 in deep, and 7 to 9 ft long were cast using both air-entrained and non-air-entrained concrete. The 28-day compressive strengths averaged approximately 3,800 psi with air contents from 3 to 3.5 percent. The specimens were moist cured for 28 days and air dried for 14 days prior to stressing The beams were subjected to third-point flexural loading producing steel stresses of from 19,700 to 49,100 psi. Over a three-year period the specimens were subjected to 312 natural freeze-thaw cycles. The results demonstrated the superior durability of air-entrained concrete. The cracking developed during stressing did not contribute to deterioration by corrosion of reinforcement.

The visible deterioration of the air-entrained beams could not be correlated with stress; however, the results of all non-air-entrained specimens did indicate a relationship between increased amounts of deterioration and increased stress, with a single exception.

A study by Rieb (1955) was concerned with durability of pretensioned prestressed concrete (*21*). Beams having dimensions of 3 by 4 by 32 in. were cast using both Types 1 and 3 cements. The concrete had 28-day compressive strengths ranging from 5,800 to 6,800 psi and air contents from 3.3 to 4.8 percent. The specimens received 3½ days of moist curing, while some were subjected to steam curing The stress levels employed were from 0 to 2,000 psi. Air drying occurred for an unspecified period while specimens were shipped to the testing location. The beams were subjected to from 400 to 800 cycles of freezing in air to 0 F and subsequent thawing in water to 40 F (ASTM C 291-52T). At the end of 400 cycles, no deterioration of specimens was observed. Measurements indicated that after as many as 800 cycles, none of the specimens had relative dynamic moduli of less than 97 percent. As a result, no differences in stress effects could be determined.

Gutzwiller and Musleh (1960) reported that stress did affect the freeze-thaw durability of concrete (*22*). This study involved freeze-thaw testing of 3- by 4- by 16-in. beams cast using Type 1 cement. The concrete had 28-day compressive strengths of 5,110 to 6,420 psi and 3,730 to 3,740 psi. The air contents ranged from 1.7 to 5.2 percent After 28 days of moist cure, specimens made using the higher strength concrete were stressed to 2,000 psi in compression by post-tensioning the reinforcement. The specimens were then tested according to ASTM C 291-52T with apparently little if any air drying. Results of weight loss and sonic measurements indicated that prestressed concrete was more durable than unstressed specimens of either the same or the leaner mix Pop-outs, D-line cracking, and map cracking were the types of deterioration noted.

The results of a thorough study of stress effects were reported in the Russian literature by Moskvin and Podvalnyi (*23*). Although the effects of flexural stressing were emphasized, the effects of tensile and compressive stresses on freeze-thaw durability were investigated as well. The 2¾- by 2¾- by either 13¾- or 8⅔-in. specimens were cast using only non-air-entrained concrete having a water-cement ratio of 0.65.

The beams were moist cured for a minimum of one month and up to the time of testing. Specimens were subjected to third-point flexural loading ranging from 20 to 70 percent of the ultimate strength The freeze-thaw testing consisted of 8 hr of freezing in air at −17 C and 4 hr of thawing in water at 15 to 20 C. Resulting from the study was a direct relationship between the relative magnitude of stress and rate of deterioration which was measured by sonic methods. For stresses below 20 percent of ultimate, the relationship did not apply. Figure 1 shows typical results from this study. Figure 1a shows results for individual specimens; Figure 1b shows the average result for four specimens. In both figures, curve 1 indicates specimens subjected to 35 percent of the ultimate flexural strength. Curves 2 and 3 are results for specimens stressed to the 20 percent level and those remaining unstressed, respectively. In Figure 1a, it should be noted that the rate of change of the dynamic modulus for stressed specimens increases with increasing number of cycles of freezing and thawing. The same relationship is not seen in Figure 1b. This is because as some specimens deteriorated at a faster rate and were discarded the average would then consist of only the more durable companion specimens, resulting in an apparent decrease in slope.

To determine the effect of salts on freeze-thaw durability of stressed specimens, a study was made by freezing the specimens in 5 percent sodium sulfate solution. The results indicated that the rate of deterioration was uniformly increased for every stress level.

The results of a study of tensile stress effects also produced the conclusion that the increase in rate of deterioration was in proportion to the stress level employed. Conclusions concerning the effect of compressive stress were obtained from further examination of flexural specimens. One interesting investigation involved the use of phosphoric dye. A flexural specimen stressed to 35 percent of the ultimate strength and subjected to 20 freeze-thaw cycles was subsequently placed on its side in a shallow container partly filled with the phosphoric dye. The phosphor was found, on examination of the cross section, to rise to a significantly higher level in the tensile zone than in the com-

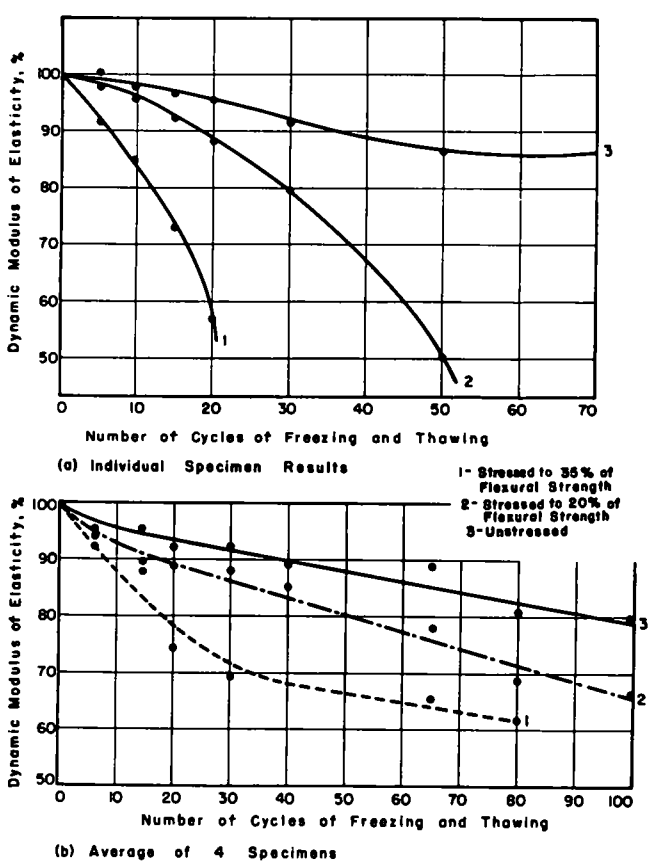

Figure 1. Influence of amount of stress on durability of plain concrete (23).

pression zone of the flexural specimen and resulted in a fairly linear slope downward from the region of maximum tensile stress to the region of maximum compressive stress. This was used to explain the ability of a tensile stress to produce a condition in the concrete such that additional moisture is made available for deterioration due to freezing and thawing. Conversely, compressive stresses tend to inhibit the presence of moisture, thereby decreasing deterioration. This was somewhat confirmed by porosity and absorption results. From the research results, the following general conclusions were drawn The rate of deterioration of non-air-entrained concrete by freezing depends on the character and intensity of the stressed state of a concrete specimen or structure Tensile stress decreases durability and longevity of concrete, whereas compression reduces or delays destructive processes. The explanation of the effects of stresses was based on the hydraulic pressure theory. The stresses were thought to have a direct influence on the distribution of moisture throughout the concrete.

Moss (*24*) conducted a study of compressive stress effects in 1966 using pretensioned specimens 2 by 4½ by 10½ in., which were stressed to a maximum of 1,200 psi. Non-air-entrained concretes having 28-day compressive strengths of 4,640 to 4,900 psi were employed using Type 2 cement. The concrete was moist cured for 14 days and air dried for 14 days. Other specimens were cured in steam at 150 F for 13½ hr. During testing either water or solutions of calcium chloride or magnesium sulfate were ponded on top by means of mortar dikes. Testing consisted of cycles of 16 hr of freezing, followed by thawing for 8 hr at room temperature. Results of the study indicated that the scaling of surface mortar was not stress dependent. The calcium chloride solution was found to cause extreme scaling It was concluded from dynamic modulus measurements that the over-all durability was moderately stress sensitive. Steam curing was observed to reduce durability.

A progress report from a continuing study of durability of prestressed concrete by the U.S. Army Corps of Engineers was published in 1967 (*25*). Thus far, no conclusions have been made with respect to the effects of stress on freeze-thaw durability.

CHAPTER THREE

LABORATORY PROCEDURES

STRESSED SURFACE STUDY

The objective of the stressed surface study was to determine the effects of uniaxial, biaxial, and flexural static stress on freeze-thaw durability of concrete.

Description of Specimens

The stress studies were designated as follows:

1. A Series.—Uniaxial tension and compression using unreinforced specimens.
2. B Series.—Uniaxial tension and compression using reinforced specimens.
3. F Series.—Flexural compression and tension (cracked and uncracked) using reinforced specimens.
4. T Series.—Biaxial stresses resulting from torsional loading of reinforced specimens.

Each of these four series was composed of several sub-series. The sub-series consisted of a number of individual specimens that were subjected to the stress conditions summarized in Table 1. In addition to stressed specimens, each sub-series contained unstressed companion specimens in order to identify any influence due to concrete batch differences. The concrete was bonded to reinforcement, except for the B Series compression specimens and the unreinforced A Series specimens.

Materials

The concretes were made using Type 1 cement. Two coarse aggregates were used: a gravel, and a crushed limestone. Both had good service records. The gravel was from the Wabash River near Covington, Ind., and consisted mainly of dolomite and limestone with minor quantities of quartz, granite, and chert. The crushed limestone was obtained from a quarry near Fairmont, Ill., and is designated as aggregate B. The fine aggregate used with both coarse aggregates was obtained from a pit near Staley, Ill. It is an outwash of the Wisconsin glaciation and consists primarily of quartz. Aggregate properties are given in Table 2.

The air-entraining agent used was a proprietary compound consisting of an aqueous solution of salts of sulfonated hydrocarbons containing a catalyst. Tap water was used in all batches.

Fabrication of Specimens

Table 3 gives mix data and the particular coarse aggregate employed for each sub-series. Table 4 summarizes the physical properties of concrete from each mix. The mixing and casting procedures employed for each study were as follows:

1. A and B Series.—Each of the A and B sub-series was cast using a 2.25-cu-ft batch mixed in a tub mixer. The dry

TABLE 1

STRESS STUDY SPECIMEN INFORMATION

Sub-series Number	Type of Loading	Specimen Dimensions, in	Reinforcement Number of Bars	Reinforcement Type	Total Number of Specimens for Each Sub-series	Number of Unstressed Specimens	Number Stressed Per Sub-series	Stressed Specimens Resulting Stresses	Stressed Specimens Magnitude
A-1	Axial	3 x 3 x 15	None		15	5	5	Tension	0 01 f'_c*
							5	Compression	0.1 f'_c
A-2	Axial	3 x 3 x 15	None		15	5	5	Tension	0.02 f'_c
							5	Compression	0.02 f'_c
A-3	Axial	3 x 3 x 15	None		15	5	5	Tension	0 025 f'_c
							5	Compression	0.25 f'_c
B-1,2,3 4,5,6,7 8,9,10 11,12	Axial	8 x 8 x 3	5	1/2" Bolts	9	3	3	Tension	0 20 f'_c
							3	Compression	0 30 f'_c
B-9	Axial	8 x 8 x 3	5	1/2" Bolts	10	5	5	Tension	0 20 f'_c
B-10, 13, 14	Axial	8 x 8 x 3	5	1/2" Bolts	10	5	5	Compression	0.30 f'_c
F-1, 2	Flexural	22 x 8 x 3	2	No 2 Bars	3	1	1	Tension	400 psi maximum
							1	Tension Cracked	Beyond Visible Cracking
F-3, 4	Flexural	22 x 8 x 3	2	No 2 Bars	5	2	1	Tension	400 psi maximum
							2	Tension Cracked	Beyond Visible Cracking
F-5	Flexural	22 x 8 x 3	2	No 2 Bars	4	1	1	Tension	400 psi maximum
F-6,8,9	Flexural	22 x 8 x 3	2	No 2 Bars	5	2	1	Tension	400 psi maximum
							1	Tension Cracked	Beyond Visible Cracking
							1	Compression	400 psi maximum
F-7, 10	Flexural	22 x 8 x 3	2	No.2 Bars	5	2	2	Tension Cracked	Beyond Visible Cracking
							2	Compression	400 psi maximum
F-C	Flexural	22 x 8 x 3	2	No 2 Bars	4	2	2	Compression	400 psi maximum
T-1, 2	Torsion	22 x 8 x 3	2	No 2 Bars	4	1	2	Biaxial	635 psi maximum
T-3, 4, 5	Torsion	22 x 8 x 3	2	No 2 Bars	5	2	3	Biaxial	635 psi maximum
X-1		96 x 36 x 6	3	No 5 Bars	1	1	0		
X-2, 3 4, 5	Flexural	72 x 36 x 6	3	No.5 Bars	2	1			
		96 x 36 x 6	3	No 5 Bars			1	Tension	f_w*
X-6, 7	Flexural	72 x 36 x 6	3	No.5 Bars	2	1			
		96 x 36 x 6	3	No 5 Bars			1	Compression	f_w
X-8, 9	Flexural	72 x 36 x 6	5	No 5 Bars	2	1			
		96 x 36 x 6	5	No 5 Bars			1	Compression	f_w
X-10,11	Flexural	72 x 36 x 6	5	No 5 Bars	2	1			
		96 x 36 x 6	5	No 5 Bars			1	Tension Cracked	f_w
X-12	Cyclic Flexural	72 x 36 x 6	3	No 5 Bars	2	1			
		96 x 36 x 6	3	No 5 Bars			1	Tension Cracked	1.5 f_w
X-13, 14	Cyclic Flexural	72 x 36 x 6	5	No 5 Bars	2	1			
		96 x 36 x 6	5	No.5 Bars			1	Tension Cracked	f_w*
X-15, 16	Cyclic Flexural	72 x 36 x 6	5	No 5 Bars	2	1			
		96 x 36 x 6	5	No 5 Bars			1	Compression	f_w
F.S.		72 x 36 x 6	3	No.5 Bars	3	1			
	Flexural	96 x 36 x 6	3	No.5 Bars			1	Tension	f_w
	Flexural	96 x 36 x 6	3	No.5 Bars			1	Compression	f_w

*f'_c refers to the 28-day cylinder compressive strength

*f_w refers to working stress of steel of 20,000 psi

TABLE 2

AGGREGATE DATA

Aggregate Designation	Cumulative Per Cent Passing Each Sieve											Fineness Modulus	Bulk Sp. Gr. SSD
	1-1/2 in.	1 in	3/4 in.	1/2 in.	3/8 in	No. 4	No. 8	No. 16	No. 30	No. 50	No 100		
Wabash River Gravel	100	94	63	29	14	1	-	-	-	-	-	7.22	2.69
CA Crushed Limestone	100	39	5	-	-	-	-	-	-	-	-	7.95	2.66
B Crushed Limestone	100	93	72	27	11	3	-	-	-	-	-	7 14	2.66
River Sand	100	100	100	100	100	98	87	69	47	16	3	2.80	2.60

ingredients were mixed for 1 min before adding the water containing the air-entraining agent. The wet mixture was then mixed for 3 min. The casting procedure consisted of placing concrete in each form and vibrating for 5 to 15 sec using external vibration. After excess concrete was removed, the surface was finished with a magnesium trowel for 30 to 60 sec.

2. F and T Series.—Sub-series T-1 was cast using the previously described mixing procedure. Sub-series F-4 was cast from a batch of the ready-mix concrete used in casting the simulated bridge deck slabs. The remaining specimens were cast with concrete mixed 5 to 6 min in a 6.5-cu-ft horizontal drum mixer. The air-entraining agent was included in the mixing water prior to its addition to the dry mixture in the drum. Each specimen was vibrated for not more than 40 sec. The actual vibration time was held to the minimum necessary to consolidate the mix.

Additional specimens to be used for modified air count readings and, in most cases, for pull-off tests were cast with each series. Compression test cylinders were cast from each batch of concrete for 28-day strength determinations, and additional cylinders were cast for the F and T Series to determine tensile strength using the splitting test.

Specimen curing differed to some degree between the various series. All specimens were subjected to 4 hr of air drying immediately after casting, followed by 20 hr of curing under wet burlap. The specimens were then removed from forms and put into a moisture room at 100 percent relative humidity for 6 days (except for sub-series A-1, which remained in the moisture room for 21 days). At the end of the curing period the specimens were placed in a constant-environment room at 50 percent relative humidity and 70 F for periods of 2 days for sub-series A-1, 7 days for sub-series A-2 and A-3, and 21 days for the other subseries. During the drying period, pull-plates were attached with epoxy to the A Series tensile specimens.

After completion of the drying period, the A Series specimens were resaturated by immersion for 24 hr prior to testing. All specimens were then subjected to the static stresses in Table 1 by means of the apparatus shown in Figure 2. The specimens were loaded using either a torque wrench on the load bolts or a universal testing machine to compress the A Series springs. See Appendix A for a discussion of actual torques used and resulting strains produced in the specimens.

Freeze-Thaw Testing

During freeze-thaw testing, Series B, T, and F specimens remained ponded with a 4 percent sodium chloride solution which was replaced only at the time of rating of scaling The solution was contained by rubber chamfer stripping cut to size and attached to the specimens by means of plastic rubber cement. Figures 2a through 2e show diked specimens properly positioned in the load frames. The apparatus shown in Figures 2f and 2g containing A Series specimens remained immersed in a 4 percent sodium chloride solution during the freezing-and-thawing cycles and were removed only at the time of rating.

The series were subjected to freeze-thaw testing in one of the following four units:

1. Constant-temperature room at 10 F for 12 hr and laboratory environment for 12 hr (i.e., one freeze-thaw cycle per day).
2. Constant-temperature upright freezers at 20 F for 12 hr and laboratory environment for 12 hr.
3. Small automatic freeze-thaw testing unit producing three cycles per day from 40 F to 0 F to 40 F (±5 F) as monitored in the center of the specimen.
4. Environmental testing unit subjected to 3 cycles per day from 36 F to 14 F to 36 F (±4 F) as monitored by thermocouples in the center of a specimen.

All of these units produced the required freezing and thawing of concrete to the center of the specimens. To compensate for possible differences in severity of freezing and thawing produced by the various systems, unstressed specimens were included in each sub-series, and the data were evaluated using a technique devised to eliminate any differences.

Rating

After a given number of cycles each specimen was rated according to the following numerical scale:

TABLE 3

STRESS STUDY CONCRETE MIX DATA

Sub-series	Max. Size Aggregate, in.	Water-Cement Ratio, gal/sk	Mix by Weight	Coarse Aggregate	Cement Factor, sk/cu yd	Slump, in.	Pressure Air, %
A-1	1	6.8	1·2.4·3.4	Limestone	6.0	3.0	4.7
A-2	1	6.8	1:2.4:3.4	Limestone	6.0	4.5	3.7
A-3	1	7.0	1:2.4:3.4	Limestone	6.0	4.5	2.6
A-4	1	6.8	1·2.4:3.4	Limestone	6.0	4.25	6.7
B-1	1	6.8	1.3.0:4.6	Gravel	4.5	3.5	4.6
B-2	1	6.8	1:3.0:4.6	Gravel	4.5	5.0	4.7
B-3	1	6.8	1·3.0:4.6	Gravel	4.5	2.5	4.6
B-4	1	6.8	1·3.0:4.6	Gravel	4.5	2.5	6.2
B-5	1	6.8	1:3.0:4.6	Gravel	4.5	3.0	6.6
B-6	1	6.8	1:3.0:4.6	Gravel	4.5	1.5	1.2
B-7	1	6.8	1:2.4.3.4	Limestone	6.0	4.0	4.6
B-8	1	6.8	1.2.4 3.4	Limestone	6.0	6.0	4.3
B-9	1	6.8	1:2.4:3.4	Limestone	6.0	5.25	4.5
B-10	1	6.8	1:2.4:3.4	Limestone	6.0	5.25	5.9
B-11	1	6.8	1 2.4:3.4	Limestone	6.0	7.0	4.1
B-12	1	6.8	1:2.4:3.4	Limestone	6.0	6.5	4.2
B-13	1	6.8	1:2.4·3.4	Limestone	6.0	6.5	5.7
B-14	1	6.8	1.2.4:3.4	Limestone	6.0	5.0	5.5
F-1	1	6.8	1:3.0:4.6	Gravel	4.5	3.0	1.4
F-2	1	6.8	1:3.0.4.6	Gravel	4.5	2.5	2.4
F-3	1	6.8	1:3.0:4.6	Gravel	4.5	5.0	5.4
F-4	1 1/2	5.2	1:2.0:3.5	Limestone	6.0	2.5	5.9
F-5	1	7.6	1:3.0 4.6	Gravel	4.5	3.0	1.5
F-6	1	7.6	1.3.0:4.6	Gravel	4.5	2.0	2.5
F-7	1	6.8	1:2.4:3.4	Limestone	6.0	4.0	3.2
F-8	1	8.4	1:3.0:4.6	Limestone	4.5	3.0	1.3
F-9	1	6.8	1.2.4 3.4	Limestone	6.0	3.5	1.9
F-10	1	6.8	1·2.4·3.4	Limestone	6.0	7.5	2.5
F-C	1	6.8	1:2.4:3.4	Limestone	6.0	6.5	6.9
T-1	1	7.6	1·3.0:4.6	Limestone	4.5	5.0	1.2
T-2	1	6.8	1:2.4:3.4	Limestone	6.0	4.0	3.2
T-3	1	6.8	1:2.4:3.4	Limestone	6.0	3.5	2.5
T-4	1	6 8	1:2.4:3.4	Limestone	6.0	1.5	3.1
T-5	1	6.8	1:2.4 3.4	Limestone	6.0	1.0	3.1
X-1	1 1/2	5.2	1:2.0:3.5	Limestone	6.0	2.0	5.2
X-2	1 1/2	5.2	1·2.0 3.5	Limestone	6.0	2.0	5.0
X-3	1 1/2	5.2	1 2.0·3.5	Limestone	6.0	3.25	5.6
X-4	1 1/2	5.2	1·2.0:3.5	Limestone	6.0	1.0	5.6
X-5	1 1/2	5.2	1·2.0:3.5	Limestone	6.0	3.5	9.3
X-6	1 1/2	5.2	1:2.0 3.5	Limestone	6.0	5.5	7.3
X-7	1 1/2	5.2	1:2.0:3.5	Limestone	6.0	2.5	2.9
X-8	1 1/2	5.2	1:2.0:3.5	Limestone	6.0	2.5	5.7
X-9	1 1/2	5.2	1:2.0:3.5	Limestone	6.0	4.0	1.9
X-10	1 1/2	5.2	1:].0:3.5	Limestone	6.0	5.0	4.0
X-11	1 1/2	5.2	1 2.0·3.5	Limestone	6.0	3.5	3.1
X-12	1 1/2	5.2	1:2.0 3.5	Limestone	6.0	2.75	4.7
X-13	1 1/2	5.2	1.2.0:3.5	Limestone	6.0	3.25	3.9
X-14	1 1/2	5.2	1:2.0:3.5	Limestone	6.0	4.0	7.0+
X-15	1 1/2	5.2	1:2.0:3.5	Limestone	6.0	2.25	5.3
X-16A	1 1/2	5.2	1:2.0:3.5	Limestone	6.0	3.5	3.8
X-16B	1 1/2	5.2	1:2.0:3.5	Limestone	6.0	4.25	4.4
F.S.	1 1/2	5.2	1:2.0:3.5	Limestone	6.0	2.5	5.9

TABLE 4

SUMMARY OF STRESSED SURFACE STUDY TEST RESULTS

Sub-series	Modified Point Count Results				Pressure Air Content, %	Pull-Off Strength, psi	Comp Strength, psi	Tensile Strength, psi	Freeze-Thaw Cycles	Max Unstr Specimen Scale Rating
	Air Content, %	Spacing Factor, in.	Paste Content, %	Air in Paste, %						
A-1	5 6	0.011	12 3	45.5	4 7	-	4190	-	291	4
A-2	4.5	0.009	20.7	21 7	3.7	-	4850	-	153	0
A-3	5.8	0 017	13.4	43 3	2.6	-	3790	-	135	6
A-4	10.1	0.014	12 4	81 5	6 7	-	4460	-	46	-
B-1	5.1	0.012	41 5	12.3	4 6	-	4640	-	304	4
B-2	4.0	0.011	46.6	8 6	4.7	-	4180	-	199	5
B-3	3.3	0 008	36.2	9 1	4 6	51	4000	-	212	5
B-4	4 4	0 007	35 5	12 4	6.2	157	3140	-	212	5
B-5	8 1	0 005	30 0	27 0	6 6	236	2950	-	172	4
B-6	2.0	0.012	40 1	5 0	1 2	95	4140	-	29	10
B-7	5.7	0 007	42.0	13.6	4.6	359	4300	-	127	3
B-8	6.6	0 011	40.9	16 1	4.3	206	3920	-	75	1
B-9	5.8	0.008	46 7	12 4	4 5	260	4710	-	11	9
B-10	4 5	0 007	49.5	9 1	5 9	278	4320	-	374	8
B-11	5 2	0 009	50 6	10 3	4 1	240	4020	-	236	6
B-12	6.1	0.008	46 9	13 0	4 2	248	4420	-	390	9
B-13	6 1	0.009	46 0	13 3	5 7	321	4240	-	403	5
B-14	5.5	0.009	46 6	11 8	5 5	317	4520	-	403	9
F-1	-	-	-	-	1 4	-	5600	557	116	10
F-2	-	-	-	-	2 4	-	5470	530	111	5
F-3	6.7	0 005	37 6	17 8	5 4	118	3600	328	126	1
F-4	7 4	0 008	35 3	21 0	5 9	71	5500	455	173	2
F-5	0 7	0.016	41.3	1 7	1 5	173	4800	526	16	10
F-6	1.4	0.011	45.6	3.1	2 5	131	5700	455	43	8
F-7	4.7	0.007	36 7	12 8	3 2	131	4900	441	88	5
F-8	0.8	0 012	39.7	2.0	1.3	243	4260	479	14	7
F-9	4 1	0.007	34 7	11 8	1.9	151	4570	421	34	10
F-10	2.9	0 007	41.4	7 0	2.5	227	6200	527	68	5
F-C	11.3	0 005	28.0	40.3	6 9	185	5140	390	77	0
T-1	0 9	0 014	40.3	2.2	1 2	127	4140	-	63	7
T-2	5.7	0.009	30.0	19.0	3 2	152	4873	441	82	8
T-3	4.1	0.007	34.7	11.8	2.5	182	4560	421	15	10
T-4	2.1	0 009	48.5	4.3	3.1	417	6210	527	130	7
T-5	2.2	0.012	48 6	4 5	3.1	260	4030	410	101	10

0—no scale.

1—scattered spots of very light scale.

2—scattered spots of light scale

3—light scale over about half the surface.

4—light scale over most of the surface.

5—light scale over most of surface, few moderately deep spots.

6—scattered spots of moderately deep scale.

7—moderately deep scale over half the surface.

8—moderately deep scale over entire surface.

9—scattered spots of deep scale; remainder moderately deep scale.

10—deep scale over the entire surface.

Scaling was considered to be *very light* when it consisted of loss of a paper-thin film of mortar from the finished surface. *Light* scaling consists of particles of mortar generally ⅛ to ¼ in. in thickness. Scaling was described as *moderate* when additional mortar was removed, resulting in easy removal of small aggregate particles. Surface deterioration resulting from pop-outs was also considered to be scaling. *Deep scaling* was said to have occurred when larger coarse aggregate particles were easily removed from the scaled surface at the time of rating.

Photographs of the specimens were taken during each rating. Immediately following the rating, the specimens were either ponded or immersed again, and freezing and thawing cycles were resumed. This periodic rating of specimens continued until the ratings became high enough to denote failure of the surface, or when the dikes leaked to such an extent that the saline solution would no longer remain ponded on the top surface. This latter condition sometimes occurred when much of the surface of the specimens remained relatively unscaled.

In addition to visual ratings, the rate of deterioration of Series A specimens was evaluated by periodic measurements of the delay of a sonic pulse traveling over a 5.25-in. gauge length using the soniscope shown in Figure 3.

Pull-Off Test

After curing was completed, one specimen from each subseries (except Series A) was selected for pull-off testing to determine the strength of the surface mortar. Prior to test-

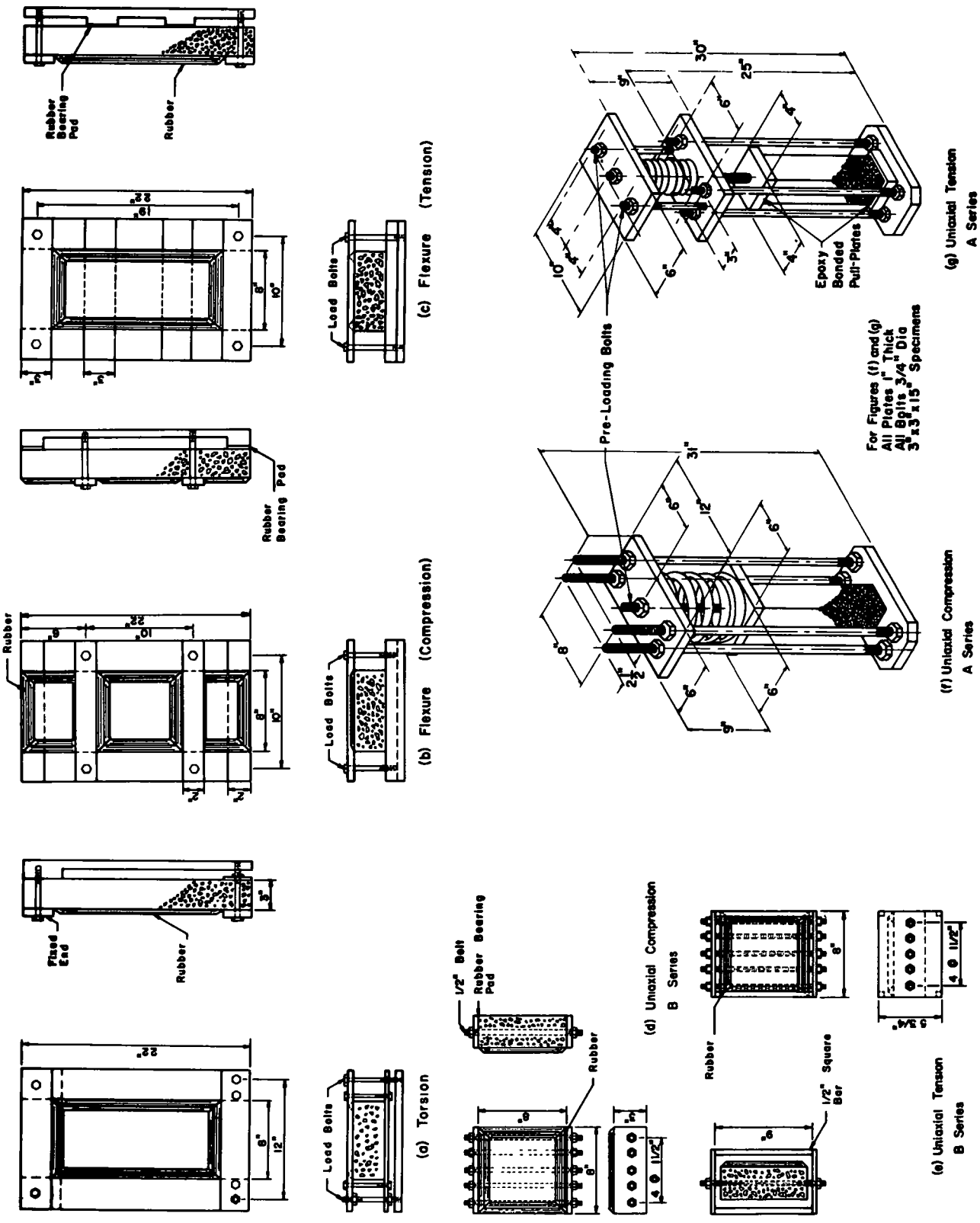

Figure 2. Loading frames for stressed surface studies.

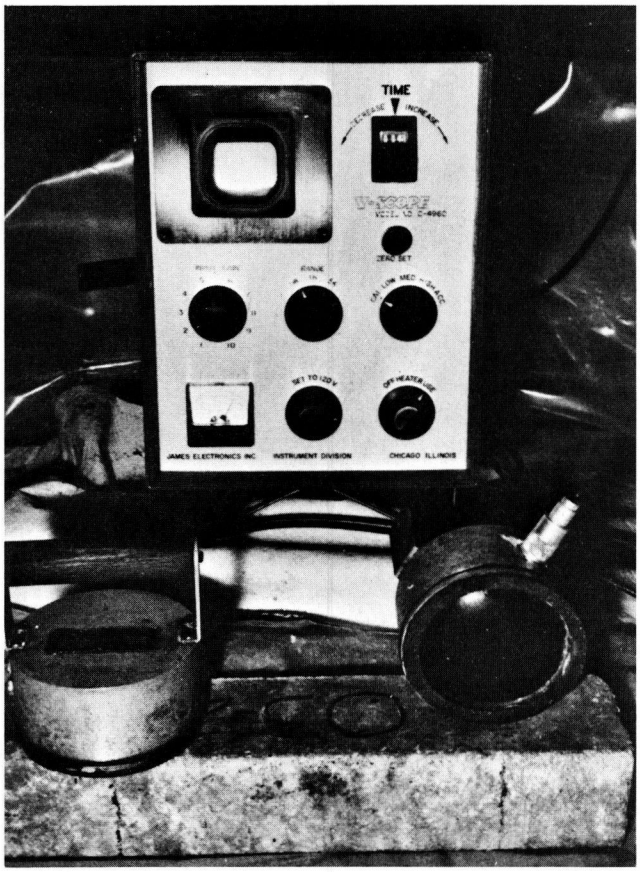

Figure 3. Sonic testing apparatus.

ing, grooves approximately ½ in. deep were cored into the finished surface using a 2-in.-diameter core bit. The bottom of the groove provided a smooth bearing surface for the pull-off tester and the presence of the groove encouraged failure to occur along the weakest plane. Steel pull-off heads of 2-in. diameter were then attached with epoxy onto the portion of the finished surface within the groove. After a minimum of 1 day of curing of the epoxy the test was performed using the apparatus shown in Figure 4a. [See Malisch et al. (*4*) for further discussion of the apparatus.] The epoxy used had sufficient bond strength so that the failure plane occurred within the concrete rather than at the epoxy-concrete or epoxy-steel interfaces. Typical failures are shown in Figure 4b.

Modified Point Count

The air void parameters of the hardened concrete were obtained using the modified point count apparatus in accordance with ASTM C 457-66T. A specimen from each sub-series was chosen to be sawed into 3- by 3-in. blocks. The finished surfaces of these blocks were then lapped until they were smooth. Only sufficient lapping to eliminate roughness was permitted, to determine as closely as possible the air content of the surface material for all series employing ponding. The A Series air void specimens were obtained by sawing 1-in. slices through the 3-in. by 3-in. cross section to obtain the average air content of the concrete.

Air voids were then counted using the modified point count apparatus. The procedure was also used to calculate paste content. Each slice was traversed individually, and eventually all traverses for one specific sub-series were combined into a single calculation of air void parameters.

SIMULATED BRIDGE DECK STUDY

This study comprised the major effort of the research program. The specimens tested under the simulated bridge deck study represent actual sections of bridge deck slabs.

Description of Specimens

The specimens included in this study were designated as follows:

1. X Series.—Laboratory flexural study with specimens subjected to positive or negative moments of either a static or cyclic nature.
2. FS Series.—Field slab flexural study consisting of specimens subjected to either positive or negative static moments.

The following criteria for the test slabs were adopted after examining a number of bridge deck designs:

1. Slab depth—6 in.
2. No. 5 bars used for both tension and compression reinforcement.
3. Longitudinal bar spacing—6 in. or 12 in.
4. Transverse bar spacing—16 in.
5. Concrete cover over top reinforcing—1½ in.

A summary of specimen information for each sub-series is given in Table 1.

Materials

The reinforcement consisted of No. 5 intermediate grade deformed bars conforming to ASTM designations A15-64 and A305-64.

The concrete was obtained from a local electronically controlled batch plant and consisted of a mix meeting the State of Illinois Division of Highways specifications for Class X bridge deck concrete.

The properties of the aggregates used are given in Table 2. The crushed limestone coarse aggregate was a mixture of 971 lb of designation CA and 974 lb of designation B per cubic yard of concrete. The source of both limestones was a quarry near Fairmont, Ill. See Table 3 for additional mix properties.

Because of an air temperature of 81 F at the time of casting of the field slabs, 9 lb of a commercial retarder was added to 3 cu yd of concrete. This was in accordance with the recommended field procedure, and was not considered necessary during casting of specimens in the laboratory.

The air-entraining agent used was the same proprietary compound described previously under "Stressed Surface Study." Type 1 cement and tap water were used in all mixes.

Fabrication of Specimens

The slabs were cast using currently recommended field procedures. All specimens, except for the FS Series, were cast in the laboratory using oiled plywood forms purchased from a commercial form manufacturer. The field slabs were cast at the site of the field exposure test using the same forms.

The concrete was transported to the casting site in 15 min or less by means of ready-mix trucks. A slump test (ASTM C143-58) and a pressure air test (ASTM C457-66T) were then conducted.

The concrete was transported by dump bucket from the truck to the slabs and a crane was used to permit dumping directly into the forms. Internal vibrators were used during placement.

Immediately after filling of the forms, excess concrete was removed, using a 2- by 4-in. board as a screed. The surface was floated using a wooden float and finishing was completed in the shortest possible time with a magnesium trowel. Concrete anchors were placed in the plastic concrete to permit easy moving of the slabs. The finishing operation was completed 30 to 40 min after the start of casting.

Twelve 6- by 12-in. cylinders and six 6- by 6- by 22-in. beams were made during the casting operation, according to ASTM C192-59.

Approximately 3 hr from the start of casting, the finished surfaces of the slabs were brushed with a straw broom. One to 2 hr later the slabs were covered with a minimum of two layers of wet burlap, which, in turn, was covered with plastic sheeting.

The following day, the cylinders and beams were removed from their forms and placed in a moisture room for 27 days of curing.

The burlap covering the slabs was moistened each day until the slabs had been cured for 7 days. The forms and the burlap were then removed and the slabs were elevated to permit air drying for 14 days. Two 3¾-in.-diameter cores were removed from the 6-ft slab, and eight 2-in.-diameter grooves were cored into the finished surface for pull-off testing (see "Pull-Off Test"). The two cores were later sliced and lapped for use in air void counting (see "Modified Point Count").

At the end of the first week of air drying the finished surfaces of the slabs were fitted with dikes made of rubber chamfer stripping (Fig. 6). The dike locations on the surface of the stressed specimen varied, depending on whether the top surfaces were to be in tension or compression; however, the unstressed specimens were always diked in the same manner. An epoxy was used to fasten the diking to the slab and at the same time epoxy was used to fasten the steel pull-off heads to the slabs. The edges of the diking were subsequently sealed with rubber cement. The diked areas were filled with tap water and remained ponded for 3 days prior to testing.

These same procedures were followed for all slabs, with one minor exception. Sub-series X-16 consisted of two separate concrete batches cast one week apart. The halves of the slabs cast first received 21 days of air drying prior to testing instead of the normal 14-day period.

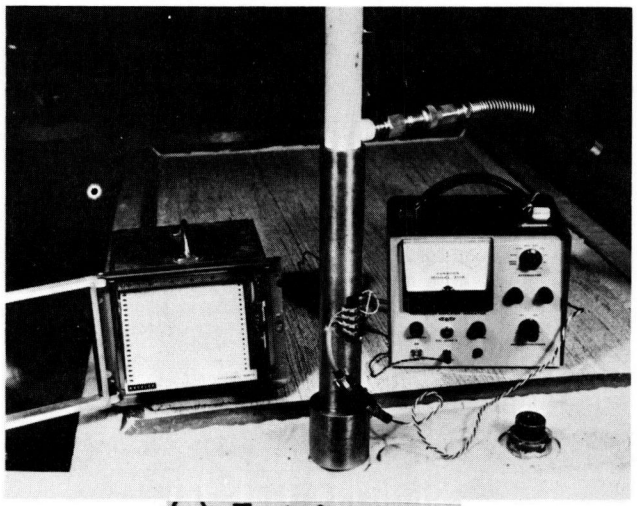

(a) Test Apparatus

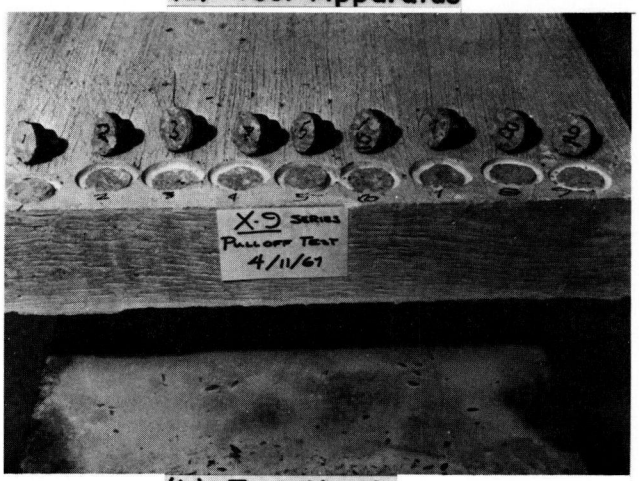

(b) Test Heads

Figure 4. Pull-off test.

Freeze-Thaw Testing

All slabs tested under the simulated bridge deck study were subjected to cycles of freezing and thawing in the environmental testing unit shown in Figure 5. This unit was designed to allow the removal of two 4- by 12-ft roof sections using an overhead crane and thereby permitted direct placement by crane of slabs onto their respective test frames. After the 8-ft slab was positioned on the I-beam attached to the hydraulic ram (Fig. 6) the top supports were replaced and bolted by tensile rods to the post-tensioned concrete load-frame base slab. The longitudinal upper and lower support locations were interchangeable, depending on whether the specimen was to be subjected to negative or positive moments. The 8-ft slab was then subjected to the desired loading using a hydraulic testing machine having both static and cyclic loading capabilities. The 6-ft unstressed companion slabs were supported by a frame at the same elevation in the environmental test unit as the stressed specimen.

After the slabs had been positioned and stressed, photo-

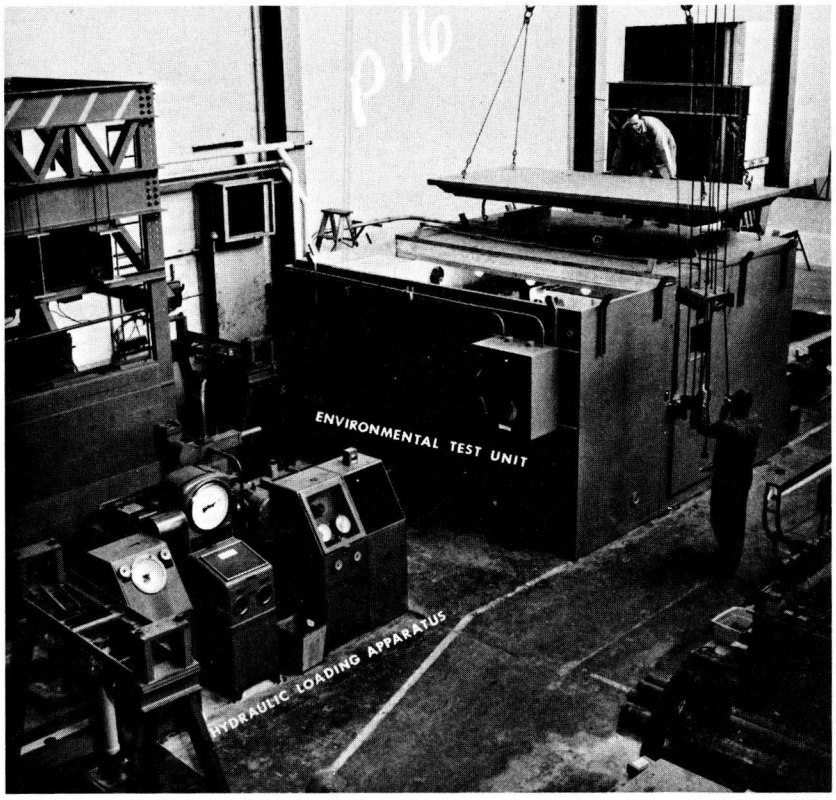

Figure 5. Laboratory environmental testing facility.

graphs were taken of the concrete surfaces enclosed by diking. Photographs were again taken after specific numbers of freeze-thaw cycles, and the severity of deterioration was evaluated using the visual rating system described previously under "Rating."

During the rating of sub-series X-5 through X-10, sonic readings were taken using the apparatus shown in Figure 3. The numbers shown on the diked surfaces of the stressed and unstressed slabs in Figure 6 denote soniscope transmitter and receiver locations. Readings were made for the following pairs of locations:

1. Compression specimen:
   a. Short readings—1-2, 3-4, 5-6, 7-8, 9-10, 11-12.
   b. Long readings—1-4, 2-3, 1-3, 2-4, 5-8, 6-7, 5-7, 6-8, 9-12, 10-11, 9-11, 10-12.
2. Tension and unstressed specimens:
   a. Short readings—2-3, 6-7.
   b. Long readings—1-4, 1-8, 4-5, 5-8, 1-5, 4-8.

The positions of transmitter and receiver were interchanged for each pair of locations to obtain an average reading.

On completion of the rating procedure, the dikes were filled with a 4 percent sodium chloride solution and the roof sections of the unit were replaced. A thermocouple serving as the temperature sensor for the programmer-controller-recorder was inserted into a precast hole at mid-depth of the slab and the environmental testing unit was activated.

THERMAL LENGTH CHANGE STUDY

The purpose of this study was to explore, using a linear comparator, the possible existence of significant thermal volume change differentials between mortars and concretes that could cause surface scaling on bridge decks.

Description of Specimens

The study was divided according to types of materials and objectives into the following sub-series:

1. C-1.—Comparator study consisting of 1:2,* 1:3, and 1:4 non-air-entrained mortars.
2. C-2.—Comparator study consisting of 1:2, 1:3, and 1:4 air-entrained mortars.
3. C-3.—Comparator study of 1:2 mortar, concrete, and no-fines specimens made from sub-series X-10 concrete.
4. C-4.—Comparator study of 1:2 mortar, concrete, and no-fines specimens made from sub-series X-12 concrete.
5. C-5.—Direct tension test using 1:1 air-entrained mortar specimens.

Sub-series C-1 through C-4 consisted of unreinforced 3- by 3- by 15-in. bars. Knurled rods having a diameter of ¼ in. and length of 2 in. were cast into the specimens with ½ in. of the rods protruding from each end. The ends of these rods were rounded to facilitate length measurements using the linear comparator shown in Figure 7.

* The mortars were designated according to cement:sand ratios by weight.

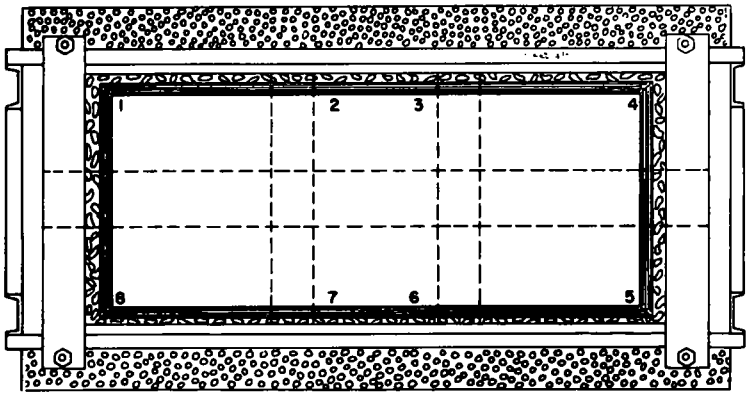

Plan View of Tension Surface

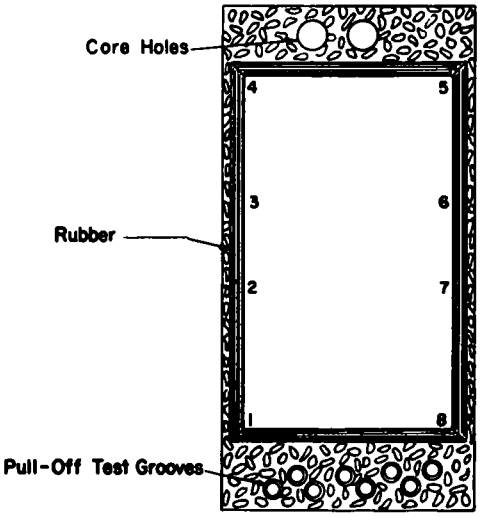

Plan View of Unstressed Slab

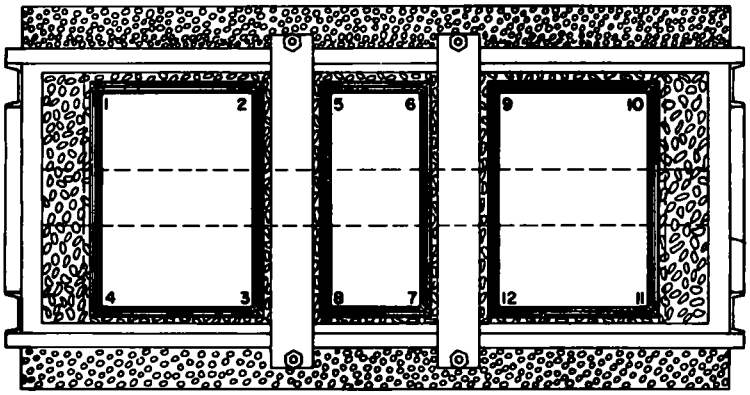

Plan View of Compression Surface

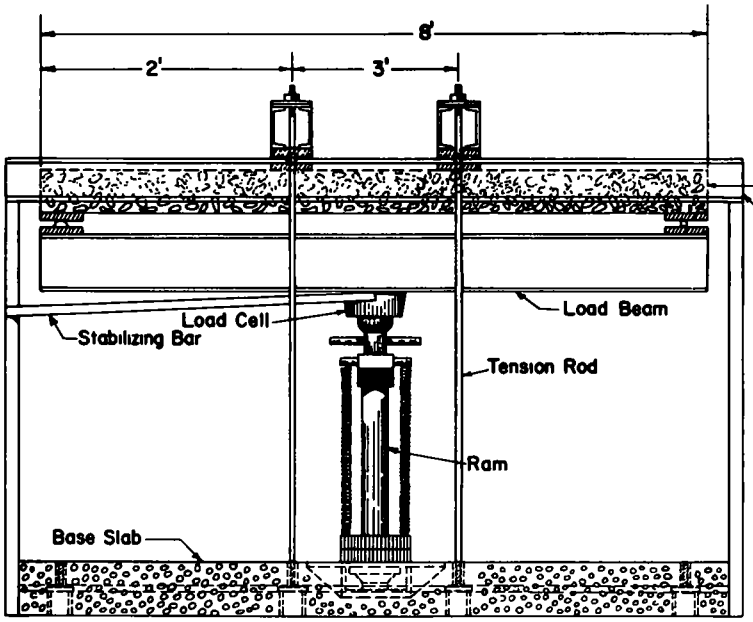

Elevation of Flexural Test Frame

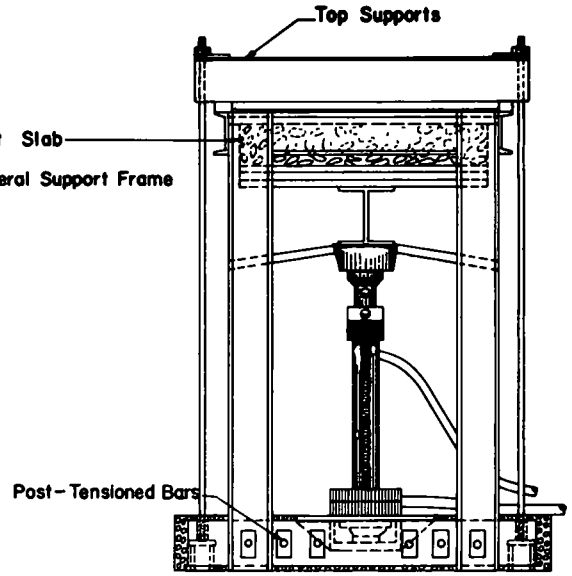

End View of Flexural Test Frame

Figure 6 Simulated bridge deck study test set-up.

TABLE 5

SUMMARY OF SIMULATED BRIDGE DECK STUDY TEST RESULTS

Sub-series	Modified Point Count Results: Air Content %	Spacing Factor in.	Paste Content, %	Air in Paste, %	Pressure Air Content, %	Pull-Off Strength, psi	Comp. Strength, psi	Tensile Strength, psi	Flexural Strength psi	Freeze-Thaw Cycles	Max. Unstr. Specimen Scale Rating
X-1	9.6	0.011	42 8	22 4	5 2	177	3960	-	-	61	1
X-2	4.2	0 010	33.2	12 7	5 0	204	4510	-	611	27	8.5
X-3	6 9	0.008	41.1	16 8	5.6	226	3520	-	609	100	0
X-4	2.5	0.009	44 8	5 6	5.6	235	5760	-	819	57	9
X-5	10.1	0 007	42.2	23 9	9.3	249	3580	433	575	74	5
X-6	7 3	0.008	43 2	16.9	7 3	227	3660	380	664	108	1
X-7	2 9	0.009	40.3	7.2	2 9	311	5180	388	758	114	0
X-8	4 7	0.010	58.0	8 1	5.7	204	4200	428	622	102	1
X-9	2.3	0.013	45.7	5 0	1.9	249	5170	413	697	58	9
X-10	6.5	0.012	39.6	16.4	4.0	282	5390	438	828	80	3
X-11	4 6	0 010	49.0	9.4	3.1	310	4410	407	701	72	7
X-12	6.5	0.007	39.5	16.5	4.7	353	4270	367	696	94	1
X-13	4.1	0.008	38 9	10.5	3.9	233	4710	419	681	105	1
X-14	10.2	0.005	24.3	42.0	7+	186	3450	304	575	110	5
X-15	5.4	0 005	36.3	14 9	5.3	162	5320	417	732	100	8.5
X-16A	3.3	0 005	34.8	9 5	3.8	314	4040	451	724	100	8
X-16B	7.9	0 006	32 8	24.0	4 4	246	4420	397	675	100	6
FS	5.2	0 007	42.9	12 1	5.9	80	4290	347	624	73	1

TABLE 6

COMPARISON OF FINAL SERIES AVERAGE SCALE RATINGS OF STRESSED SPECIMENS WITH UNSTRESSED COMPANIONS

Series	Number Higher	Per cent Higher	Number Same	Per cent Same	Number Lower	Per cent Lower
A Static Flexure						
1 Gravel						
tension (cracked)	2	40	2	40	1	20
tension (uncracked)	1	20	2	40	2	40
compression	0	0	0	0	1	100
2. Limestone						
tension (cracked)	5	83	0	0	1	17
tension (uncracked)	4	57	2	29	1	14
compression	3	50	2	33	1	17
3. Combined						
tension (cracked)	7	64	2	18	2	18
tension (uncracked)	5	42	4	33	3	25
compression	3	42	2	29	2	29
B. Cyclic Flexure						
1. Limestone						
tension (high)	1	50	1	50	0	0
tension (low)	0	0	1	100	0	0
compression	2	100	0	0	0	0
C. Uniaxial Stress						
1 Gravel						
tension (uncracked)	4	67	0	0	2	33
compression	3	50	1	17	2	33
2. Limestone						
tension (uncracked)	3	60	1	20	1	20
compression	1	14	2	29	4	57
3 Combined						
tension (uncracked)	7	64	1	9	3	27
compression	4	31	3	23	6	46
D. Combination of A and C						
tension (uncracked)	12	52	5	22	6	26
compression	7	35	5	25	8	40
E Torsional	1	20			4	80

Sub-series C-5 consisted of tensile specimens especially designed to permit strain measurements using electric resistance strain gauges during testing. These specimens (Fig. 8), have a diameter of 1 in. at the test section.

Materials

Type 1 cement, the sand and the air-entraining agent described previously in "Stressed Surface Study," and tap water were used in all specimens.

Fabrication of Specimens

Table 7 gives a summary of sub-series C-1, C-2, and C-5 mix data. The properties of C-3 and C-4 mixes were the same as those of sub-series X-10 and X-12, respectively.

The C-1, C-2, and C-5 mortars were mixed using the same procedure described previously for Series A under "Stressed Surface Study." Three 3- by 3- by 15-in. beams and four 2- by 4-in. cylinders were cast using each mix. Air contents were measured using a 0.1-cu-ft pressure meter.

The materials for casting sub-series C-3 and C-4 were obtained by separating ready-mixed concrete into two fractions using a ¼-in. screen. The coated rock retained on the screen was used to cast no-fines specimens and the material passing through the screen was used to cast mortar specimens. Sub-series C-3 consisted of four beams made from each of these materials and four made from the concrete. Sub-series C-4 consisted of three beams of each type. The forms were filled and placed on a vibrating table for 15 sec. The top surfaces were finished with a magnesium trowel.

All comparator beams were moist cured in their forms for 7 days under burlap after an initial 4-hr period of air drying. The beams were then permitted to air dry for a minimum of 14 days. The specimens were immersed for at least 3 days in tap water immediately prior to testing. The cylinders were moist cured for 28 days by immersion after an initial 4-hr drying period.

Four sub-series C-5 tensile specimens were cast in the brass molds shown in Figure 8a. The molds were placed on a vibrating table during casting to remove entrapped air. The mortar was allowed to bond to the 2.25-in.-diameter brass collars, except for the plugged lower 1 in. of the bottom collar and the top 1 in. of the upper collar. Six 2- by 4-in. cylinders were also cast from the same mix. The air content was determined using a 0.1-cu-ft pressure meter.

After 4 hr of air drying the plugs were removed from the bottom collars and the filled molds were immersed in a tank containing tap water. Three days later all of the specimens were de-molded and re-immersed in the tank. After 7 days of moist curing the specimens were allowed to air dry in the laboratory for 14 days. Toward the end of this period, electric resistance strain gauges were attached to diametrically opposite surfaces of the reduced sections of the direct tension specimens after the surfaces had been smoothed and cleaned.

Testing Procedures

Control temperatures for the thermal length change study were measured using a thermister cast in the center of one 3- by 3- by 15-in. mortar beam.

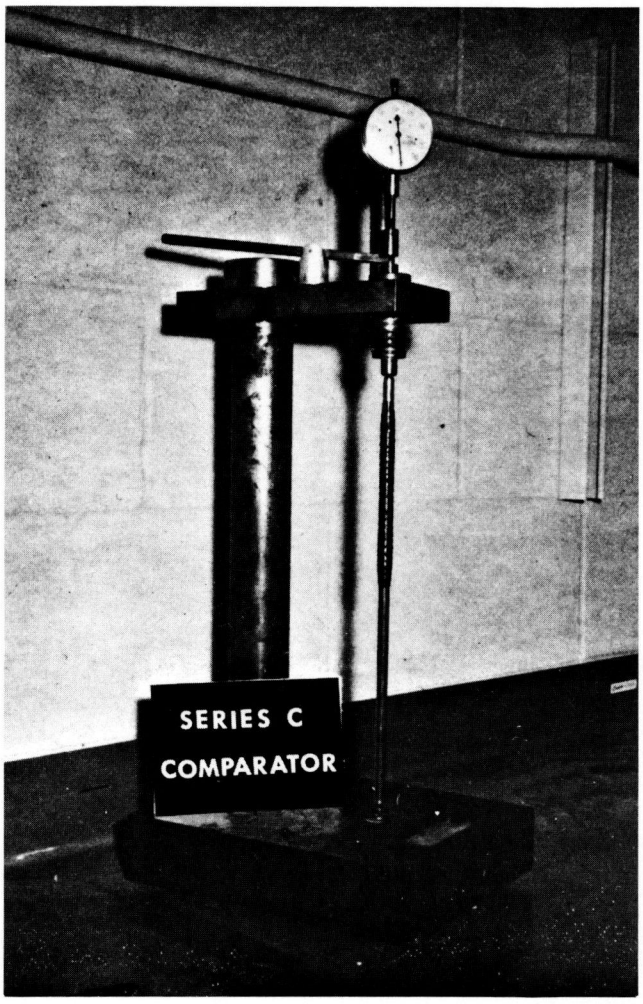

Figure 7. Apparatus for measuring length change.

The specimens were subjected to one of the following freeze-thaw cycles:

1. Sub-series C-1 and C-2:
   a. Frozen in solvent cooled by dry ice to a specimen temperature of 20 F in 30 min.
   b. Thawed in heated tap water to a specimen temperature of 70 F in 20 min.
2. Sub-series C-3:
   a. Frozen in air in a commercial freezer to a specimen temperature of −15 F in 12 hr.
   b. Thawed in 4 percent sodium chloride solution to a specimen temperature of 64 F in 4 hr.
3. Sub-series C-4:
   a. Frozen in solvent cooled by dry ice to a specimen temperature of 0 F in 20 min.
   b. Thawed in heated tap water to a specimen temperature of 70 F in 17 min.

Once the specific temperature was reached, the specimens were removed in a random order and comparator readings were made as quickly as possible. A brass standard bar was measured using the comparator before each set of readings

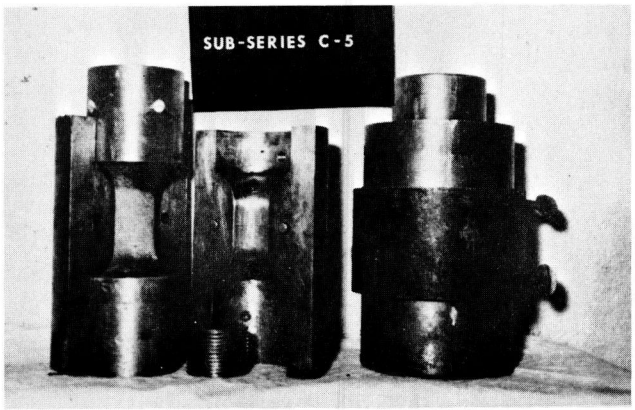

(a) Tensile Specimen and Mold

(b) Tension Test Set-Up

Figure 8. Axial tension test for mortar.

was taken (Fig. 7). All length differences were referenced to the reading of the brass standard.

At the end of each thawing period, sonic readings were made on sub-series C-1 and C-2 beams over a 7-in. gauge length using the soniscope shown in Figure 3.

Sub-series C-5 specimens were tested to failure in tension using the screw-type mechanical testing machine (Fig. 8b). The upper end of the specimen was rigidly attached to the load cell. The lower end of the bottom coupling was affixed to a threaded plug which was immersed in a pot containing molten Wood's metal attached to the moveable cross-head. After cooling of the Wood's metal, the test was started, and the strains were recorded to the instant of failure. Three of the 2- by 4-in. cylinders were tested on their sides as an indirect tension test and three cylinders were tested in compression.

REINFORCEMENT CORROSION STUDY

The purpose of this study was to provide information concerning bridge deck deterioration attributed to deep-seated disruptions not in evidence during the laboratory freeze-thaw testing and to determine the effects of external loading on this type of deterioration. The investigation was divided into two series:

1. Series D.—A study of the effects of crack widths and depth of cover on corrosion of reinforcement.
2. Series E.—A study of the pressures that must be developed during corrosion of reinforcement to produce spalling of concrete.

Description of Specimens

The D Series laboratory corrosion study was divided into sub-series D-1, D-2, and D-3. Each sub-series consisted of eight 4- by 8- by 22-in. specimens reinforced with two 20-in. No. 3 longitudinal bars and four 6-in. No. 4 transverse bars. The transverse bars were helically wrapped with 12-in. strips of copper foil ¼ in. wide. The copper, which is higher in the electromotive series than iron, was used to accelerate the rate of corrosion of the reinforcement. Each transverse bar was weighed and labeled prior to being wired

TABLE 7

LENGTH CHANGE STUDY MIX DATA

Sub-series	Cement-Sand Ratio by Weight	Water-cement Ratio, gal/sk	Pressure Air, %	28 Day Compressive Strength, psi
C-1	1:2	5.5	3.7	8300
	1:3	6.4	4.1	6670
	1:4	8.1	4.2	4780
C-2	1:2	5.2	8.0	7140
	1:3	5.9	12.0	6130
	1:4	7.5	15.0	3900
C-5	1:1	4.6	10.7	4710*

*Specimens were moist cured for 7 days and air dried for 21 days.

TABLE 8

REINFORCEMENT CORROSION STUDY MIX DATA

Sub-series	Maximum Size Agg. in.	Water-Cement Ratio gal/sk	Mix by Weight	Cement Factor sk/ cu yd	Slump in.	Pressure Air %	Compressive Strength lb/in.^{2}
D-1	1.5	5.2	1·2.0 3.5	6.0	2.75	4.7	4270
D-2	1	6.6	1.2 4·3 4	6 0	2.75	3.0	4270
D-3	1	6 6	1 2.4·3.4	6 0	2.5	3.0	5310
E-1	1	6 6	1 2.4:3.4	6.0	2.25	3.7	5310
E-2	1	6.6	1 2.4.3.4	6.0	2 5	3.8	5240
E-3	1	6 6	1 2 4:3.4	6.0	4 5	3.5	5150
E-4	1.5	5.2	1 2.0.3.5	6.0	2.75	4.7	4270
E-5	1	6.6	1·2 4 3.4	6.0	2.75	3.0	5280
E-6	1	6.6	1 2 4·3.4	6.0	2.5	3 0	5310
E-100	1 5	5 2	1·2.0·3 5	6.0	4.0	7+	3450

to the longitudinal bars. The sub-series were divided into specimens having average measured crack widths of either 0 in., 0.006 in., or 0.012 in. The cracks were formed by stretched strips of teflon-coated fiberglass cloth 0.002, 0.004, or 0.006 in. thick extending from the tops of the transverse bars to above the surface of the concrete. By supporting the ends of the longitudinal bars at different heights, the transverse reinforcement was provided with depths of concrete cover ranging from ¼ in. to 2 in., as specified in Table 10.

The E Series pressure study was divided into sub-series E-1, E-2, E-3, E-4, E-5, E-6, and E-100. Sub-series E-1 through E-6 consisted of 6- by 12- by either 18- or 36-in. specimens; sub-series E-100 consisted of one 12- by 12- by 36-in concrete specimen. Instead of conventional transverse reinforcement, ⅜-in. galvanized iron pipe was cast into the concrete at design depths of cover ranging from ½ in. to 4¼ in., as given in Table 9. One end of each pipe was capped and a ⅛-in. slit was milled into the pipe for a length of 8½ in. This slit was covered with a thin rubber membrane to prevent entrance of concrete into the pipe during casting. The pipes were supported by wire chairs at the prescribed height with the slit on the top. The threaded open ends of the pipes extended 3 in. beyond the edges of the specimens. Sub-series E-1 and E-2 included pipe spacings of 6 and 12 in.; however, all subsequent sub-series included only 6-in. pipe spacings. The specimens containing longitudinal reinforcement are so designated in Table 9. This reinforcement was situated approximately 1 in. below the bottom of the pipes.

Materials

Table 8 is a summary of mix data for Series D and E. Class X bridge deck concrete was used in casting sub-series D-1, E-4, and D-7. The materials used in this mix are described in "Simulated Bridge Deck Study." All other sub-series were cast using the materials described previously in "Stressed Surface Study." The coarse aggregate employed was the class B crushed limestone.

Fabrication of Specimens

Sub-series D-1, E-4, and E-100 were cast using the procedure described in "Simulated Bridge Deck Study" for the Series X slabs. Sub-series E-4 and D-1 were cast from the same ready-mixed concrete batch used for the X-12 slabs, and E-100 was cast from the sub-series X-14 concrete.

The remainder of the sub-series were cast from concrete mixed in the laboratory. The mixing and casting procedures were the same as those described in "Stressed Surface Study" for Series A, with the exception that internal vibrators were used. Sub-series E-1, E-2, and E-3 required two batches of concrete each. Sub-series E-5 and D-2 were cast together from four batches of the laboratory mix. Sub-series E-6 and D-3 were cast together using three laboratory batches.

The concrete was allowed to air dry for approximately 4 hr and was cured under wet burlap for 20 hr. At the end of this period the specimens were removed from their plywood forms and cured for 6 days in a moisture room. They were then air dried in the laboratory for 21 days.

Testing Procedures

At the time of removal from the moisture room, the D Series specimens were loaded in flexure the minimum amount needed for removal of the fiberglass strips from the cracks. On the final day of air drying an optical micrometer was used to measure the resulting crack widths. The averages of these measurements are given in Table 10.

The slabs were placed on their sides in shallow tanks containing 3 in. of 4 percent sodium chloride solution. Heat lamps were placed approximately 1 ft above the tops of the slabs. These lamps remained on for the entire exposure period, maintaining the temperature of the water at approximately 89 F. Additional quantities of salt solution were added periodically to the tanks to maintain the desired 3-in depth. Toward the end of the exposure period, tap water was added to reduce excessive salt build-up at the water level of the specimens.

After 4 months of exposure the specimens were removed from the tanks and the final crack widths were measured

TABLE 9

PRESSURE STUDY RESULTS

Sub-series	Spec No	Pipe No	Pipe Spacing (in)	Design Depth (in)	Actual Depth (in)	Pressure at Failure (lb/in ^{2})	With Lat Reinf	Pre-cracked Vertically
E-1	1	A	12	2	1-7/8	2100		
		B	12	2	1-7/8	1600		
		C	12	2	2	2150		
	2	A	12	3/4	3/4	800		X
		B	12	3/4	3/4	1000		X
		C	12	3/4	3/4	1100		X
	3	A	6	2	1-15/16			
		B	6	2	1-15/16	2200		
		C	6	2	1-15/16	1500		
	4	A	6	3/4	3/4	900		X
		B	6	3/4	11/16	700		X
		C	6	3/4	11/16	800		X
E-2	1	A	6	1-1/4	1-1/4	1000		
		B	6	1-1/4	1-5/16	1300		X
		C	6	1-1/4	1-3/8			
	2	A	12	1-1/4	1-3/16	700		X
		B	12	1-1/4	1-3/16	1100		X
		C	12	1-1/4				
	3	A	6	1	7/8	850		X
		B	6	1	13/16	850		X
		C	6	1	13/16	1000		X
	4	A	12	1	1	1100		X
		B	12	1	7/8	600		X
		C	12	1	7/8	1000		X
E-3	1	A	6	1-3/4	1-11/16	1900		
		B	6	1-3/4	1-11/16			
		C	6	1-3/4	1-5/8	1250		
		D	6	1-3/4	1-11/16	1400		
		E	6	1-3/4	1-11/16	1150		
		F	6	1-3/4	1-3/4	1100		
	2	A	6	1-1/2	1-7/16	850		
		B	6	1-1/2	1-7/16	900		
		C	6	1-1/2	1-7/16	1050		
		D	6	1-1/2	1-1/2	1350		
		E	6	1-1/2	1-7/16	1200		
		F	6	1-1/2	1-1/2	1300		
	3	A	6	1-1/4	1-1/4	1000		
		B	6	1-1/4	1-3/16	1100		
		C	6	1-1/4	1-1/4	1000		
	4	A	6	1-1/4	1	1000		
		B	6	1-1/4	1-1/8	850		
		C	6	1-1/4	1-3/16	1150		
E-4	1	A	6	1-1/4	1-3/16	1100	X	
		B	6	1-1/4	1-1/8	1200	X	
		C	6	1-1/4	1-3/16	1100	X	
	2	A	6	1-1/4	1-1/8		X	
		B	6	1-1/4	1-1/16	1100	X	
		C	6	1-1/4	1-1/8	1050	X	
	3	A	6	2	1-7/8	1750	X	
		B	6	2	1-15/16	2000	X	
		C	6	2	1-15/16	2050	X	
		D	6	2	1-15/16	1800	X	
		E	6	2	1-15/16	2800	X	
		F	6	2	1-7/8	2050	X	
	4	A	6	1-3/4	1-11/16	1800	X	
		B	6	1-3/4	1-5/8		X	
		C	6	1-3/4	1-5/8	1400	X	
		D	6	1-3/4	1-9/16	1350	X	
		E	6	1-3/4	1-9/16	1600	X	
		F	6	1-3/4	1-5/8	1800	X	
	5	A	6	1-1/2	1-1/2	1400	X	
		B	6	1-1/2	1-1/2	1550	X	
E-4	5	C	6	1-1/2	1-1/2	1350	X	
		D	6	1-1/2	1-7/16	1350	X	
		E	6	1-1/2	1-1/2	1500	X	
		F	6	1-1/2	1-1/2	1550	X	
	6	A	6	1	1-1/16	675	X	
		B	6	1	1	1125	X	
		C	6	1	1-1/16	1000	X	
		D	6	1	1	1050	X	
		E	6	1	1	1175	X	
		F	6	1	15/16	1050	X	
E-5	1	A	6	1-1/2	1-5/16	1800	X	
		B	6	1-1/2	1-7/16	1600	X	
		C	6	1-1/2	1-1/2	1800	X	
	2	A	6	1-1/2	1-1/2	1850	X	
		B	6	1-1/2	1-9/16	1800	X	
		C	6	1-1/2	1-1/2	1800	X	
	3	A	6	1-1/4	1-3/8	1350	X	
		B	6	1-1/4	1-1/4	1300	X	
		C	6	1-1/4	1-1/8	1250	X	
		D	6	1-1/4	1-1/4	1400	X	
		E	6	1-1/4	1-5/16	1225	X	
		F	6	1-1/4	1-5/16	1400	X	
	4	A	6	2	1-15/16	2250	X	
		B	6	2	1-7/8	2000	X	
		C	6	2	1-7/8	2200	X	
		D	6	2	1-15/16	2100	X	
		E	6	2	1-15/16	2400	X	
		F	6	2	2-1/16	2575	X	
	5	A	6	1-3/4	1-7/8	2350	X	
		B	6	1-3/4	1-7/8	1950	X	
		C	6	1-3/4	1-7/8	2150	X	
		D	6	1-3/4	1-15/16	2200	X	
		E	6	1-3/4	1-15/16	1950	X	
		F	6	1-3/4	1-7/8	2250	X	
	6	A	6	1	1	1100	X	X
		B	6	1	1	1100	X	X
		C	6	1	1-1/16	1175	X	X
		D	6	1	1-1/16	1100	X	X
		E	6	1	1-1/8	1225	X	X
		F	6	1	1-3/16	1350	X	X
E-6	1	A	6	3/4	7/8	1000	X	X
		B	6	3/4	7/8	1000	X	X
		C	6	3/4	7/8	910	X	X
		D	6	3/4	13/16	1050	X	X
		E	6	3/4	7/8	410	X	X
		F	6	3/4	7/8	975	X	X
	2	A	6	1/2	9/16	610		X
		B	6	1/2	3/4	610		X
		C	6	1/2	1/2	375		X
		D	6	1/2	9/16	375		X
		E	6	1/2	5/8	490		X
		F	6	1/2	1/2	610		
	3	A	6	1/2	5/8	675	X	
		B	6	1/2	5/8	610	X	
		C	6	1/2	9/16	850	X	
		D	6	1/2	5/8	675	X	
		E	6	1/2	5/8	675	X	
		F	6	1/2	5/8	725	X	X
E-100	1	A	6	4-1/4	4-3/8	2700	X	
		B	6	4-1/4	4-3/8	1800	X	
		C	6	4-1/4	4-1/4	2000	X	
		D	6	4-1/4	4-1/4	2200	X	

with an optical micrometer. The specimens were then broken up with an impact hammer, and the transverse reinforcing bars were removed, cleaned, and reweighed to determine the weight loss due to corrosion.

The testing procedure for Series E consisted of applying a hydraulic pressure to the pipes using a 10,000-psi pump. A pressure transducer was inserted into the hydraulic line to record the failure pressures. The responses from the transducer were monitored with a strip recorder. The recorded test data were later compared with a calibration curve to determine failure pressures. After failure had occurred the pumping of oil was allowed to continue to enlarge the resulting cracks. The specimens were then sliced with a concrete saw and photographs were taken of each pipe cross section as well as of the cracking patterns on the top surface.

CYCLIC WETTING AND DRYING

Actual bridge decks are subjected to a multiplicity of environmental conditions in addition to freezing and thawing. This study was conducted to determine the effects of conditions of wetting and drying on freeze-thaw durability of concrete. Investigations were conducted with cyclic wetting and drying occurring either during, before, or after freeze-thaw testing.

Cyclic Drying During Freeze-Thaw Testing

Sub-series A-2 and A-4 were used to investigate the effects of cyclic wetting and drying on concrete durability when it occurred periodically during the freeze-thaw testing. Both of these sub-series consisted of 3- by 3- by 15-in. specimens cast and moist cured using the procedures described in "Stressed Surface Study" for Series A. Mix data for the two concretes are given in Table 3.

The freeze-thaw testing consisted of subjecting specimens immersed in 4 percent sodium chloride solution to temperature cycles of 60 to −2 to 60 F at a rate of 8 F per hour. After a given number of freeze-thaw cycles (usually three) the specimens were removed from the environmental test unit and weighed in a saturated-surface-dry condition. A specific set of specimens from each study was placed into an oven at 230 F and dried to a constant weight. The remaining specimens were continuously immersed in the saline solution. The dry specimens were allowed to cool to air temperature, and were re-immersed in the solution. All specimens were then returned to the environmental test unit, and the temperature cycling was resumed.

Sub-series A-2 consisted of seven specimens for this study. Five of the specimens were the unstressed companions of the A-2 uniaxial stress study which had been previously subjected to 153 cycles of freezing and thawing without showing any signs of surface deterioration. The remaining two specimens were not included in the stressed surface study and were subsequently referred to as "virgin" specimens. Two of the stress study specimens and one virgin specimen were subjected to the cyclic drying while the remainder of the specimens were continuously immersed.

TABLE 10

CORROSION STUDY RESULTS

Concrete Cover in	Number of Specimens	Average Initial Crack Width in	Average Crack Expansion %	Average Weight Loss g
1/4	3	0	0	1 6
	2	0 006 ± 0 001	317	1 9
	2	0 012 ± 0 003	105	1 4
1/2	3	0	0	1 3
	5	0 006 ± 0 002	81	1 8
	4	0 012 ± 0 003	245	1 8
3/4	3	0	0	0.8
	5	0 006 ± 0 002	202	2 0
	4	0 014 ± 0.002	37	1 2
1	3	0	0	0.7
	4	0 004 ± 0 001	278	2.5
	3	0.015 ± 0.002	-14	2 0
1 1/4	3	0	0	0 4
	4	0 005 ± 0.003	136	1 9
	2	0 019 ± 0 006	88	1 1
1 1/2	3	0	0	0.1
	3	0 005 ± 0.002	32	2 5
	6	0 011 ± 0 003	25	2 2
1 3/4	3	0	0	0.7
	4	0.006 ± 0 002	195	1 8
	5	0.013 ± 0 003	33	2.4
2	3	0	0	0 2
	2	0 007 ± 0 003	228	2 4
	5	0 015 ± 0 004	61	1.8
0	3		.	3 0

Sub-series A-4 consisted of five freeze-thaw specimens, of which three were subjected to the cyclic drying and two remained continuously immersed.

Cyclic Drying Before and After Freeze-Thaw Testing

Sub-series X-13 and X-14 simulated bridge deck study specimens were used to determine possible influences on concrete durability of cyclic wetting and drying both before and after freezing and thawing.

Prior to freeze-thaw testing both of the sub-series X-13 specimens were subjected to 35 wetting and drying cycles consisting of approximately 8 hr of wetting by a 4 percent sodium chloride solution followed by 16 hr of drying under heat lamps to a maximum temperature of 90 F. During this period the stressed specimen was also subjected to the prescribed cyclic loading. The wetting and drying cycling immediately preceded the regular freeze-thaw testing.

A second study consisted of the 8-ft specimens of sub-series X-13 and X-14. On completion of freeze-thaw testing these specimens were removed from the environmental test unit and located in an adjacent area of the laboratory where they were subjected to 30 cycles of wetting by 4 percent sodium chloride solution and drying under heat lamps at a maximum surface temperature of 105 F. The cycles were the same as those described in the previous paragraph. On completion of the last drying cycle, the concrete covering the reinforcing bars along the tensile cracks was removed and the bars were inspected for corrosion.

CHAPTER FOUR

RESULTS

The emphasis of this chapter is on the results of the stress study, which are presented herein; however, in the course of the research, many additional observations were made.

In the first section the physical properties of the stress study concretes are examined with respect to possible correlations with freeze-thaw deterioration. The results of an investigation of possible causes of freeze-thaw deterioration observed during laboratory testing are then discussed. Following sections contain the results of the corrosion study and a discussion of the air void distribution in the simulated bridge deck slabs. The cyclic wetting and drying results also are discussed.

CONCRETE PROPERTIES

A comparison of the results of the various physical tests listed in Tables 4 and 5 with respect to the corresponding freeze-thaw test results revealed no single property that could be consistently used as an indicator of relative durability. This can be seen in Figures 9 and 10, which are plots of paste air contents and air void spacing factors, respectively, versus the corresponding durability factors. The durability factor was obtained by dividing the final number of freeze-thaw cycles for a series by its average maximum scale rating of unstressed specimens. If this rating was zero, the divisor used was one-half.

Generally, the modified point count air contents were higher than the pressure meter values. Because, with the exception of the Series A concretes, the modified point count readings were made on surface mortar having higher paste contents than the average values for the concrete, the mortar air contents should be higher. The sub-series having lower mortar air contents generally were for concretes having relatively low pressure air contents. One notable exception to this trend was sub-series X-4. This series had a mortar air content of 2.5 percent, compared with a pressure air value of 5.6 percent, and experienced appreciable surface scaling after 14 freeze-thaw cycles. This could pass as an example of a concrete that had been subjected to either over-vibrating, over-finishing, or washing-out of air from the surface mortar; however, all Series X concretes were placed and finished in exactly the same way. Extreme care was exercised to ensure that every batch was treated the same. It should also be emphasized that of the 18 batches of concrete used in the simulated bridge deck study only one showed this significant reduction in the air content of the surface mortar when compared with pressure air values. The cause of the reduction was not apparent.

Figure 11 shows micrographs obtained using scanning electron microscopy of X Series surface mortars. The results of freeze-thaw tests disclosed that sub-series X-5 (Fig. 11b) having high air contents was not as durable, for example, as sub-series X-3 (Fig. 11a) with a lower air content. Microscopic examination of the mortar indicated a high air void accumulation at paste-aggregate interfaces of the X-5 specimen which could have a detrimental effect on durability by weakening the bond strength.

All concretes used in the simulated bridge deck study were obtained from a single ready-mixed concrete supplier who consistently used cement and aggregates from the same sources. On examining freeze-thaw test data, however, one finds that the series could be divided into two classes: those suffering little or no scaling and those experiencing significant deterioration. Examples of these two classes are shown

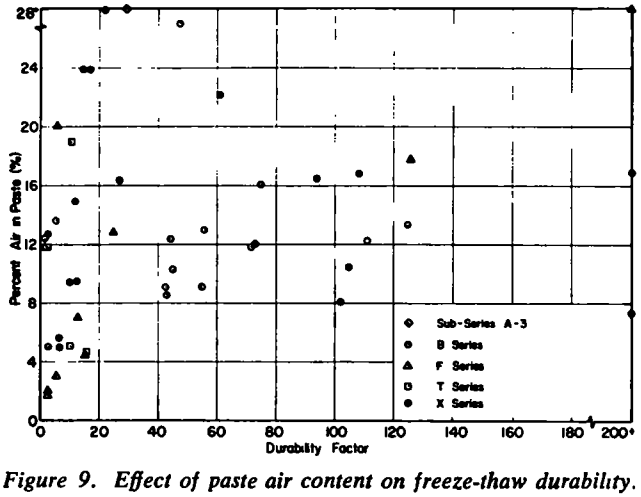

Figure 9. Effect of paste air content on freeze-thaw durability.

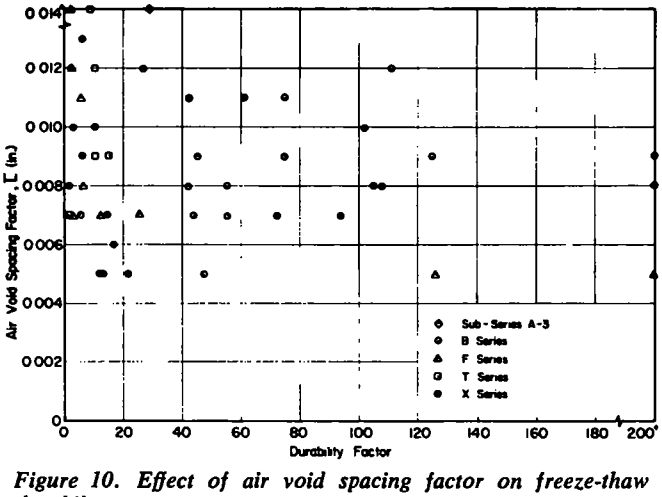

Figure 10. Effect of air void spacing factor on freeze-thaw durability

in Figures 12 and 14. Because none of the measured physical properties provided any insight into the reasons for this division, additional observations were made. Figures 20a and 20b show magnified views of sawed sections of sub-series X-8 and X-9 slabs. These pictures show a significant difference in the composition of the fine aggregates of the two slabs. The less durable X-9 specimen contained numerous brightly colored particles that cannot be seen in the X-8 concrete.

During the pressure study, all E Series specimens were sliced with a diamond saw to examine planes of failure. This procedure produced additional observations that were unrelated to the pressure test results. Figures 21a and 21b show cracks attributed to settlement of concrete away from the reinforcement. In both pictures, portions of steel chairs used to support reinforcement can be seen. Although this type of cracking was not prevalent in the majority of cases, it was not uncommon in specimens cast using the 1½-in. maximum size aggregates and having lower slumps. Figures 22a and 22b show a more common type of cracking. This was seen as a small vertical crack directly above the top reinforcement. This cracking was more prevalent in the ¾-in. maximum size aggregate mixes and those mixes having the higher slumps. It was generally not observed in specimens having more than 1½ in. of concrete cover. The pressure specimen shown in Figure 22a had not been subjected to testing. The specimen shown in Figure 22b was cast from sub-series X-14 concrete.

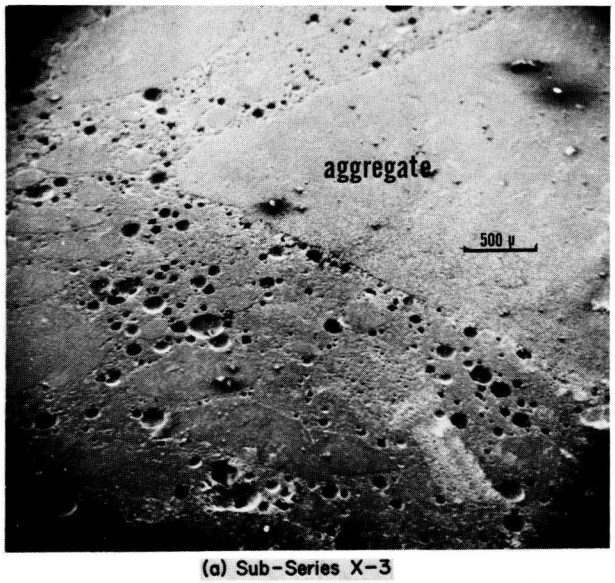

(a) Sub-Series X-3

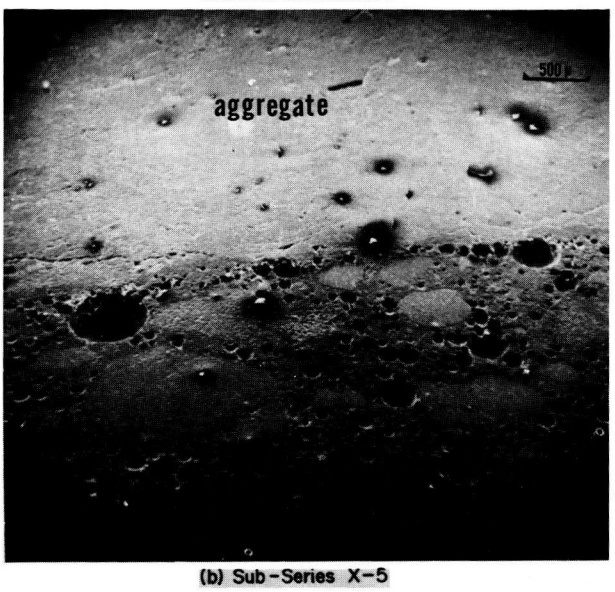

(b) Sub-Series X-5

Figure 11. Electron micrographs of X Series surface mortar specimens.

STRESS EFFECTS

The results presented in this section are divided according to the type of stress employed. The first sub-section contains a general discussion of methods used in evaluating stress effects, together with a description of the method employed in evaluating Series B, F, and T results. The second sub-section includes the results of both the stressed surface and simulated bridge deck studies. The remainder of the sub-sections consider only results of the stressed surface study.

Methods of Evaluation

Owing to the nature of freeze-thaw deterioration of concrete, it is very difficult if not impossible to produce consistent results from a set of specimens subjected to the same treatment, whether it is stress or another variable such as the amount of surface finishing under study. These inconsistencies are even more apparent when, as was the case in these studies, all of the specimens were not cast from a single batch of concrete. It was therefore necessary to test as many specimens as possible, representing each state of stress, to determine trends in the effect of stress. The number of specimens used in each sub-series is given in Table 1.

The majority of the stressed surface specimens were tested in freeze-thaw apparatus permitting only one cycle per day. Owing to the amount of time needed to produce a significant number of freeze-thaw cycles it was important for the specimens to exhibit deterioration within a reasonable period of time while still satisfying the requirement that air-entrained concrete be tested. Consequently, adjustments were continually being made in the air content of the concretes. As a result, the various series behaved differently with respect to rate and characteristics of the deterioration.

The diking procedure was not perfected until the beginning of the simulated bridge deck study; consequently, freeze-thaw testing of Series B, F, and T specimens continued until either a rating of 10 was reached or until the bond between diking and concrete deteriorated sufficiently to prevent continuous ponding of salt solution on the surface. This diking failure was apparent for the more durable concretes after relatively large numbers of freeze-thaw cycles had occurred. Therefore, the ultimate surface rating

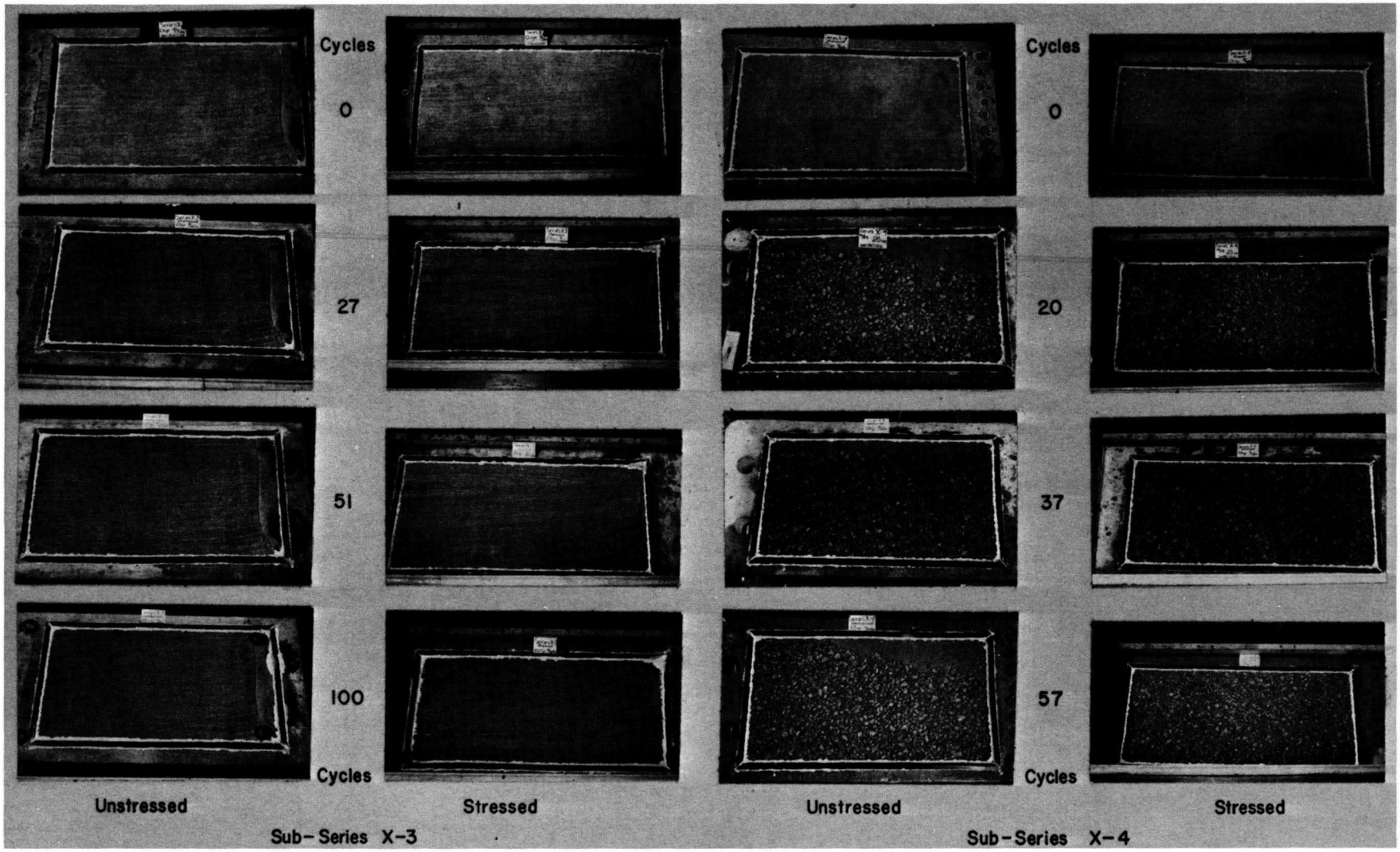

Figure 12. Freeze-thaw test results of simulated bridge deck study—static tension—low stress level.

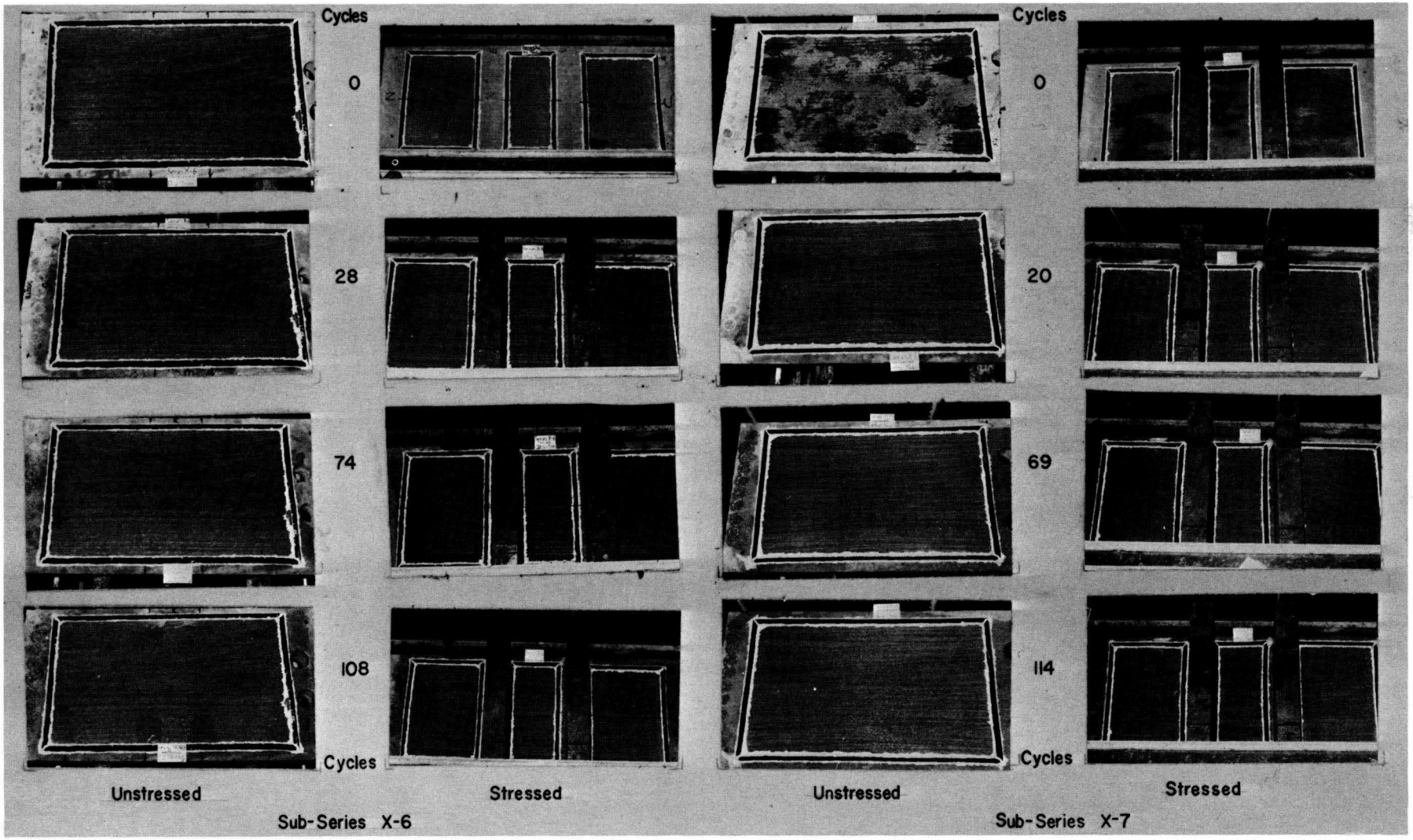

Figure 13. Freeze-thaw test results of simulated bridge deck study—static compression—low stress level.

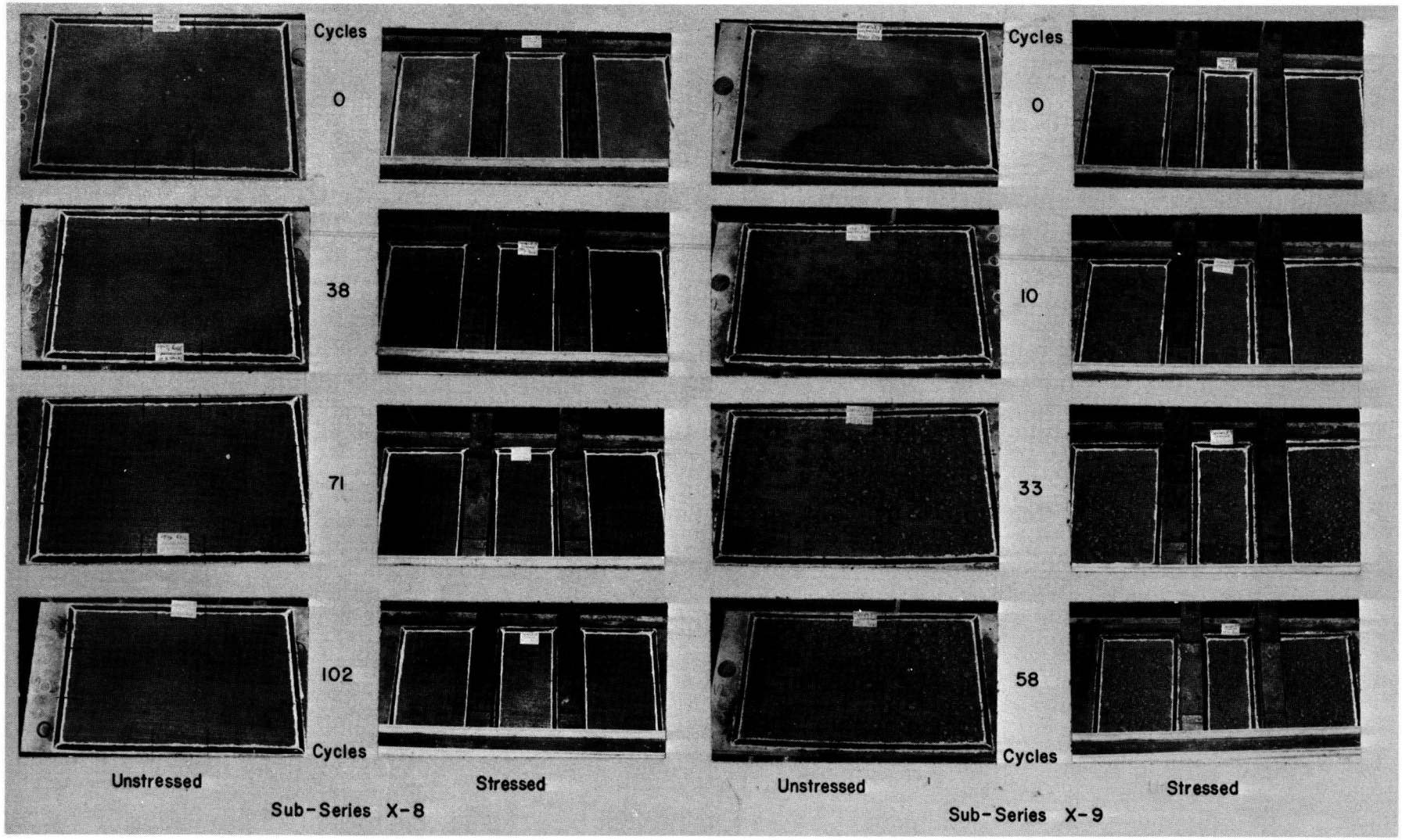

Figure 14. Freeze-thaw test results of simulated bridge deck study—static compression—high stress level.

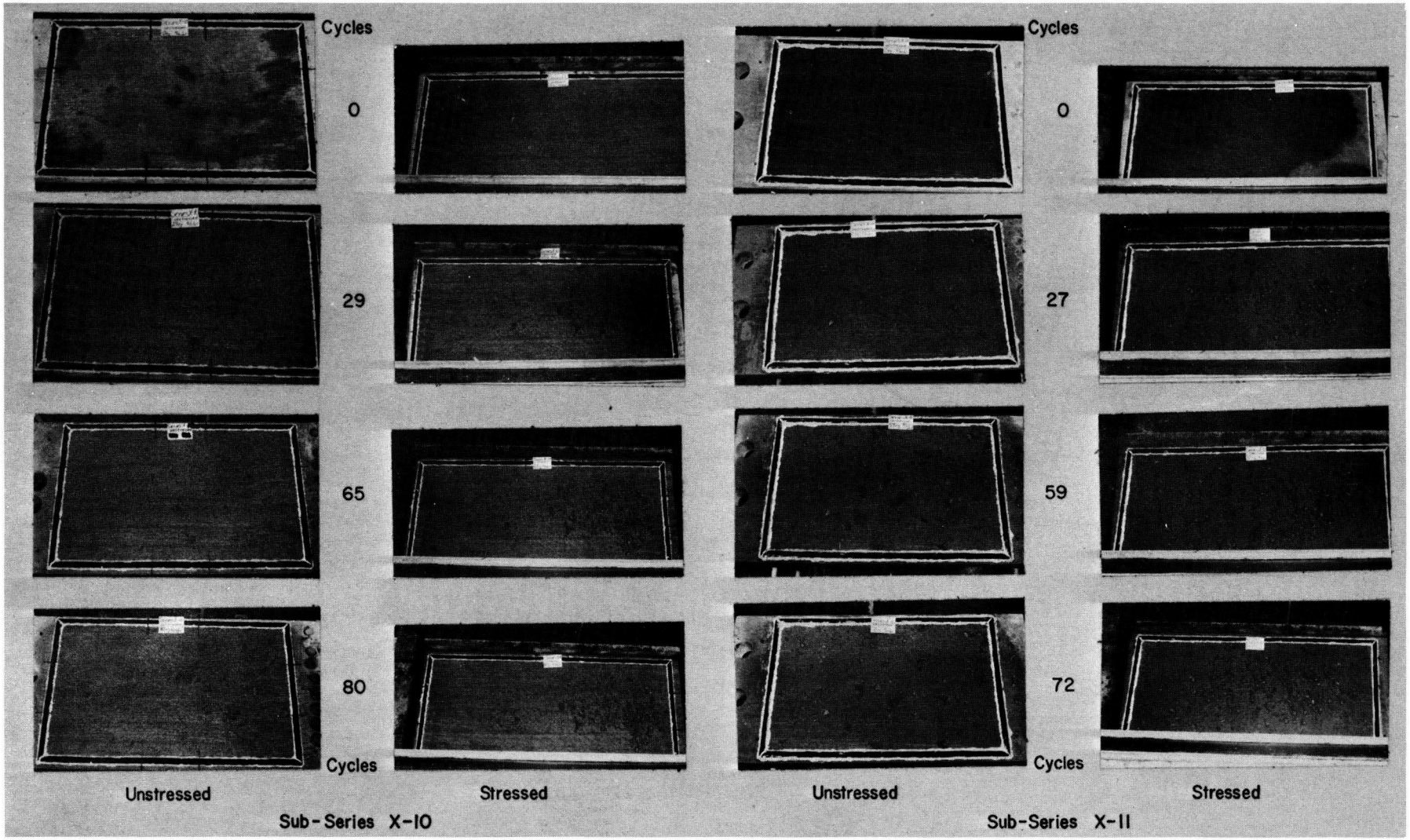

Figure 15. Freeze-thaw test results of simulated bridge deck study—static tension—high stress level.

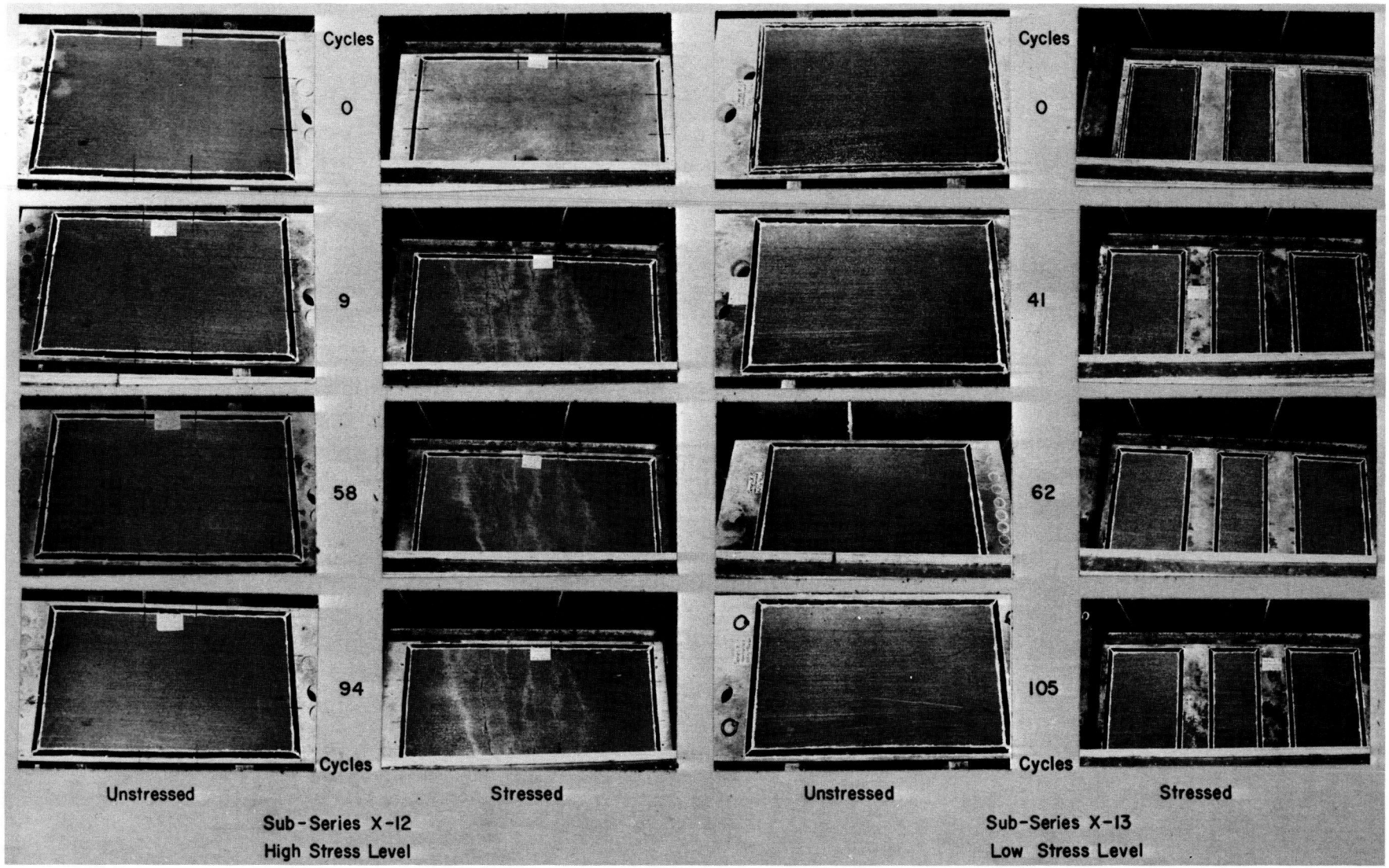

Figure 16. Freeze-thaw test results of simulated bridge deck study—cyclic tension.

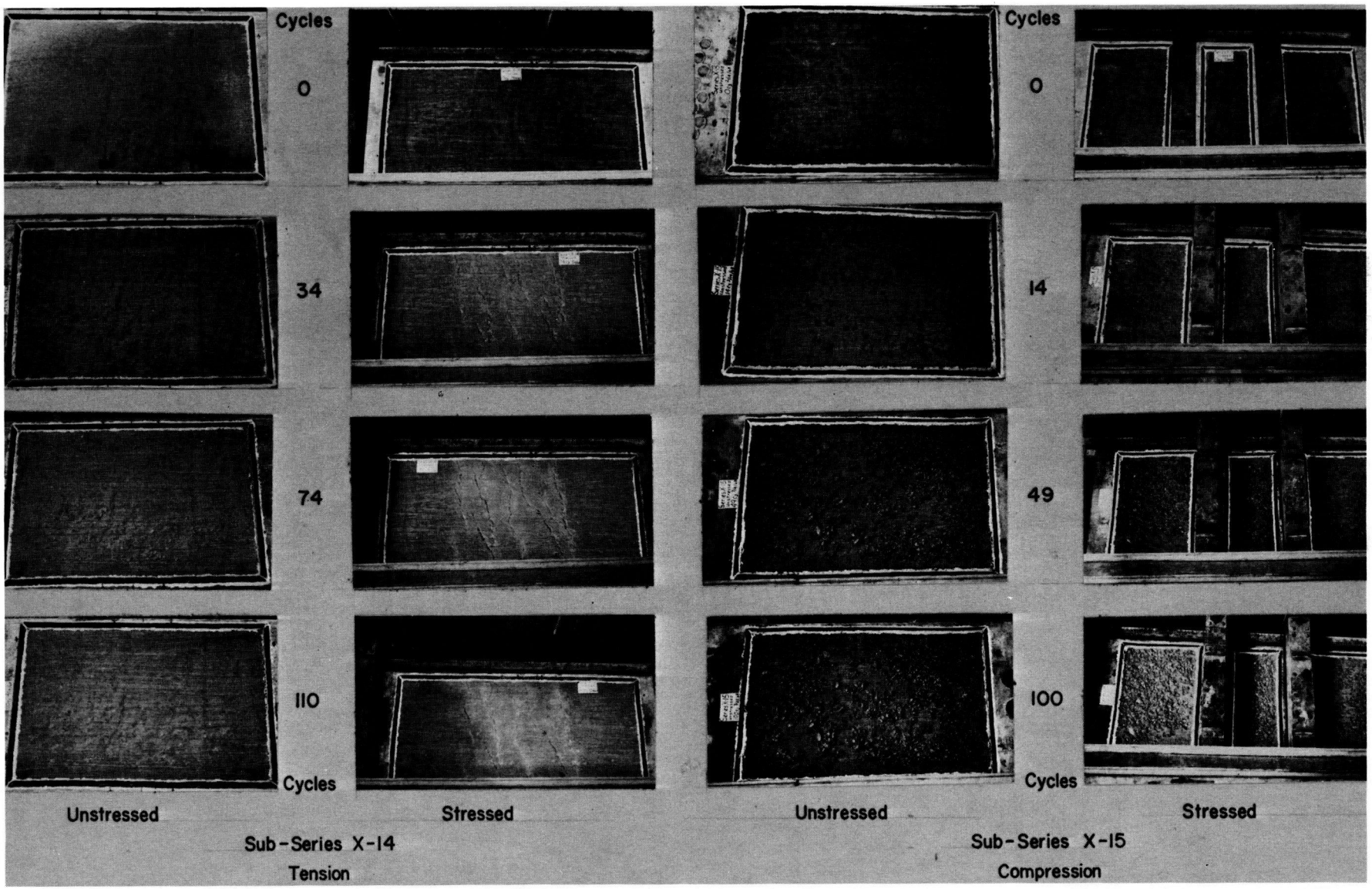

Figure 17. Freeze-thaw test results of simulated bridge deck study—high stress level—cyclic loading.

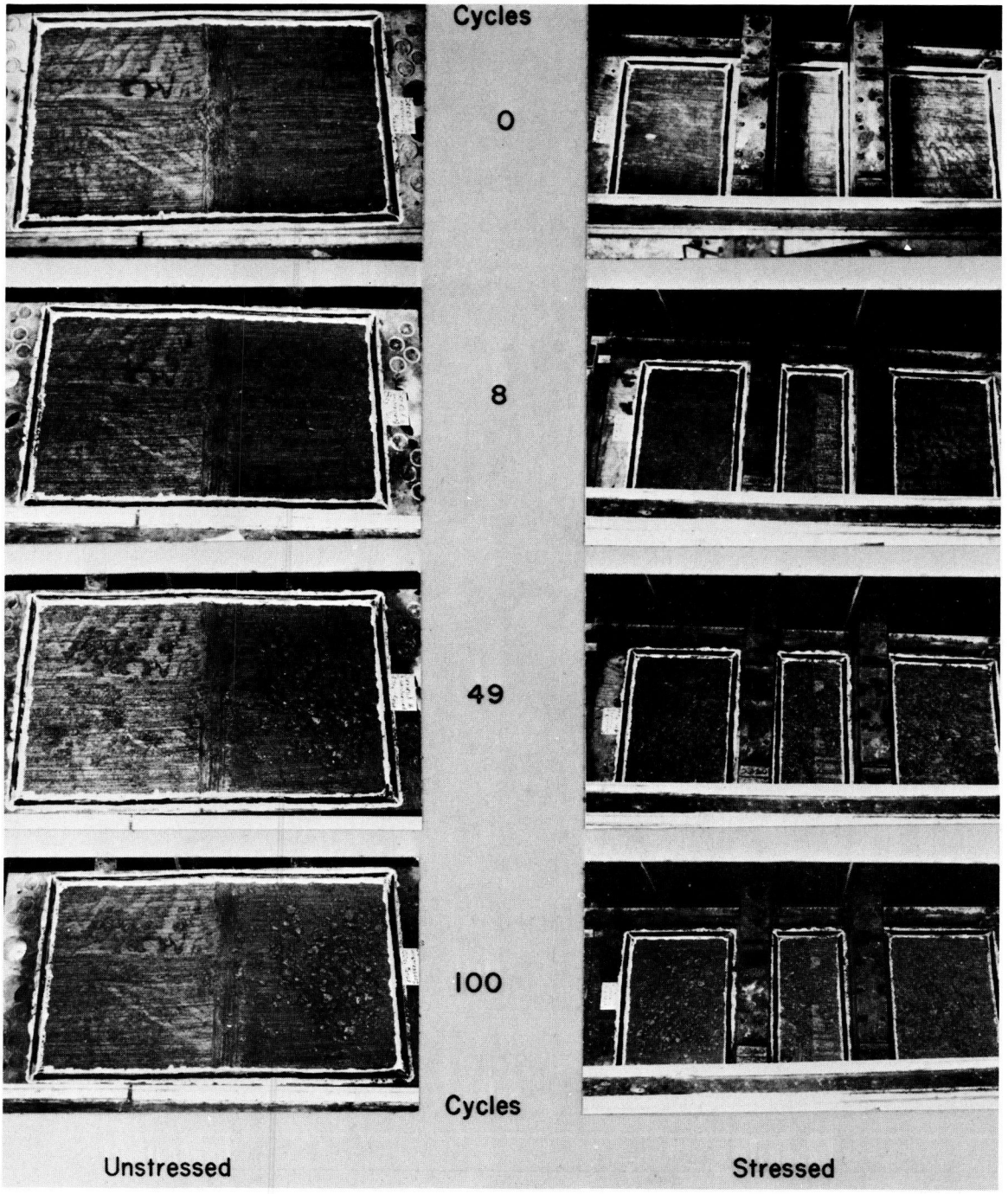

Figure 18. Freeze-thaw test results for sub-series X-16 with construction joint—high cyclic compressive stress.

attained for these series does not represent necessarily failure of the surface but rather that a significant amount of damage had occurred.

A graphic technique was used to represent the relative rate of deterioration of the stressed surface study subseries and isolate the effects of the single variable, stress, while eliminating large differences in durability. Plots were prepared of average ratings for each stress condition and the corresponding number of freeze-thaw cycles. These plots are shown as Figures 23 through 66. Series A was not included in these figures because it was evaluated using only sonic methods.

To isolate the stress effects from other variables, plots were prepared using two dimensionless ratios—(1) percent life, and (2) damage ratio.

The percent life at a given time is the ratio, in percentage, of the number of freeze-thaw cycles up to that time to the eventual number of cycles the series underwent.

The damage ratio is the numerical scale rating at the chosen time divided by the largest average specimen rating

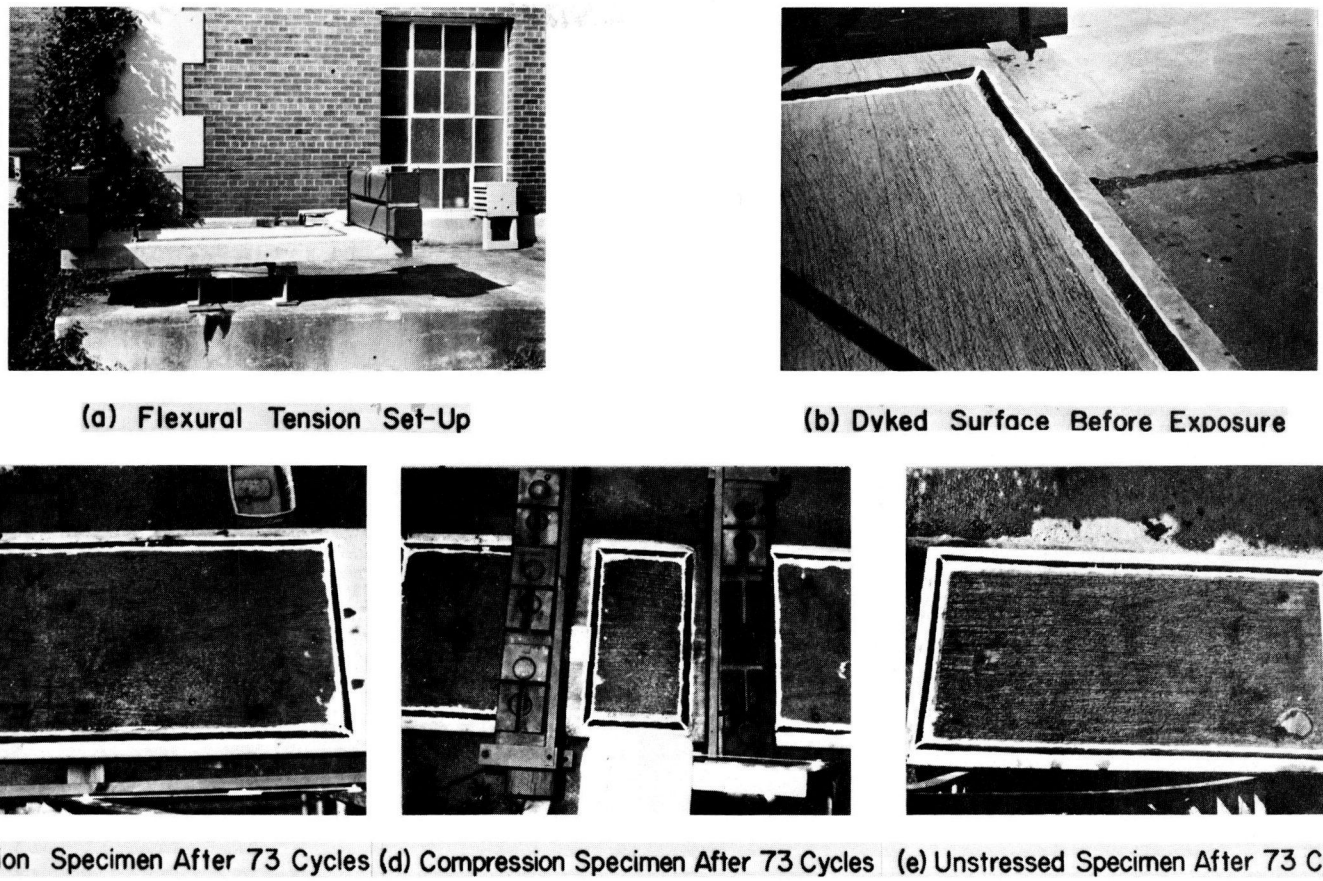

Figure 19. Field slab series.

achieved during testing, regardless of its stress state.

The damage ratio versus percent life plots for Series B, F, and T are shown in Figures 67 through 95. These curves were used to prepare summary plots for each series by dividing the percent life scale into 10 equal increments (i.e., 10, 20, 30, . . ., 100 percent). The numerical average of the damage ratios recorded at a specific percent life for each stress condition was then calculated. The plots of these average damage ratios are shown in Figures 96 through 102. These curves depict average relative rates of freeze-thaw deterioration of concrete subjected to various stress states; however, they do not show the results of each and every sub-series. The observed differences in behavior of some of the sub-series negate the possible use of statistical methods of data analysis.

Flexural Stress

Stressed Surface Study

The average curve for sub-series F-1, F-2, F-3, F-5, and F-6 (Fig. 99) indicates that specimens stressed to cracking with tensile stresses on the diked surface displayed the most rapid rate of deterioration. Next in order of rate of deterioration was tension without cracking; this was followed, in turn, by unstressed specimens and those having compressive stresses on the diked surface. All of these specimens were cast using the natural river gravel. The actual differences between the top three curves on this graph were not particularly significant; however, the compression curve was well below the rest of the curves. It should be noted that only one of the five sub-series included compression specimens; therefore, there is some doubt as to how representative this summary compression curve actually was. Sub-series F-1, F-2, and F-5 (Figs. 81, 82, 84) deteriorated fairly rapidly and the number of ratings is fewer than would be desirable.

Figure 100 consists of the average damage ratio curves for the five flexural sub-series cast using crushed limestone aggregate. Again, the same order of deterioration was observed as is shown in Figure 99. There appeared to be little difference between rates of deterioration of the bottom three curves, whereas the specimens subjected to flexural tension beyond cracking on the diked surface appeared to have deteriorated at a significantly greater rate. For this group, sub-series F-9 and F-10 (Figs. 89, 90) had less than a desirable number of ratings. The tests shown in Figure 100 included a sufficient number of flexural compression specimens. Because sub-series F-C specimens failed to deteriorate during freeze-thaw testing, they were not included in the curves.

In general, there appeared to be little difference between flexural specimens cast using the two types of aggregates in terms of the effect of stress on freeze-thaw durability. The

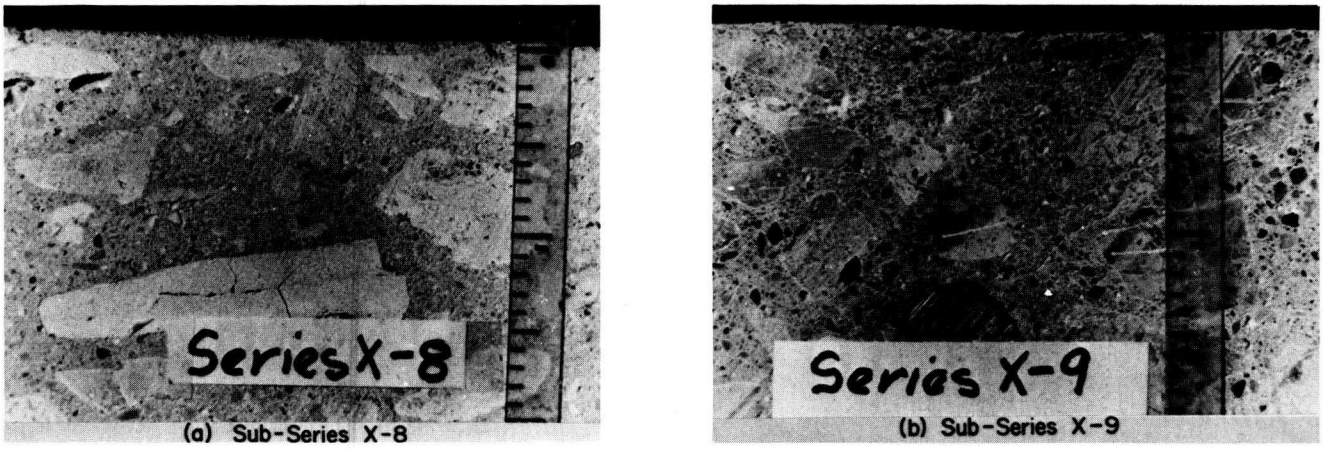

Figure 20. Close-up of X Series concrete.

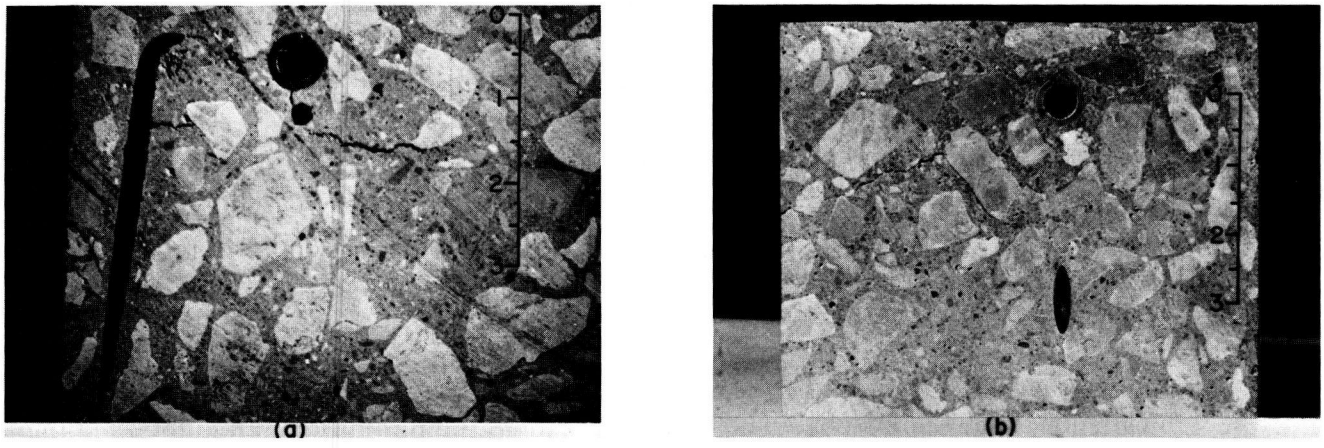

Figure 21. Cracking due to settlement of plastic concrete.

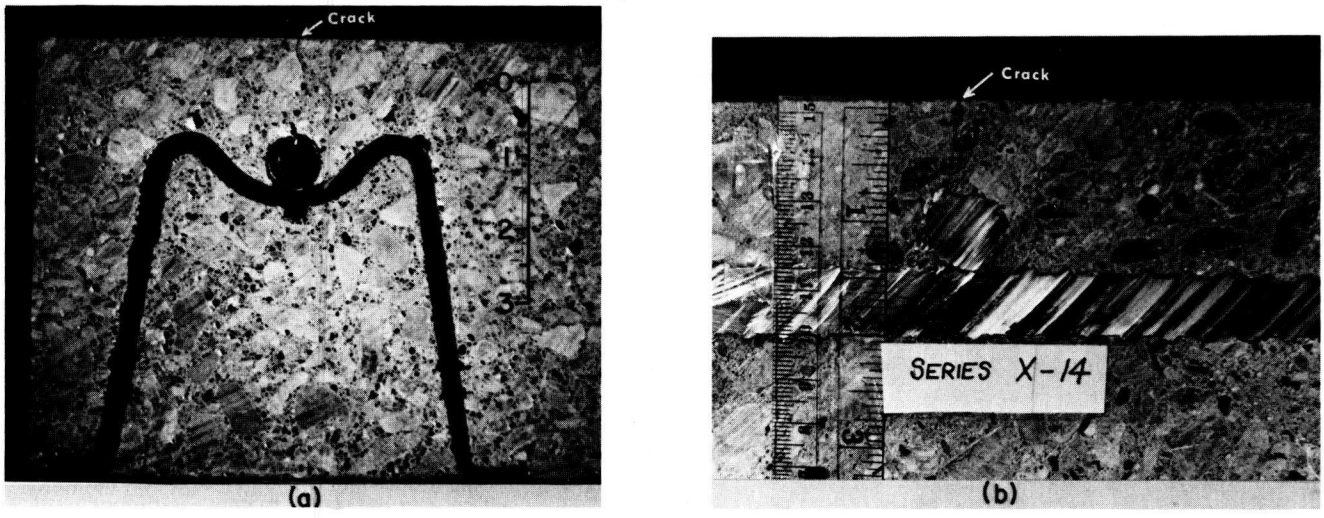

Figure 22. Vertical cracking of concrete above reinforcement.

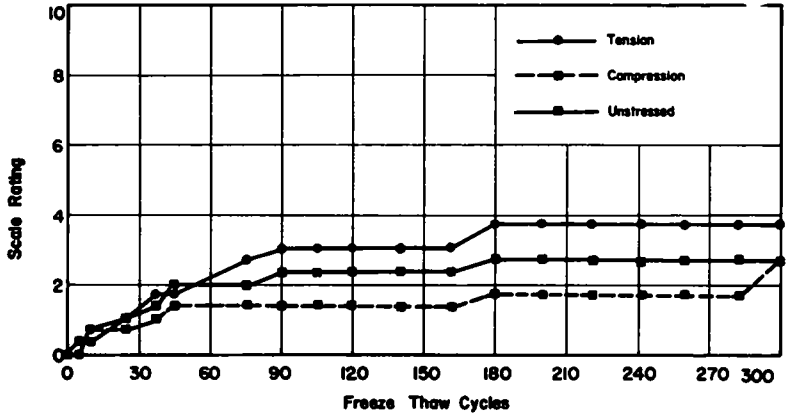

Figure 23. Ratings of scaling, sub-series B-1—uniaxial stress.

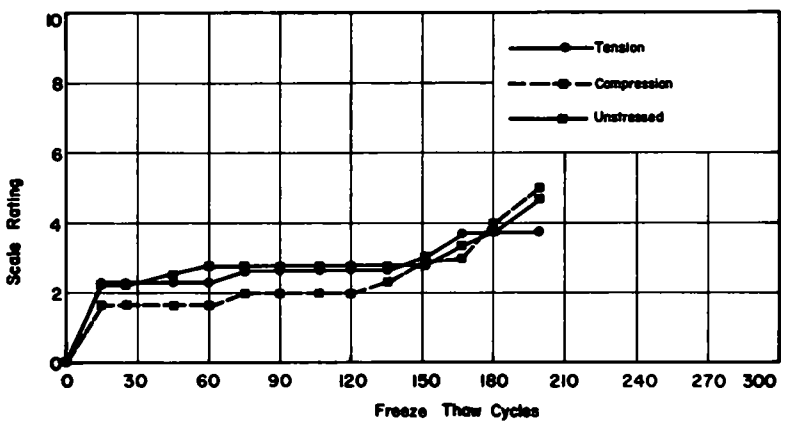

Figure 24. Ratings of scaling, sub-series B-2—uniaxial stress.

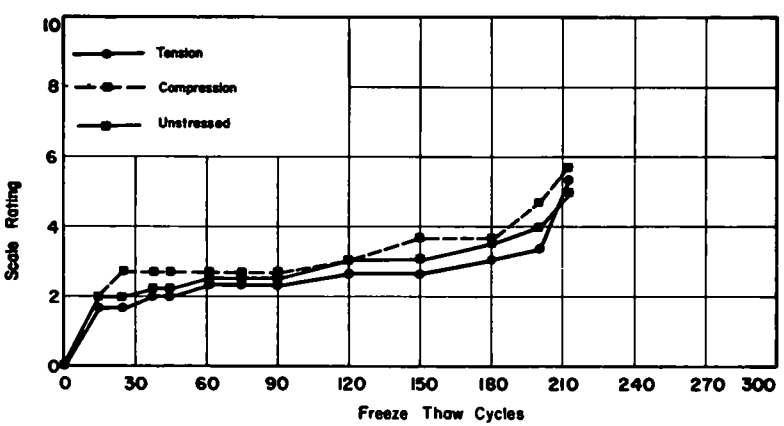

Figure 25. Ratings of scaling, sub-series B-3—uniaxial stress.

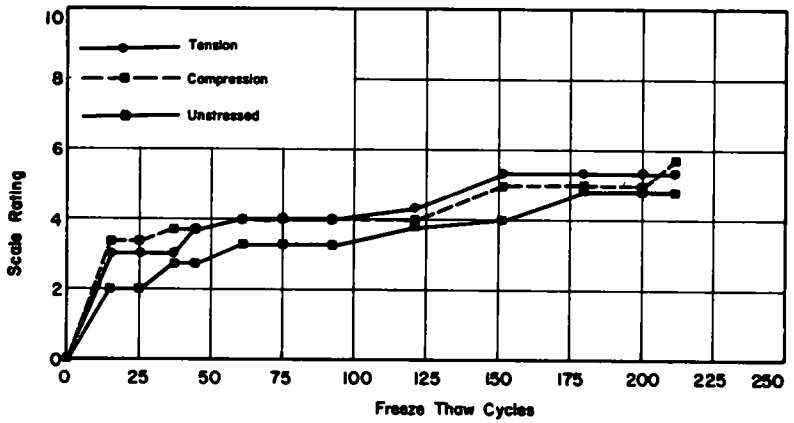

Figure 26. Ratings of scaling, sub-series B-4—uniaxial stress.

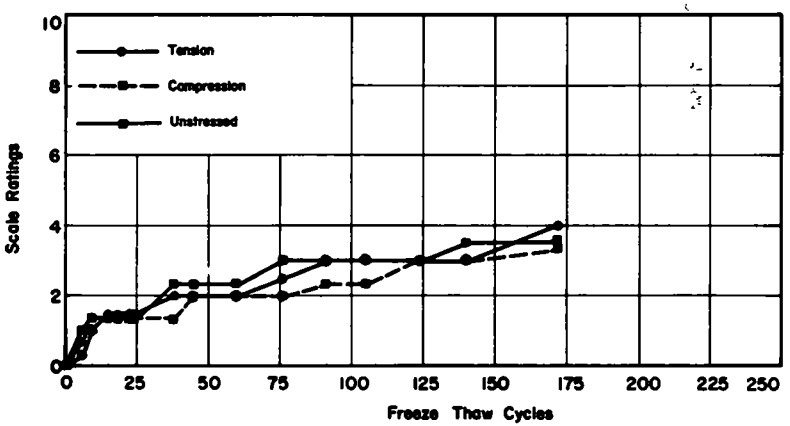

Figure 27. Ratings of scaling, sub-series B-5—uniaxial stress.

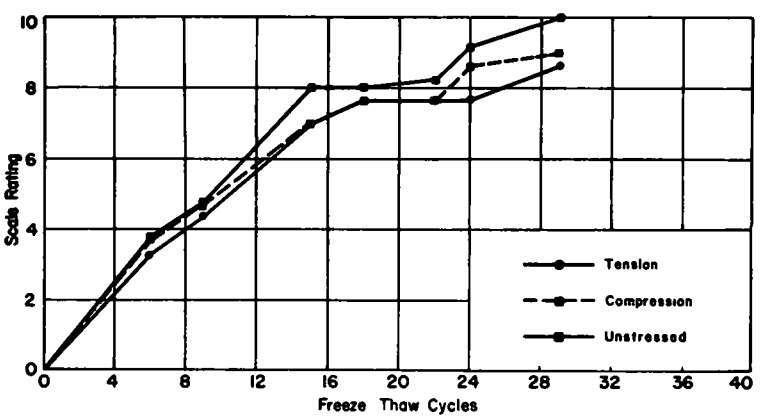

Figure 28. Ratings of scaling, sub-series B-6—uniaxial stress.

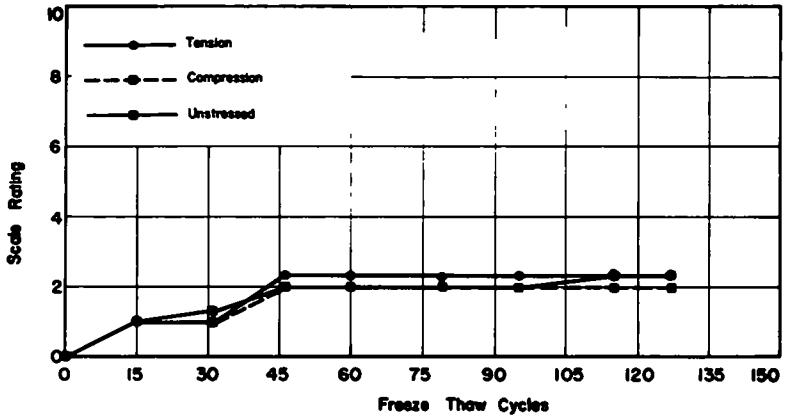

Figure 29. Ratings of scaling, sub-series B-7—uniaxial stress.

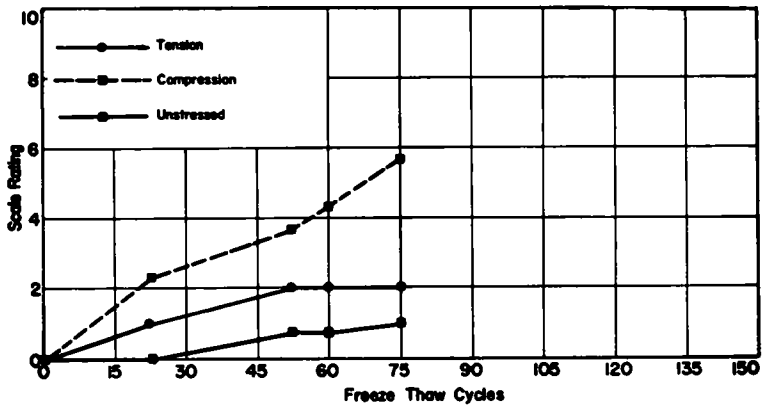

Figure 30. Ratings of scaling, sub-series B-8—uniaxial stress.

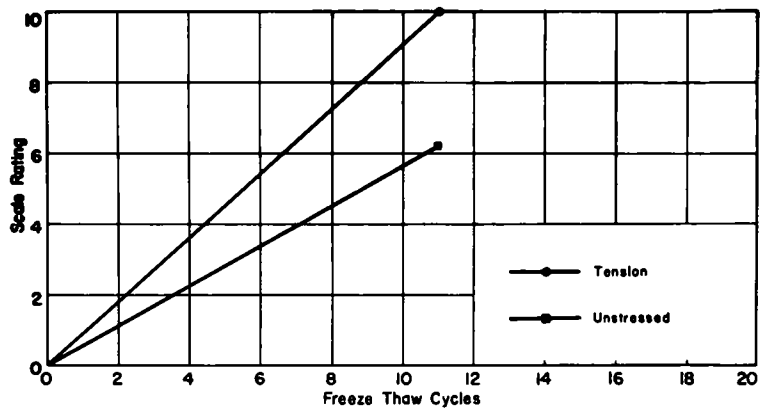

Figure 31. Ratings of scaling, sub-series B-9—uniaxial stress.

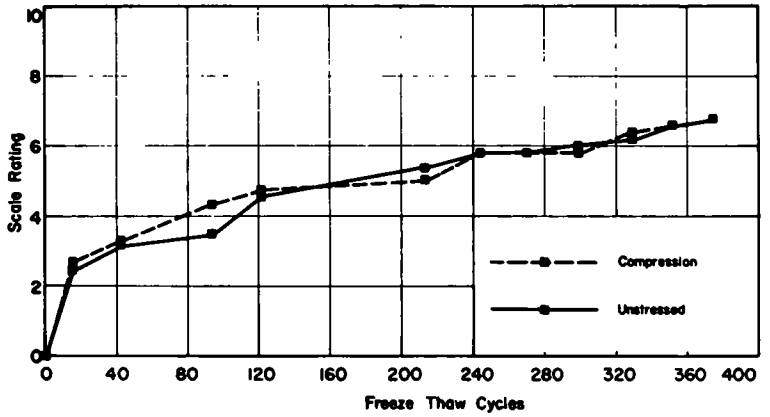

Figure 32. Ratings of scaling, sub-series B-10—uniaxial stress.

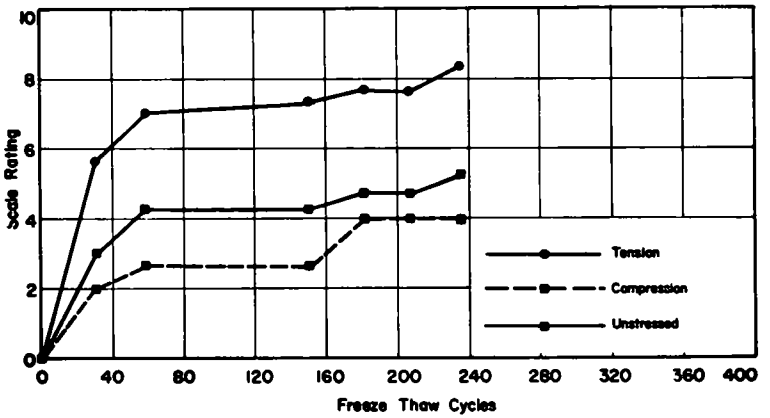

Figure 33. Ratings of scaling, sub-series B-11—uniaxial stress.

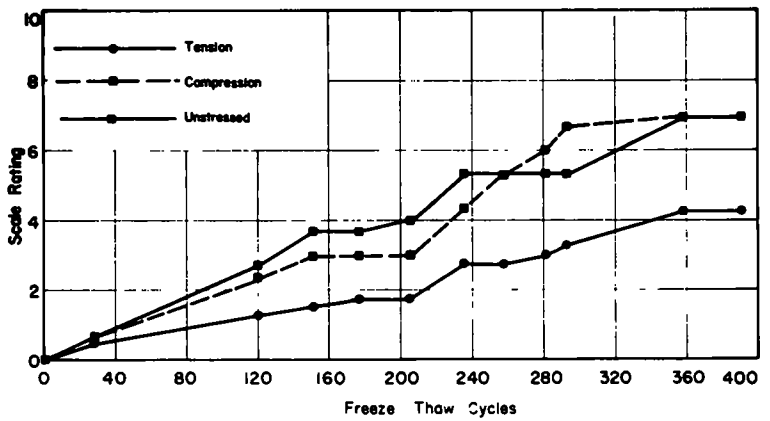

Figure 34. Ratings of scaling, sub-series B-12—uniaxial stress.

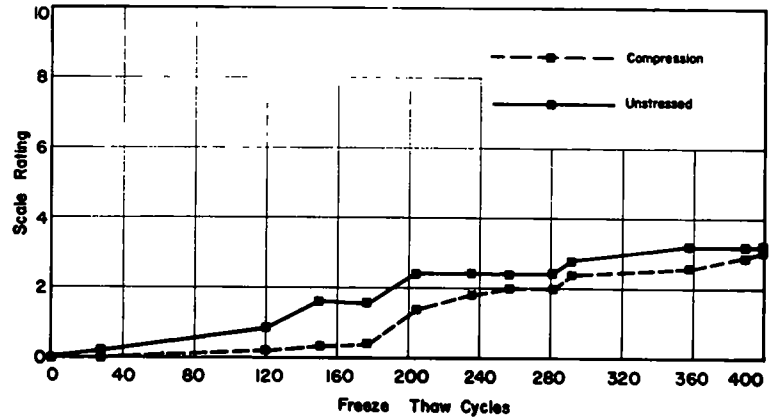

Figure 35. Ratings of scaling, sub-series B-13—uniaxial stress.

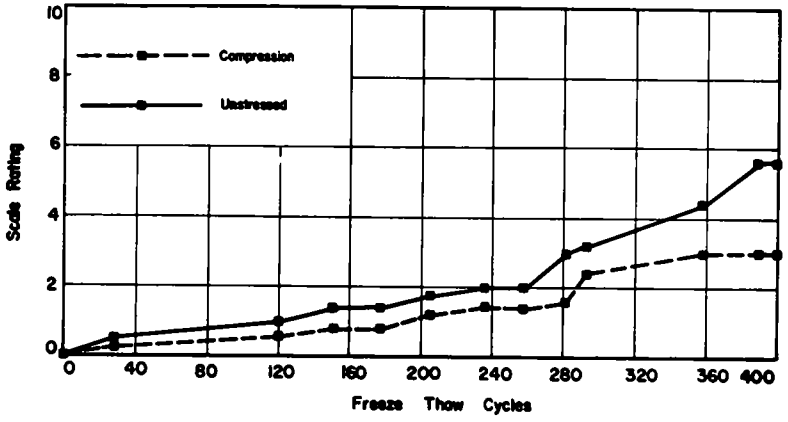

Figure 36. Ratings of scaling, sub-series B-14—uniaxial stress.

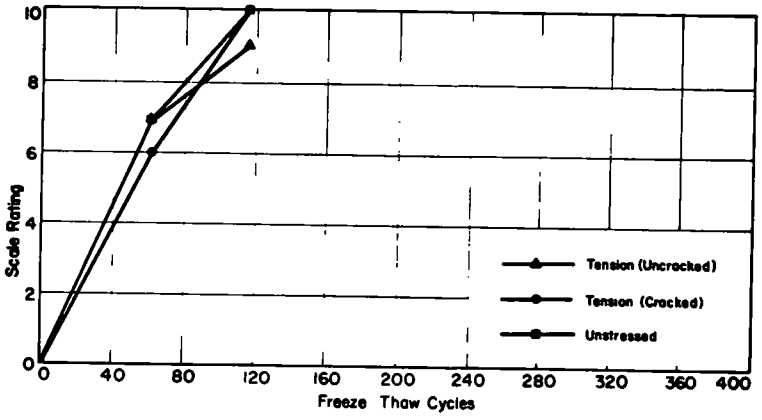

Figure 37. Ratings of scaling, sub-series F-1—flexure.

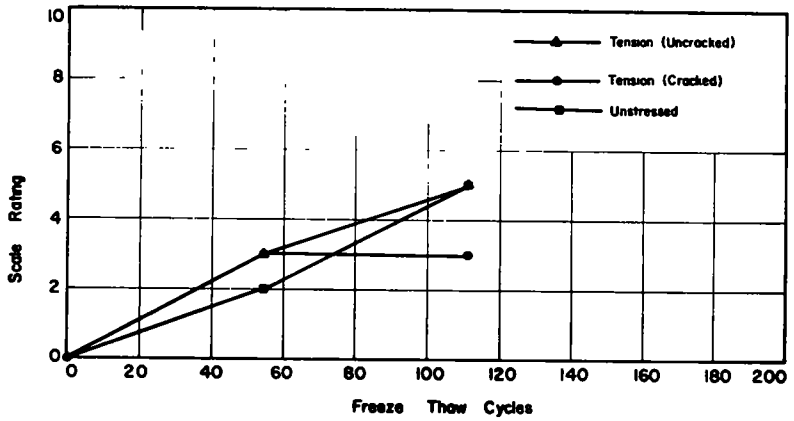

Figure 38. Ratings of scaling, sub-series F-2—flexure.

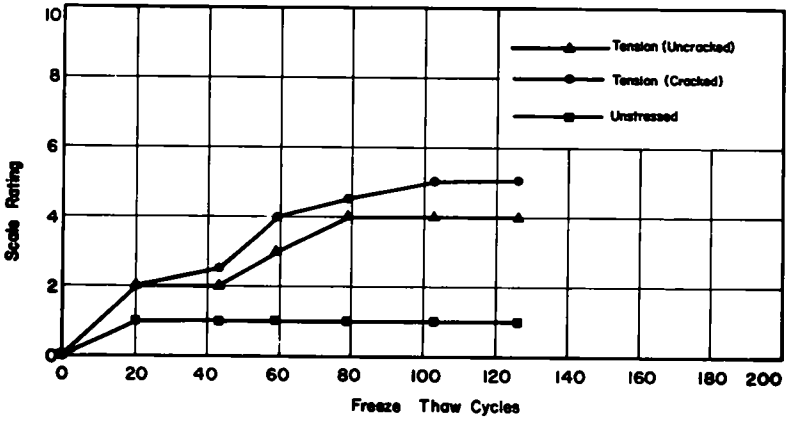

Figure 39. Ratings of scaling, sub-series F-3—flexure.

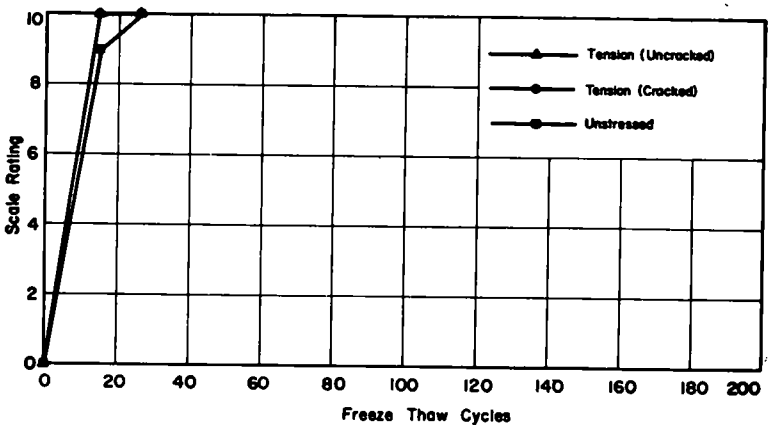

Figure 40. Ratings of scaling, sub-series F-5—flexure.

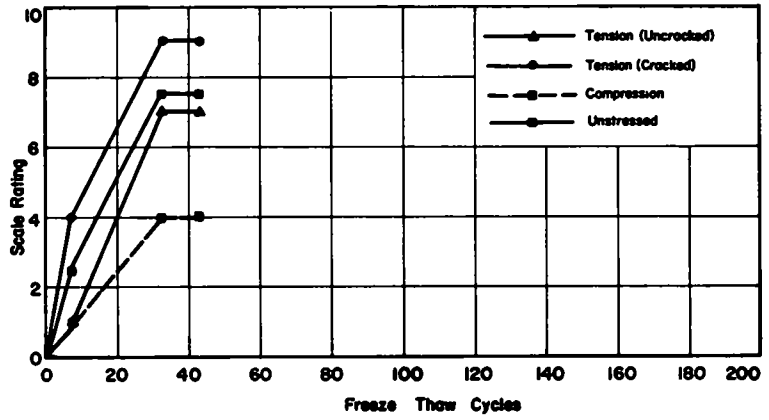

Figure 41. Ratings of scaling, sub-series F-6—flexure.

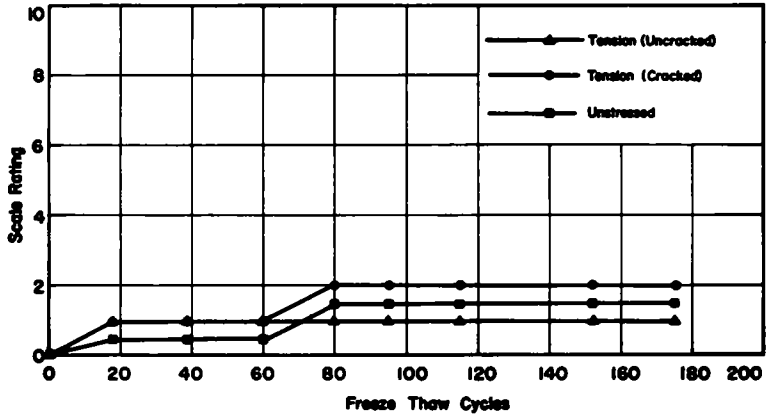

Figure 42. Ratings of scaling, sub-series F-4—flexure.

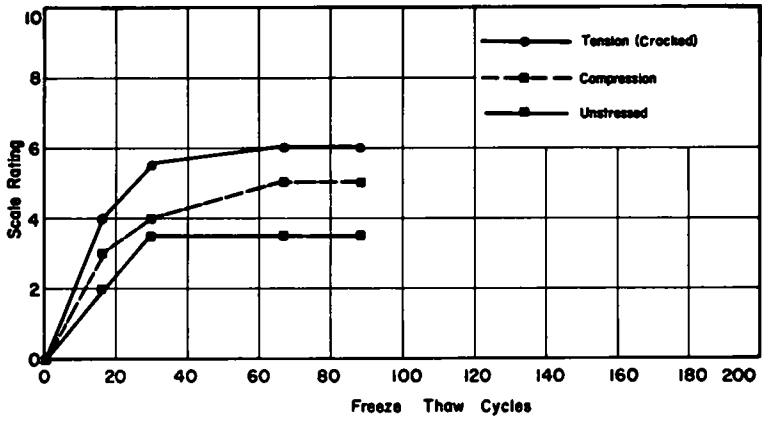

Figure 43. Ratings of scaling, sub-series F-7—flexure.

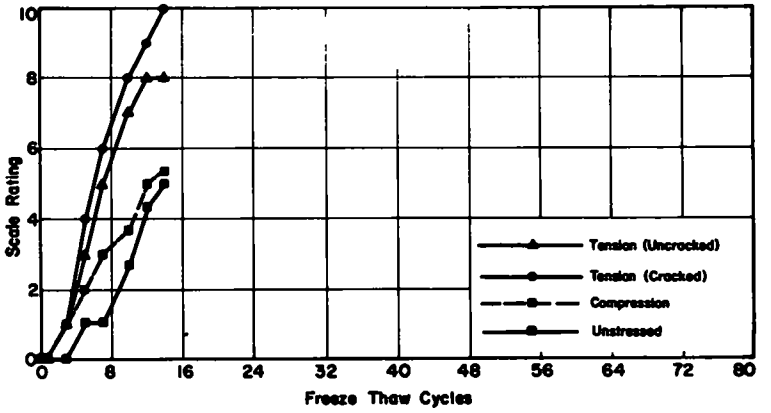

Figure 44. Ratings of scaling, sub-series F-8—flexure.

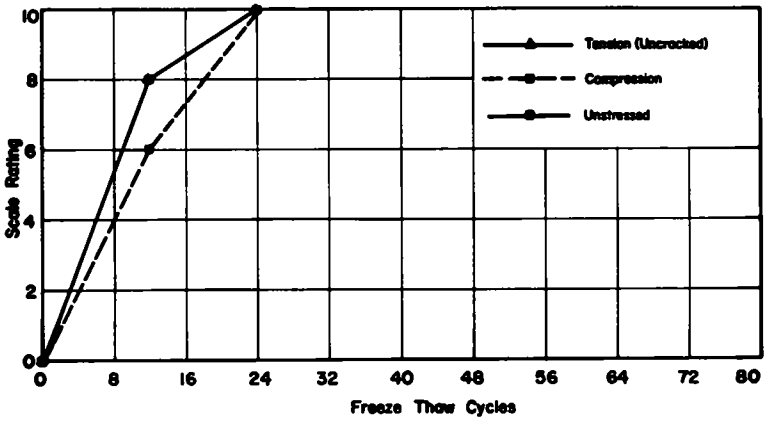

Figure 45. Ratings of scaling, sub-series F-9—flexure.

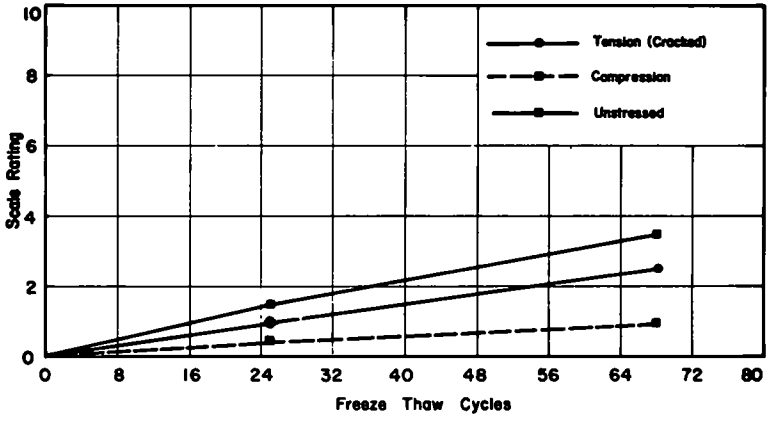

Figure 46. Ratings of scaling, sub-series F-10—flexure.

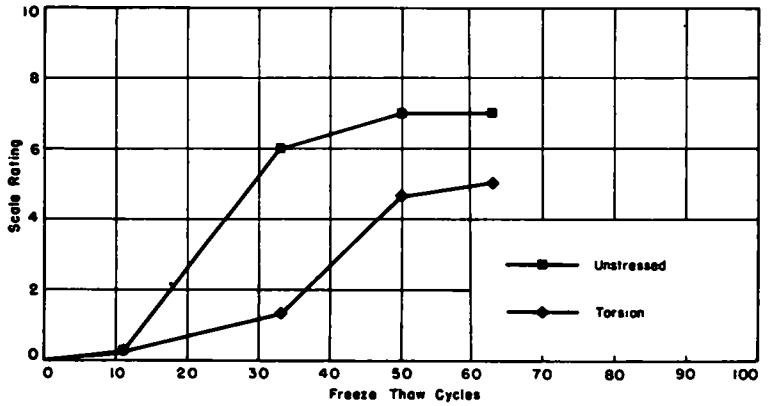

Figure 47 Ratings of scaling, sub-series T-1—torsion

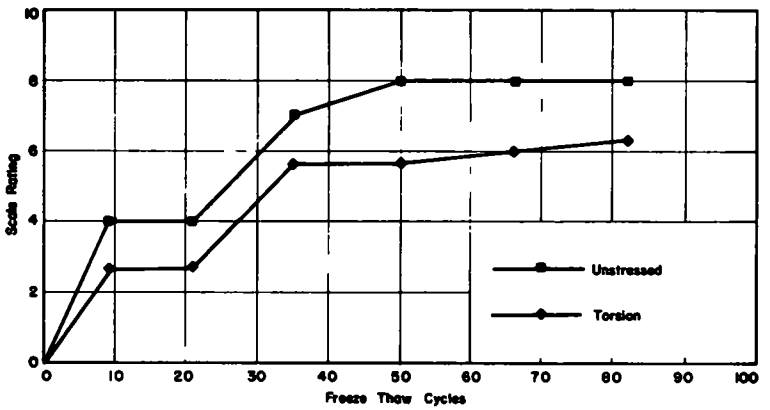

Figure 48 Ratings of scaling, sub-series T-2—torsion.

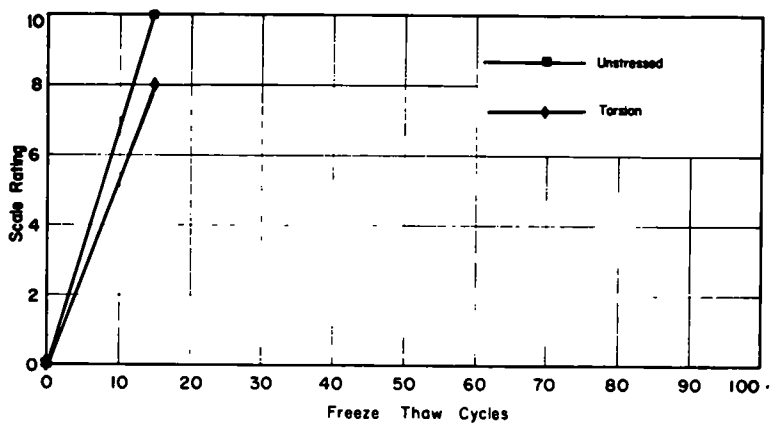

Figure 49. Ratings of scaling, sub-series T-3—torsion.

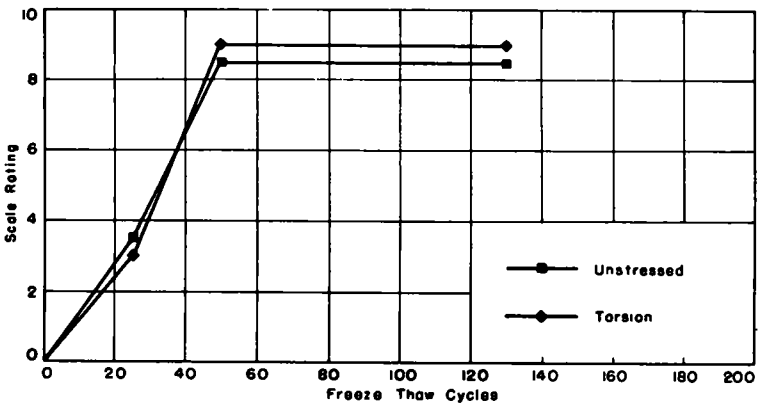

Figure 50. Ratings of scaling, sub-series T-4—torsion.

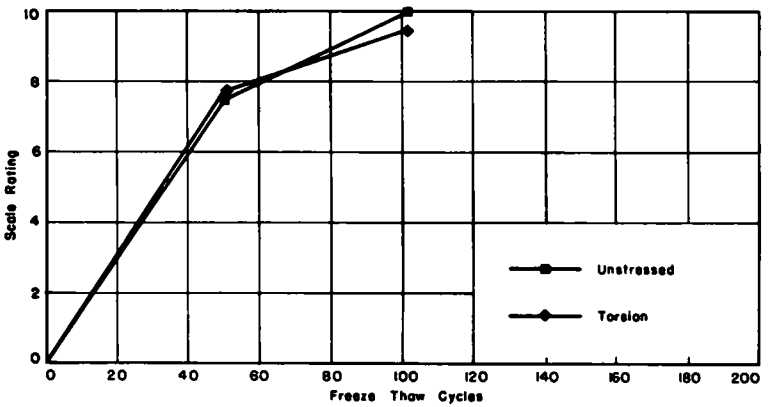

Figure 51. Ratings of scaling, sub-series T-5—torsion.

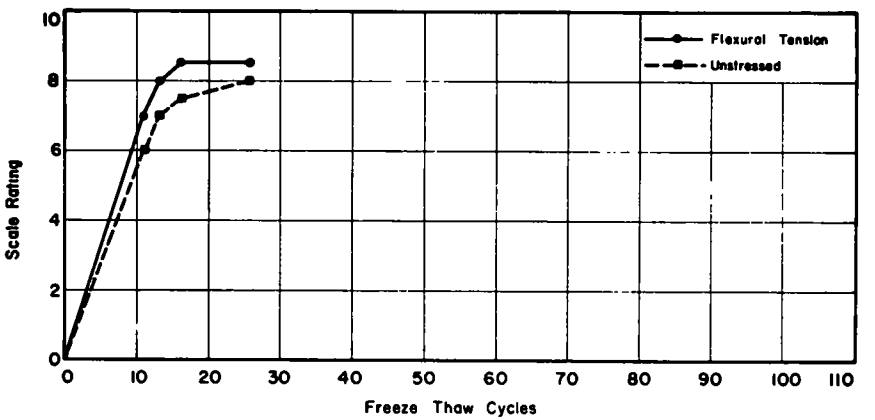

Figure 52. Scale ratings of sub-series X-2, simulated bridge deck slabs, low static stress.

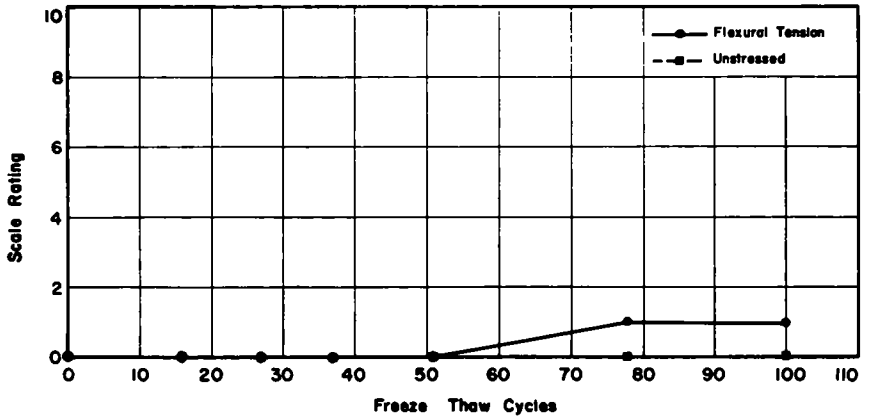

Figure 53 Scale ratings of sub-series X-3, simulated bridge deck slabs, low static stress

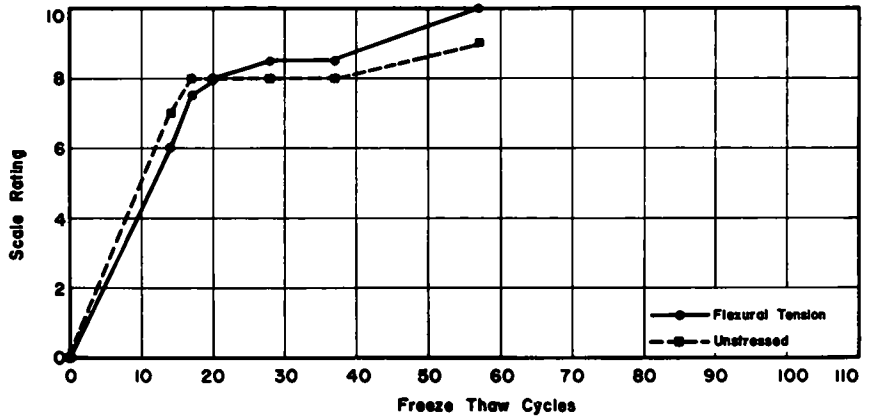

Figure 54. Scale ratings of sub-series X-4, simulated bridge deck slabs, low static stress.

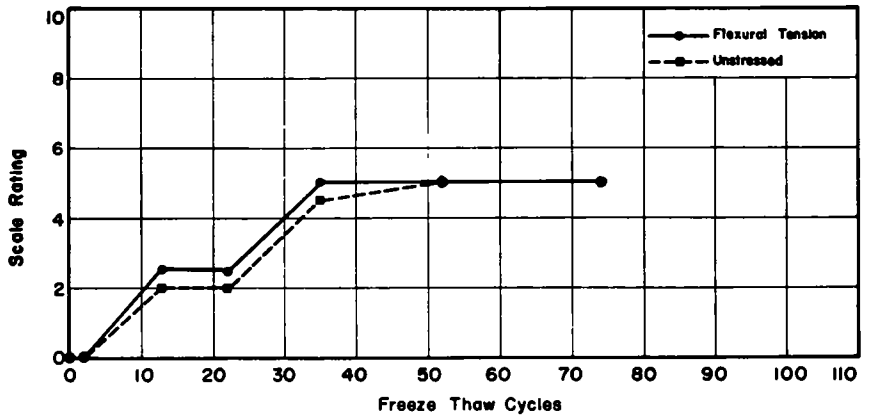

Figure 55. Scale ratings of sub-series X-5, simulated bridge deck slabs, low static stress.

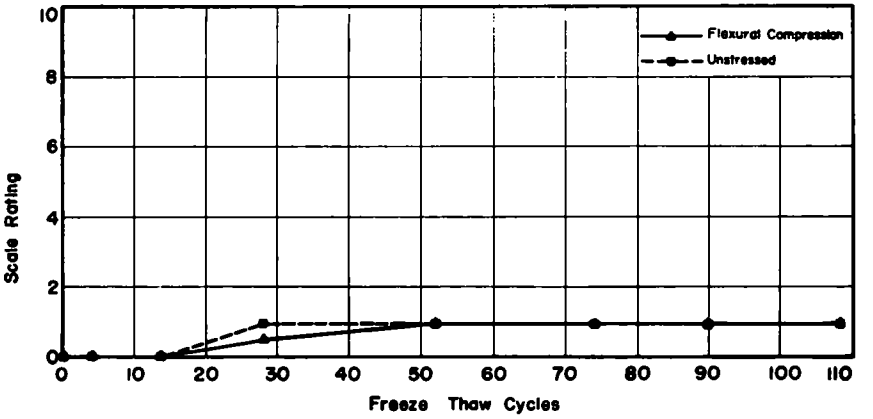

Figure 56. Scale ratings of sub-series X-6, simulated bridge deck slabs, low static stress.

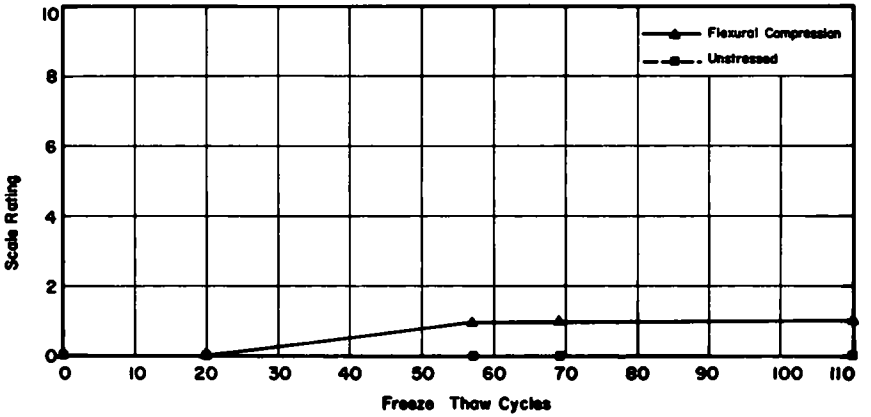

Figure 57. Scale ratings of sub-series X-7, simulated bridge deck slabs, low static stress.

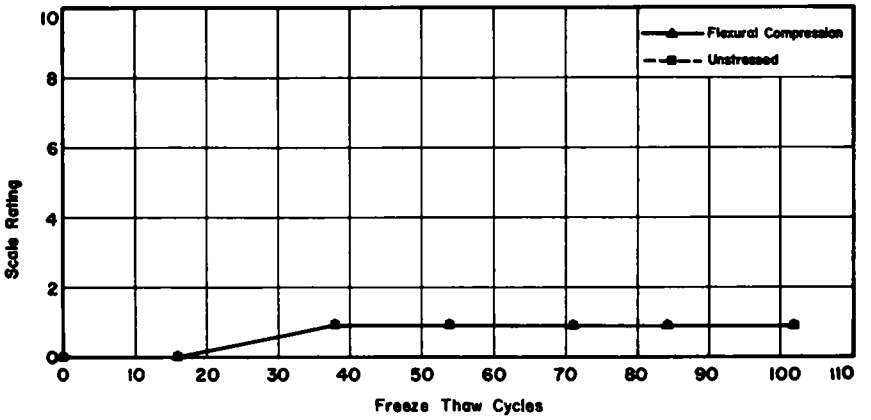

Figure 58. Scale ratings of sub-series X-8, simulated bridge deck slabs, high static stress.

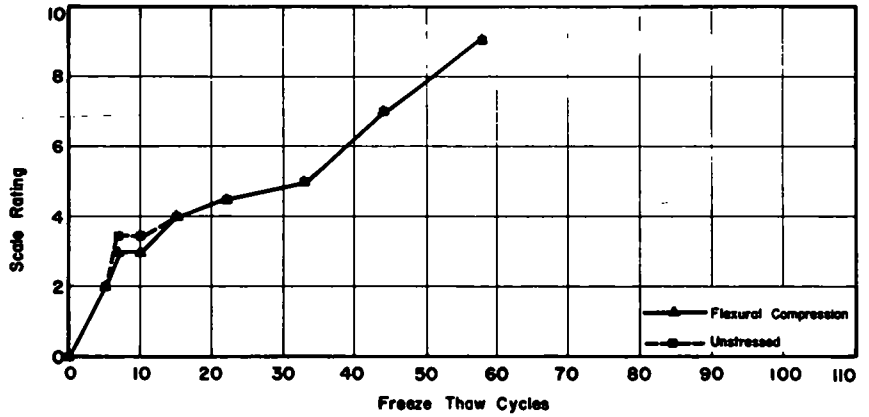

Figure 59. Scale ratings of sub-series X-9, simulated bridge deck slabs, high static stress.

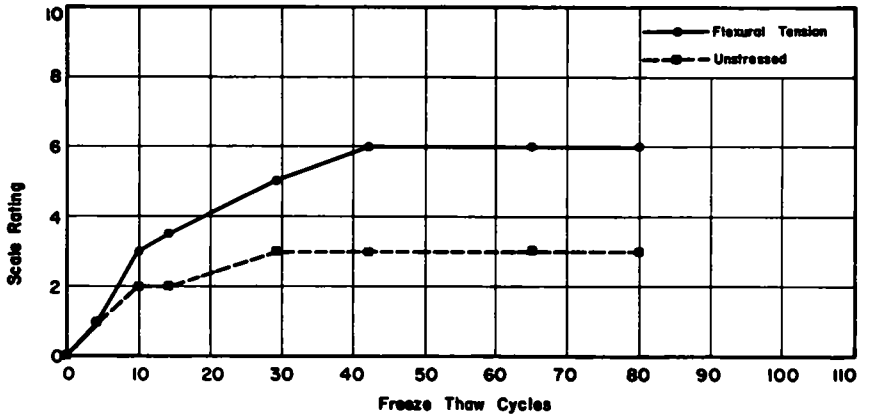

Figure 60 Scale ratings of sub-series X-10, simulated bridge deck slabs, high static stress.

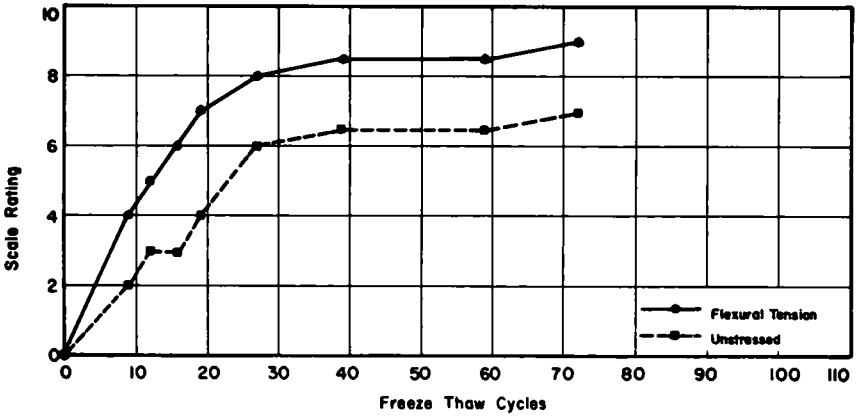

Figure 61. Scale ratings of sub-series X-11, simulated bridge deck slabs, high static stress.

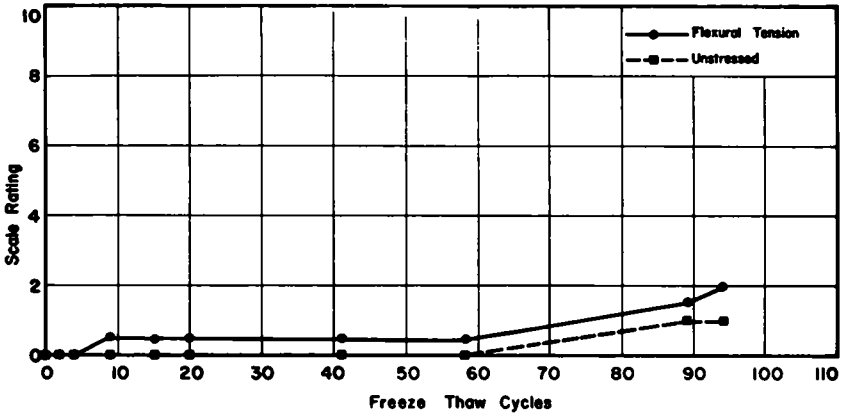

Figure 62. Scale ratings of sub-series X-12, simulated bridge deck slabs, high cyclic stress.

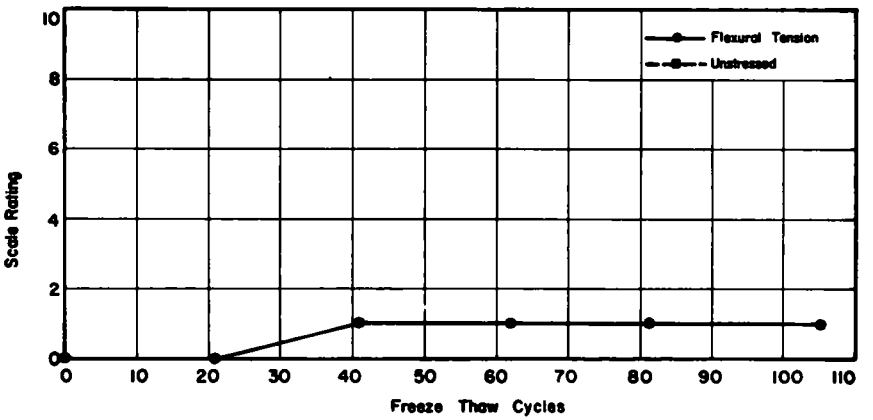

Figure 63. Scale ratings of sub-series X-13, simulated bridge deck slabs, low cyclic stress

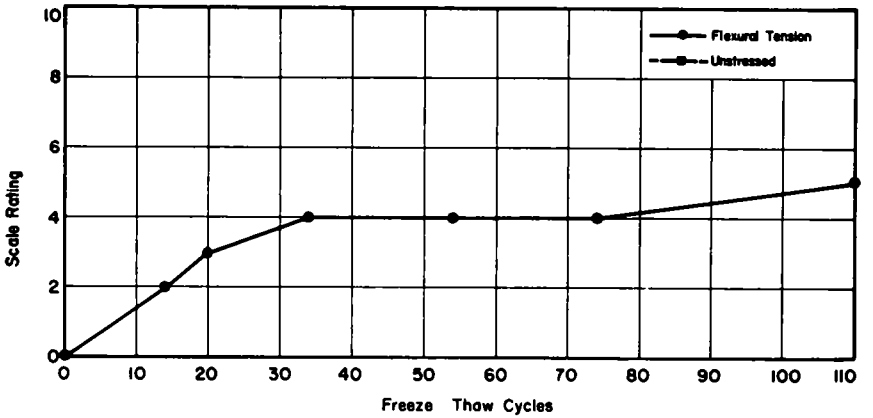

Figure 64. Scale ratings of sub-series X-14, simulated bridge deck slabs, high cyclic stress.

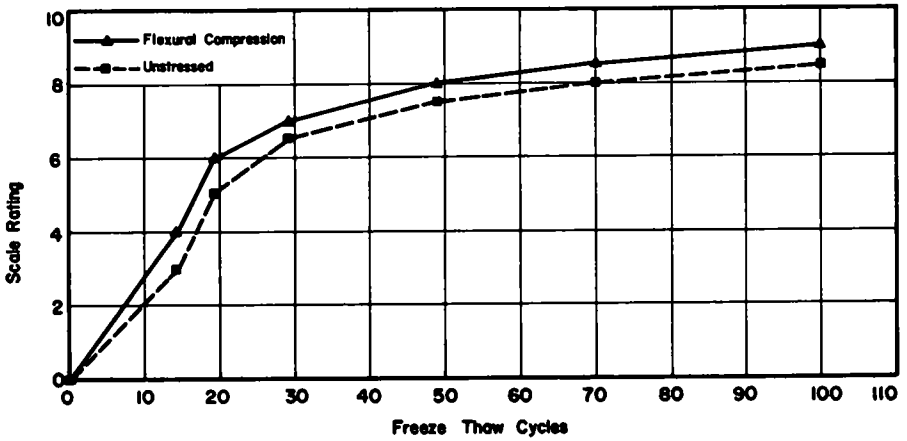

Figure 65. Scale ratings of sub-series X-15, simulated bridge deck slabs, high cyclic stress.

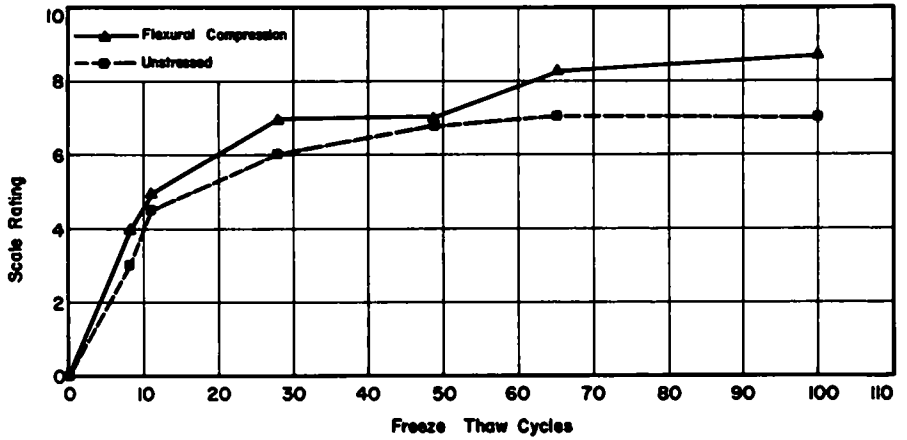

Figure 66. Scale ratings of sub-series X-16, simulated bridge deck slabs, high cyclic stress.

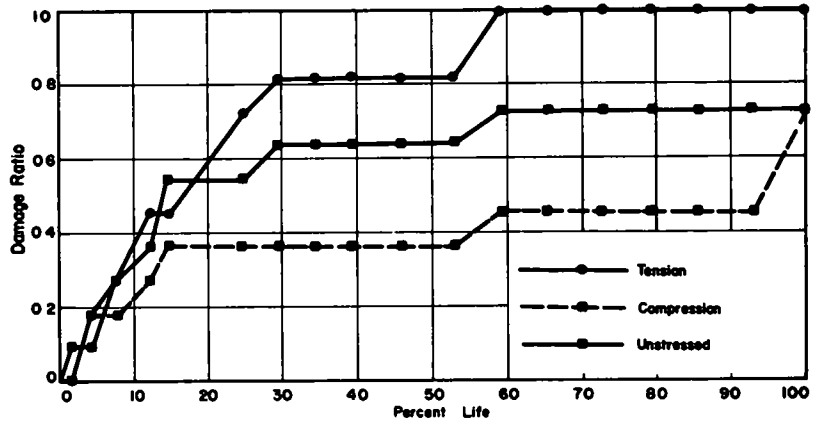

Figure 67. Freeze-thaw test results, sub-series B-1—uniaxial stress.

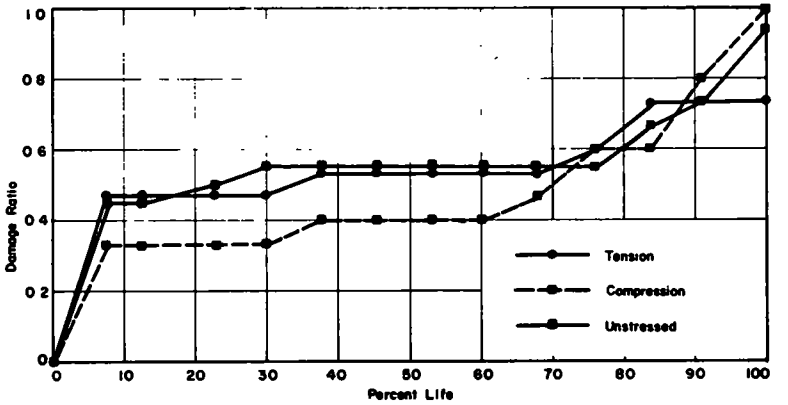

Figure 68. Freeze-thaw test results, sub-series B-2—uniaxial stress.

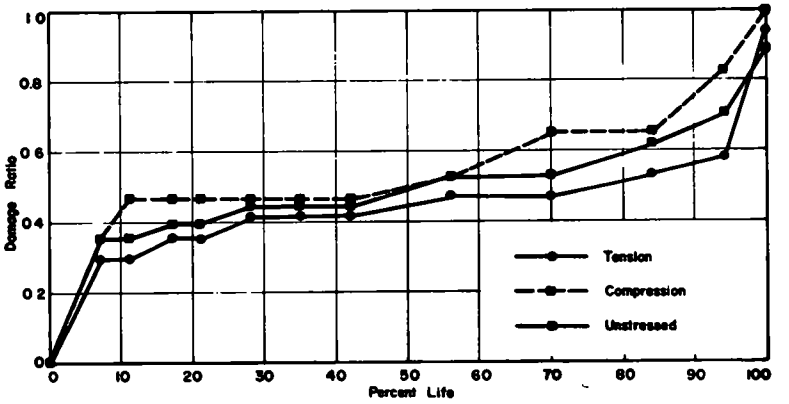

Figure 69. Freeze-thaw test results, sub-series B-3—uniaxial stress.

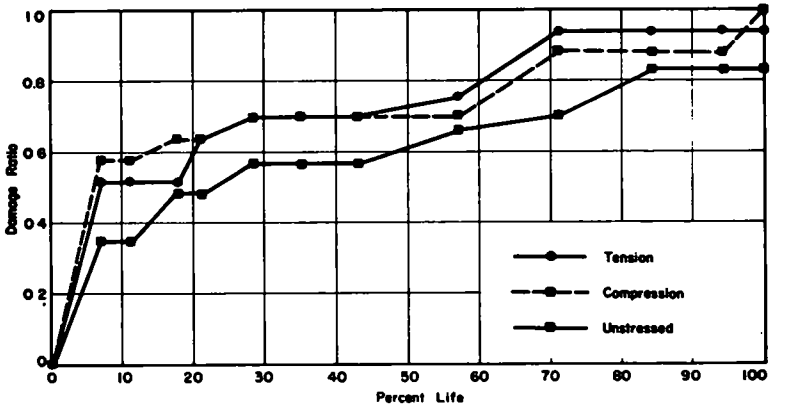

Figure 70. Freeze-thaw test results, sub-series B-4—uniaxial stress.

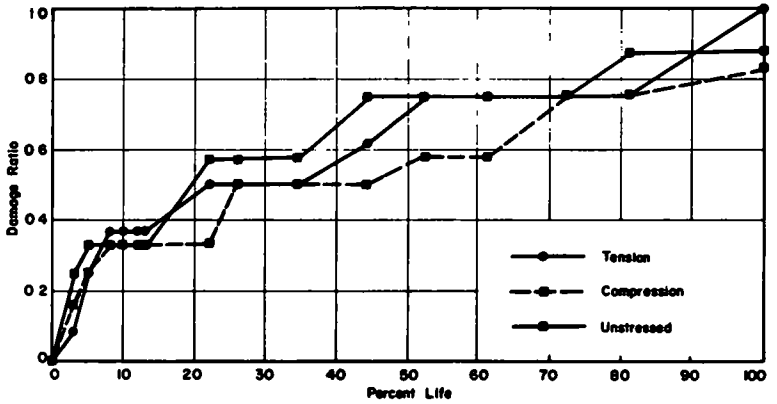

Figure 71. Freeze-thaw test results, sub-series B-5—uniaxial stress.

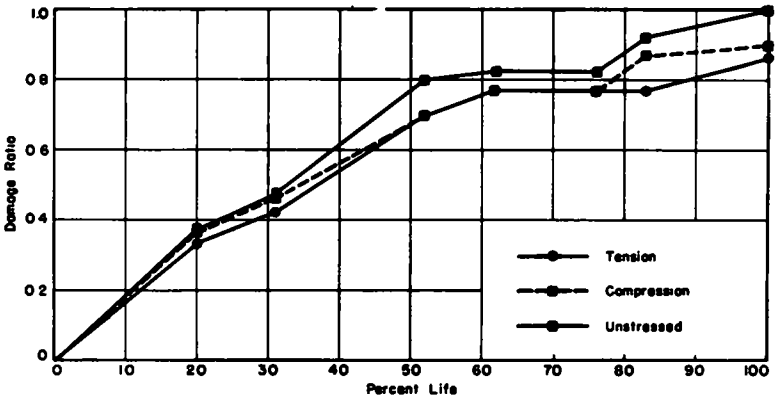

Figure 72. Freeze-thaw test results, sub-series B-6—uniaxial stress.

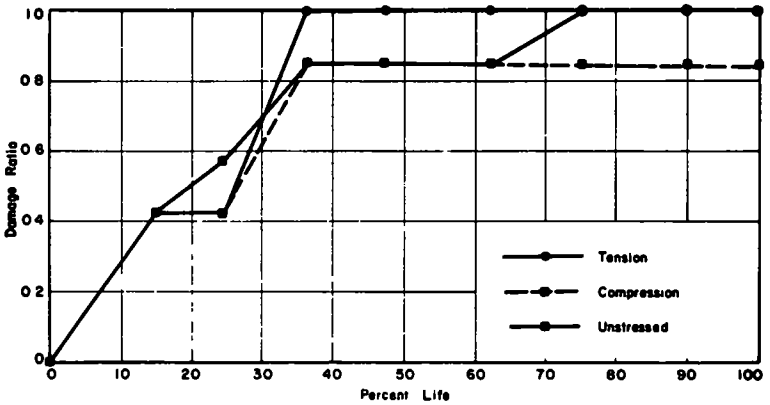

Figure 73. Freeze-thaw test results, sub-series B-7—uniaxial stress.

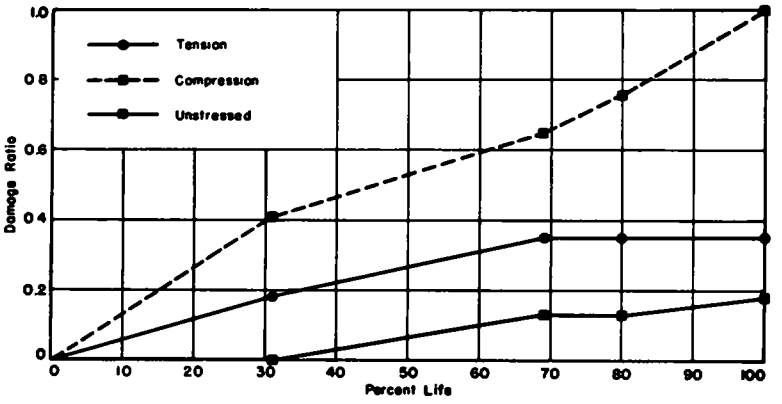

Figure 74. Freeze-thaw test results, sub-series B-8—uniaxial stress.

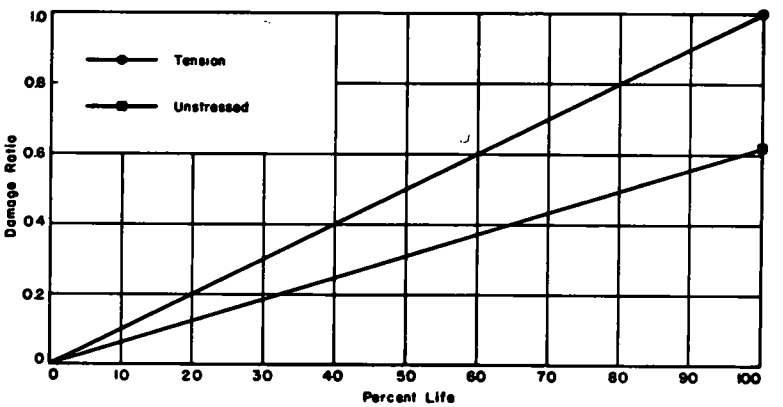

Figure 75. Freeze-thaw test results, sub-series B-9—uniaxial stress.

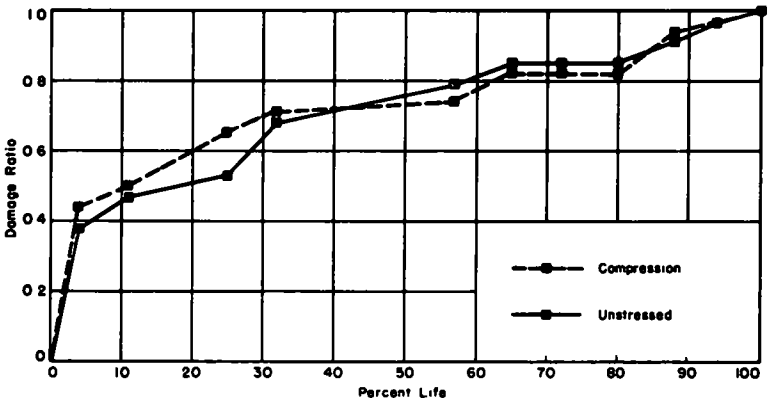

Figure 76. Freeze-thaw test results, sub-series B-10—uniaxial stress.

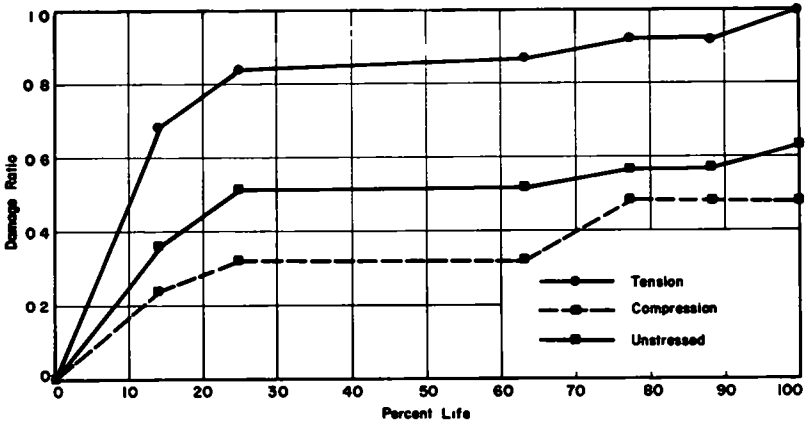

Figure 77. Freeze-thaw test results, sub-series B-11—uniaxial stress.

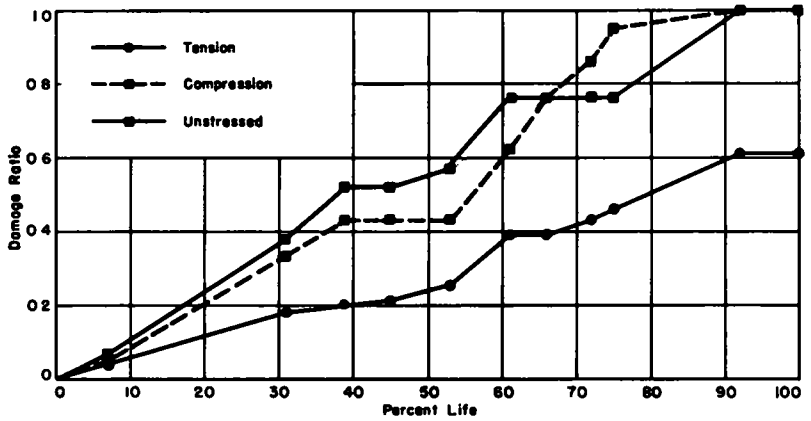

Figure 78. Freeze-thaw test results, sub-series B-12—uniaxial stress.

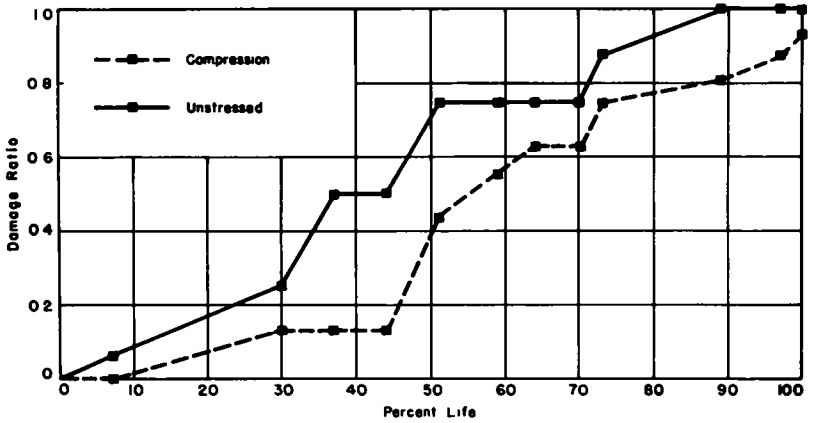

Figure 79. Freeze-thaw test results, sub-series B-13—uniaxial stress.

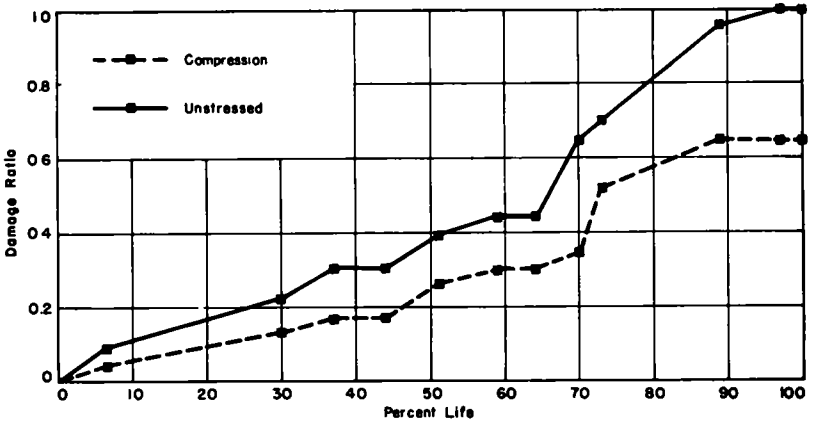

Figure 80. Freeze-thaw test results, sub-series B-14—uniaxial stress.

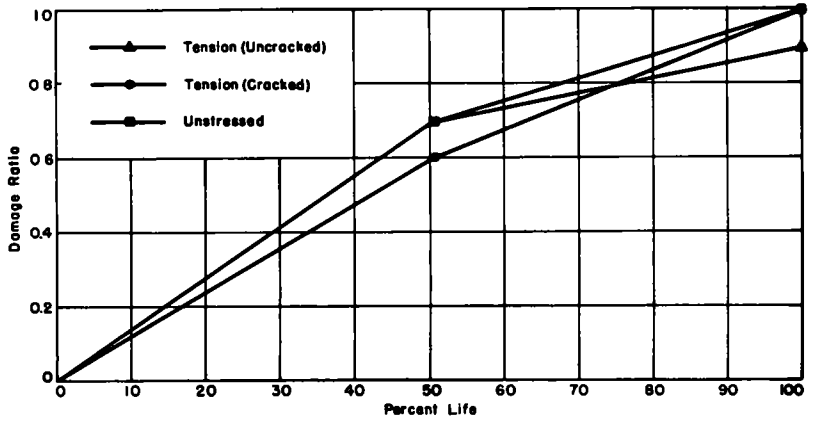

Figure 81. Freeze-thaw test results, sub-series F-1—flexure.

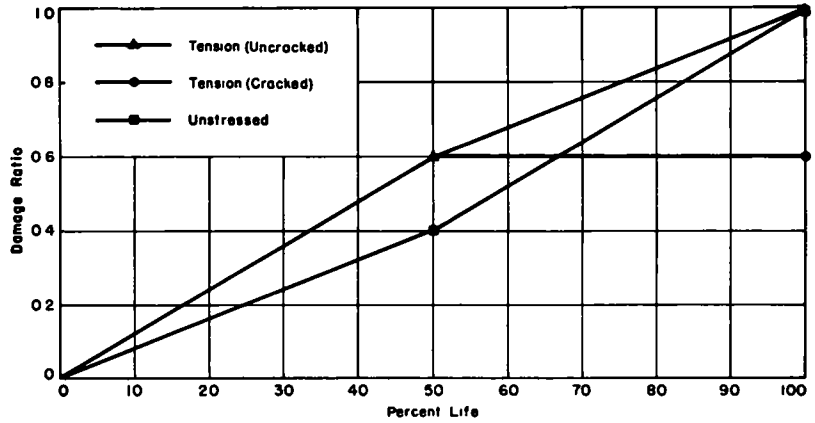

Figure 82. Freeze-thaw test results, sub-series F-2—flexure

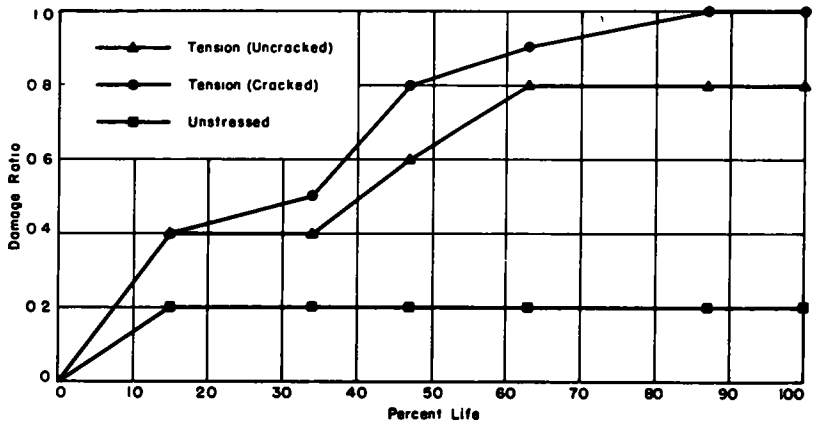

Figure 83. Freeze-thaw test results, sub-series F-3—flexure

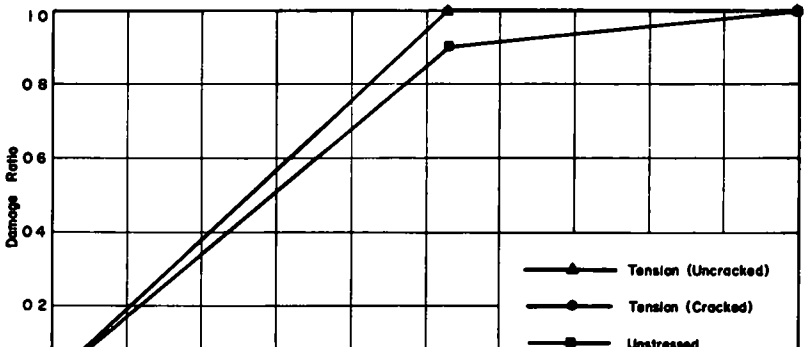

Figure 84 Freeze-thaw test results, sub-series F-5—flexure.

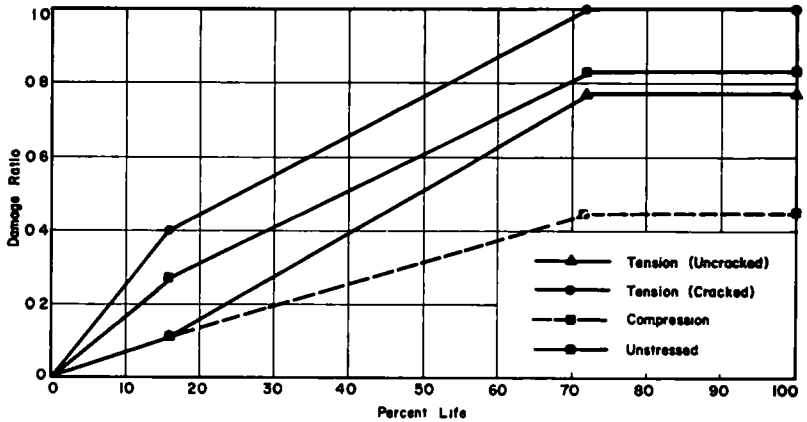

Figure 85. Freeze-thaw test results, sub-series F-6—flexure.

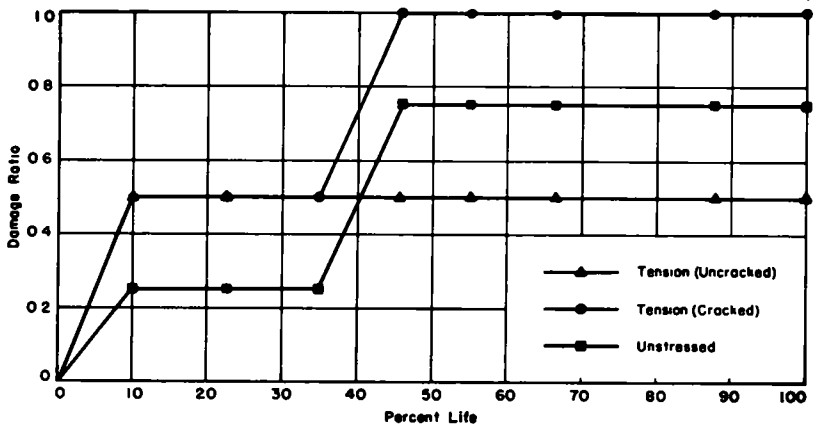

Figure 86 Freeze-thaw test results, sub-series F-4—flexure.

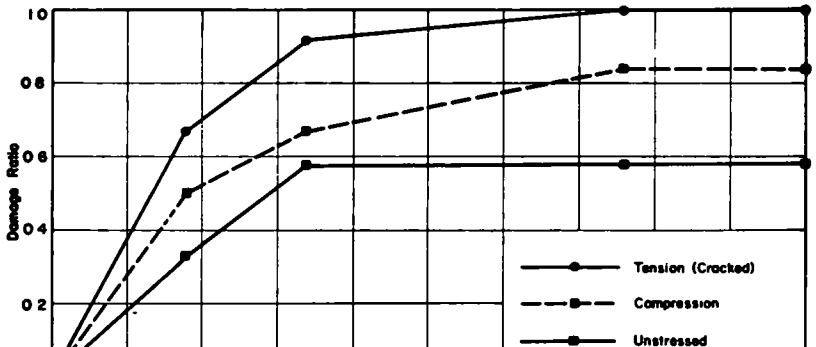

Figure 87. Freeze-thaw test results, sub-series F-7—flexure.

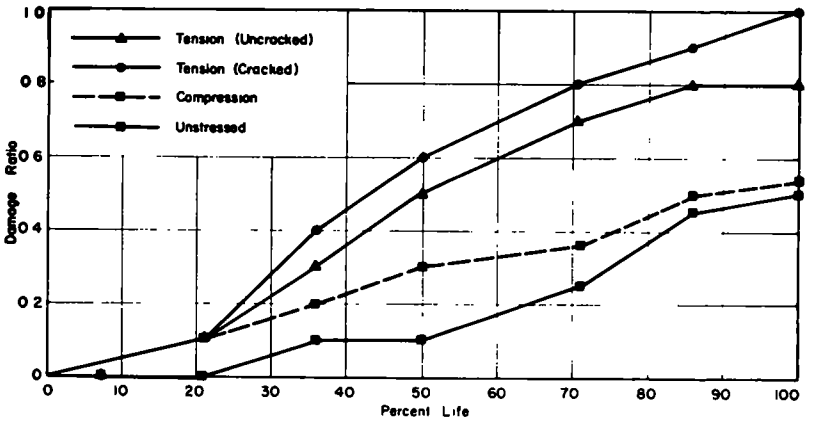

Figure 88. Freeze-thaw test results, sub-series F-8—flexure.

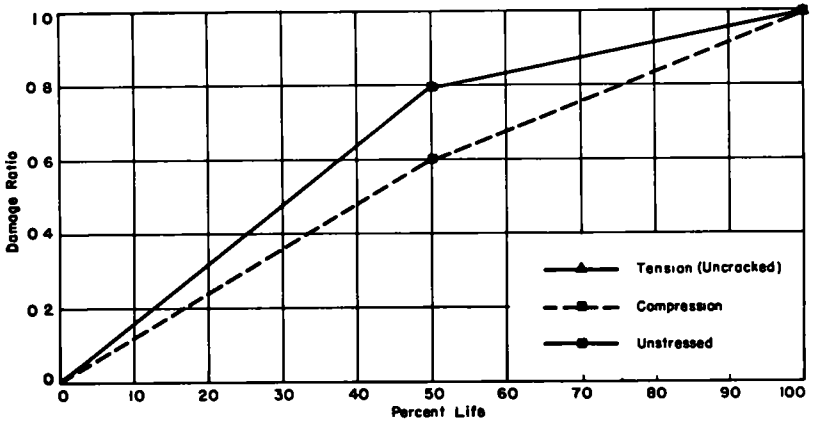

Figure 89. Freeze-thaw test results, sub-series F-9—flexure.

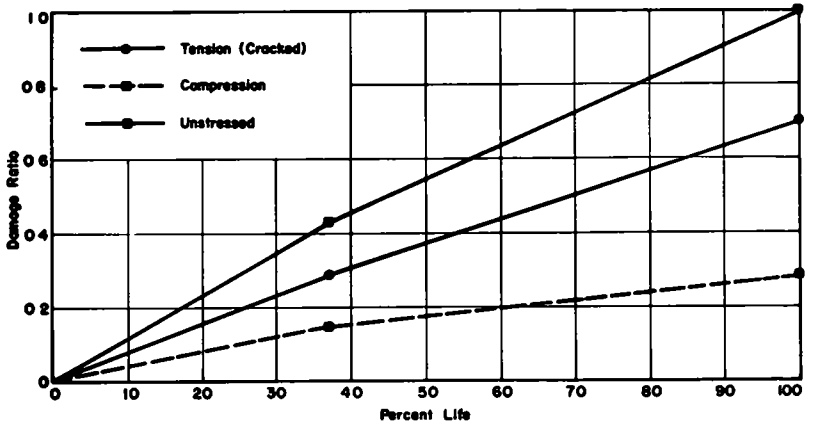

Figure 90. Freeze-thaw test results, sub-series F-10—flexure.

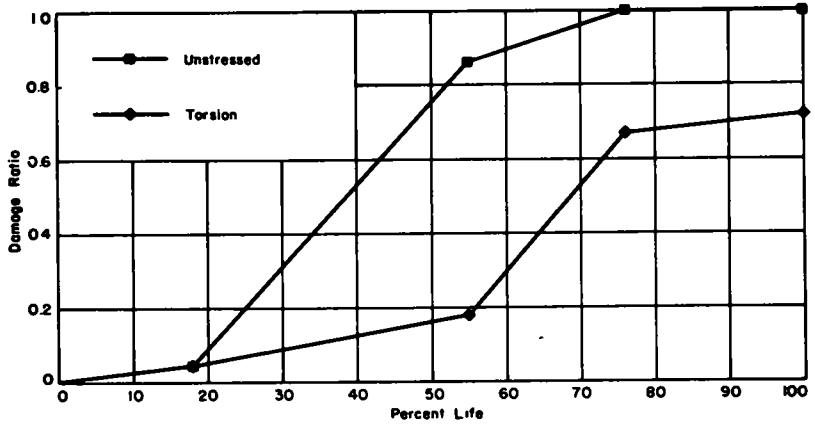

Figure 91. Freeze-thaw test results, sub-series T-1—torsion.

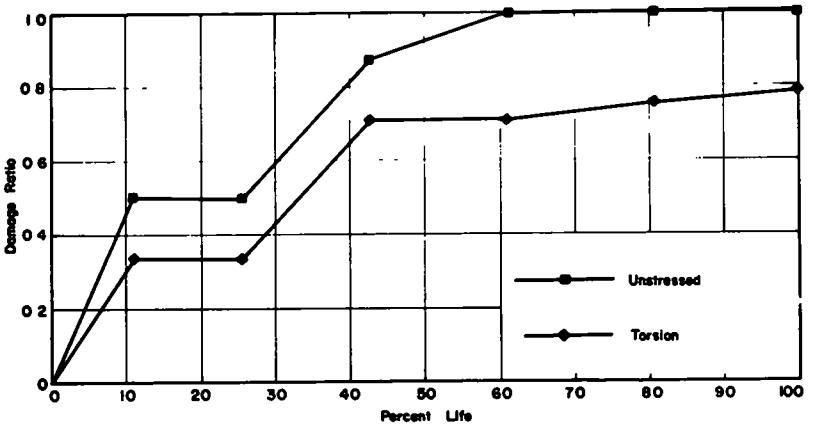

Figure 92. Freeze-thaw test results, sub-series T-2—torsion.

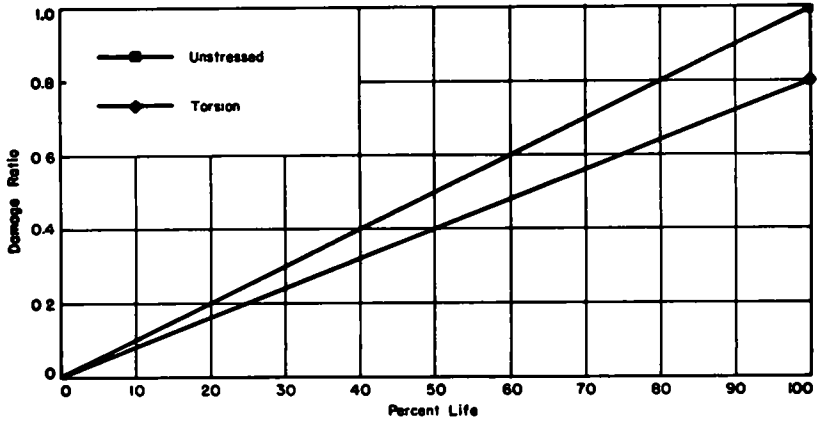

Figure 93. Freeze-thaw test results, sub-series T-3—torsion.

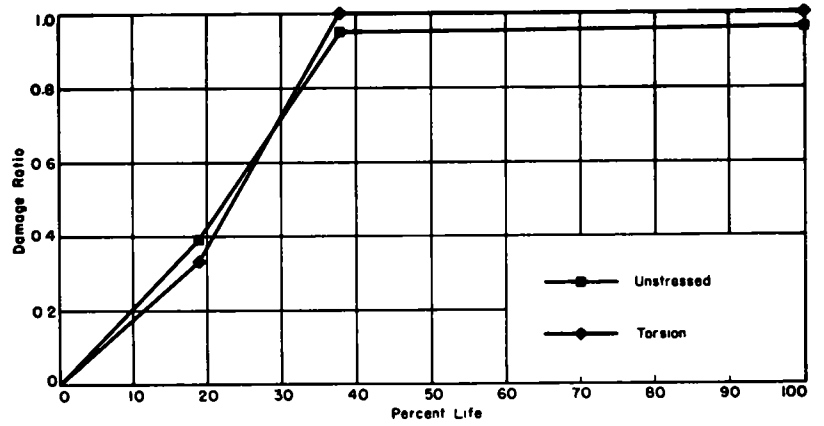

Figure 94. Freeze-thaw test results, sub-series T-4—torsion.

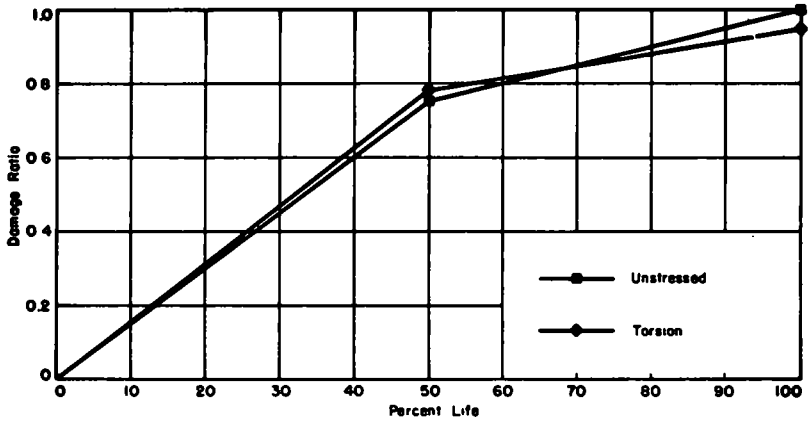

Figure 95. Freeze-thaw test results, sub-series T-5—torsion.

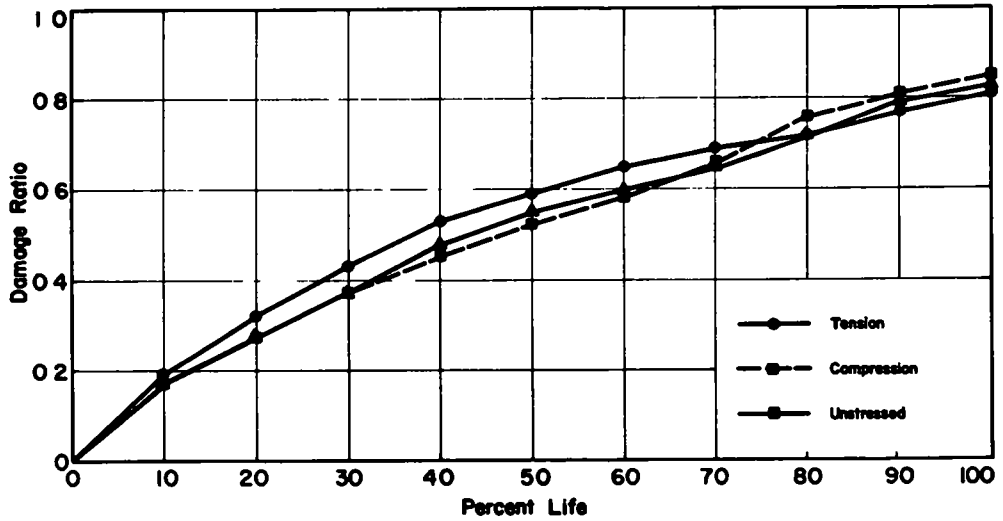

Figure 97. Freeze-thaw test results for average of uniaxially stressed sub-series B-7, 8, 9, 10, 11, 12, 13, and 14.

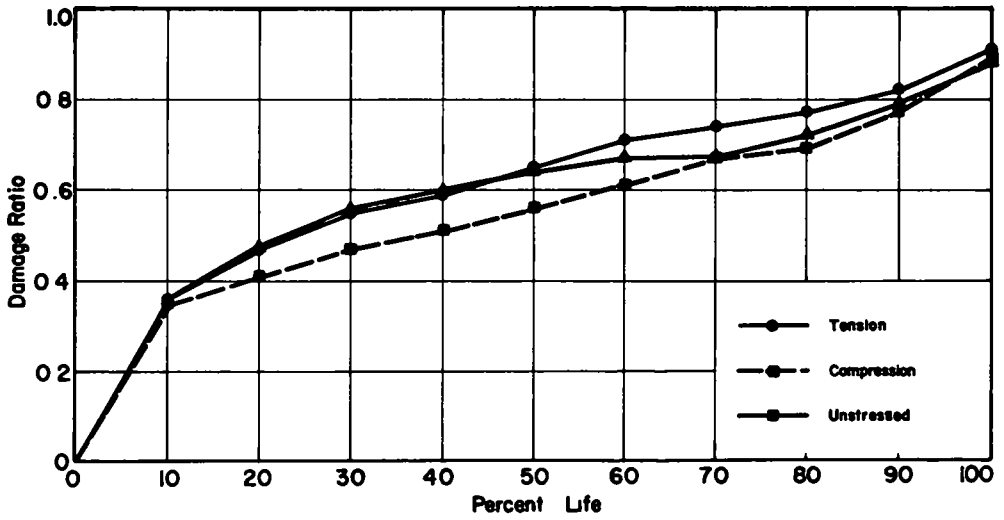

Figure 96. Freeze-thaw test results for average of uniaxially stressed sub-series B-1, 2, 3, 4, 5, and 6.

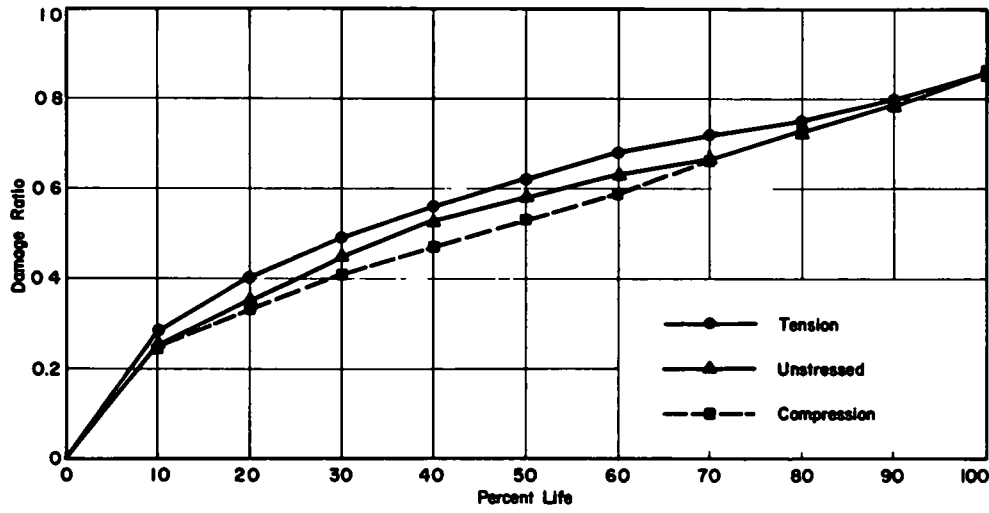

Figure 98. Combined freeze-thaw results for average of all uniaxially stressed sub-series of the stressed surface study (excluding Series A).

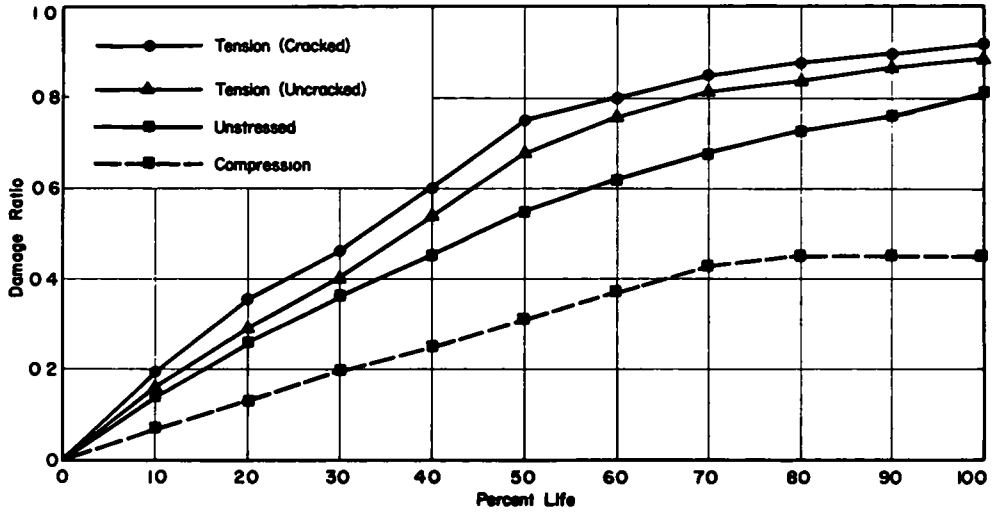

Figure 99. Freeze-thaw test results for average of flexural sub-series F-1, 2, 3, 5, and 6.

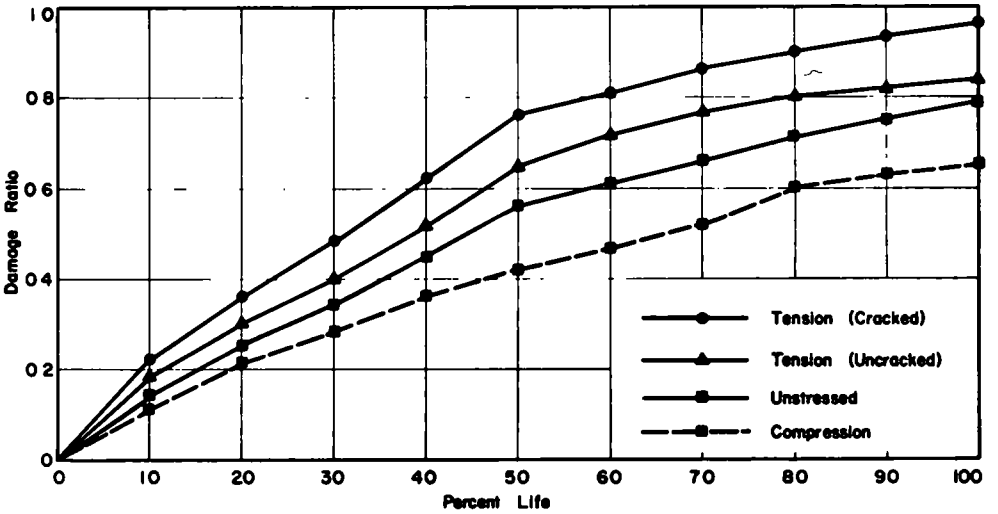

Figure 101. Combined freeze-thaw test results for average of all flexural sub-series of the stressed surface study.

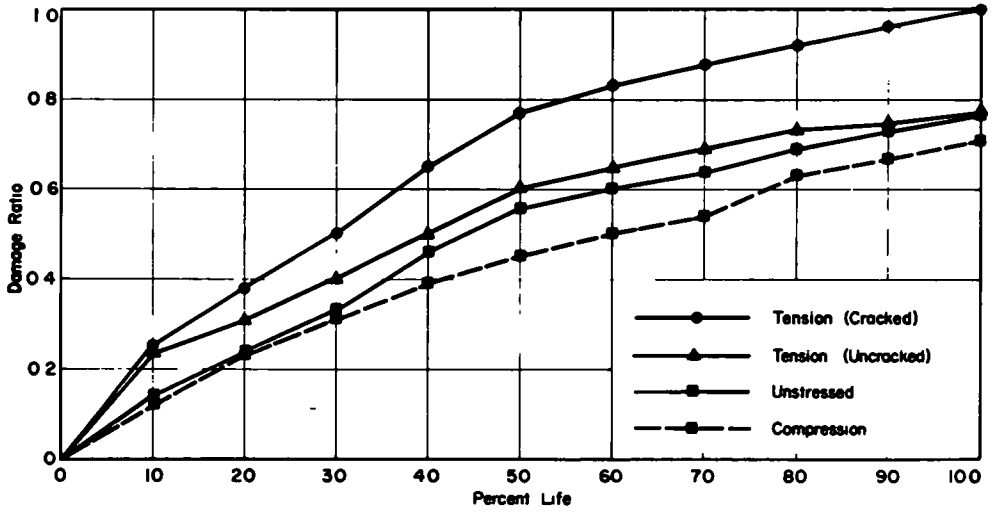

Figure 100. Freeze-thaw test results for average of flexural sub-series F-4, 7, 8, 9, and 10.

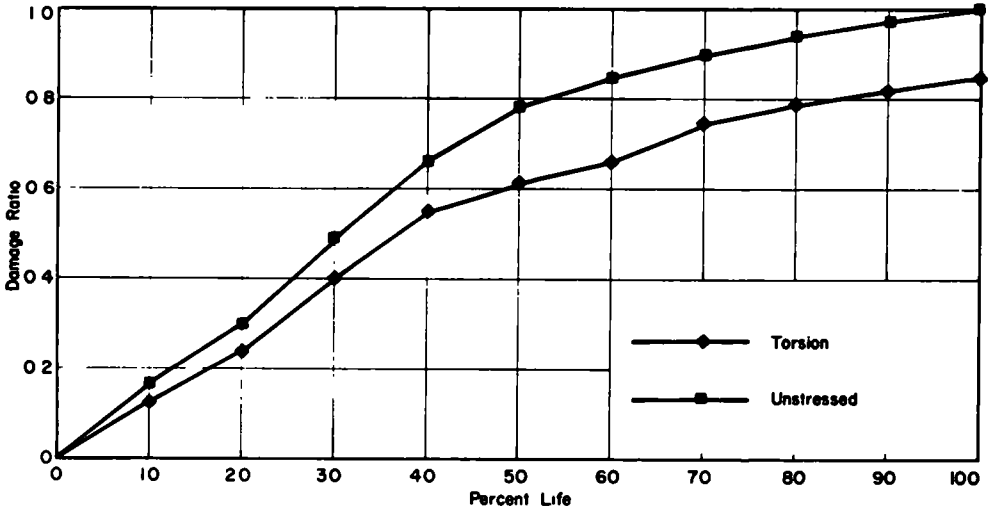

Figure 102. Combined freeze-thaw test results for average of all torsional sub-series of the stressed surface study.

close grouping of the three top curves in Figure 99 could possibly be attributed to the frequent occurrence of pop-outs, which could tend to conceal stress effects.

Figure 101 is a plot of the average damage ratio curves for all flexural sub-series. When the averages of all sub-series were used, the various curves became almost equally spaced. The general trend for the stressed surface flexural tests indicates that cracked specimens subjected to tensile stresses on the ponded surface deteriorated more rapidly than the rest of the specimens. Next in order of rate of deterioration were uncracked specimens subjected to tension, followed by unstressed specimens. The compression specimens had the slowest rate of deterioration. The only types of deterioration observed were scaling of surface mortar and pop-outs.

Simulated Bridge Deck Study

The simulated bridge deck study consisted of 16 pairs of slabs, one stressed and one unstressed, which were subjected to one of two stress levels of either a static or cyclic nature. Included in this study were also a set of three field slabs, two stressed and one unstressed, which were subjected to static loading resulting in the lower of the two concrete stress levels. The slabs tested at the low stress level contained three No. 5 deformed bars as tensile reinforcement and were subjected to computed steel stresses of 20 ksi based on the usual straight-line theory, assuming no tension in the concrete. This loading condition was selected to produce uncracked concrete and resulted in a maximum tensile stress of 310 psi, calculated using the transformed uncracked section. The slabs having a high stress condition contained five No. 5 bars as tensile reinforcement which were loaded to the same computed steel stress of 20 ksi. The maximum concrete tensile stress calculated for the transformed uncracked section was 530 psi, however, these slabs were designed to develop cracked tensile concrete sections, and did. The high stress slabs having 6-in. bar spacing are more typical of actual bridge decks.

The slabs are discussed in groups, according to their prescribed loading conditions.

Sub-series X-2, X-3, X-4, and X-5 were subjected to *static loading* at the *lower tensile stress* level on the diked surface. Two of these sub-series, X-2 and X-4, consisted of specimens that deteriorated readily; sub-series X-5 deteriorated at a much slower rate, and sub-series X-3 deteriorated a minimal amount. It was consistently found that the slabs subjected to tensile flexural stress deteriorated at a slightly faster rate than the unstressed companion specimens; however, there was little significance in the differences. The results of these tests are shown in Figures 52 through 55. Figure 12 shows the diked surfaces of sub-series X-3 and X-4 specimens. It shows the extreme difference in durability of the two sets of slabs. Sub-series X-5 was the first of a series of six pairs of slabs evaluated using sonic readings. The results are shown as Figures 103 and 104 for long and short sonic readings, respectively. It would be expected that the less durable of the two slabs would have a greater decrease in relative dynamic modulus; however, the curve for the unstressed slab remains lower for both long and short readings. The difference between the two slabs was insignificant for the short readings, and little change in modulus with increasing numbers of freeze-thaw cycles was seen. The sonic readings did not appear to show the progressive deterioration observed and plotted in Figure 55. Visual observations of the stressed specimens failed to reveal any tensile cracks during the period of freeze-thaw testing.

Sub-series X-6 and X-7 were subjected to *static loading* at the *lower compressive stress* on the diked surface. There was little difference in the durability of the two series and little difference in the rate of deterioration of the pairs of slabs, however, the X-7 stressed slab appeared to have deteriorated slightly more than its unstressed companion (Fig. 57). In Figures 105 and 106 there appears to be a negligibly small difference in the relative dynamic moduli of the X-6 slabs for either long or short readings and, as should be the case for these durable slabs, there was little change in the moduli with increasing freeze-thaw cycles. Figures 107 and 108 show considerably more difference between the two X-7 slabs. The long readings showed the curve for the compression specimen to be lower than that of its unstressed companion; however, at 70 freeze-thaw cycles the two had virtually the same readings. These differences were not as significant for the short readings. The photographs of these two series in Figure 13 confirm the fact that there was no significant difference in observable behavior of the two sets of slabs.

Figures 58 and 59 consist of the results of tests of slabs subjected to *static loading* at the *high compressive stress* level. By chance, these sub-series also represented the two basic freeze-thaw behavior patterns. Sub-series X-8 slabs (Fig. 58) experienced a negligible amount of deterioration, whereas both of the X-9 slabs (Fig. 59) scaled appreciably. The differences in the two sets of slabs can easily be seen in Figure 14; however, for both extremes of durability there was virtually no difference in the rate of scaling of stressed and unstressed specimens. The long sonic readings for the X-8 slabs (Fig. 109) showed considerable difference between the two, with the unstressed slab having appreciably lower relative dynamic modulus values. This difference, however, was not seen in the short sonic readings (Fig. 110) of the same two slabs. The same trend seen in Figure 109 was also apparent in Figures 111 and 112, with the X-9 unstressed slab having the lower relative dynamic modulus for both long and short sonic readings. This is generally assumed to indicate that the unstressed slab was less durable than its stressed companion specimen.

Sub-series X-10 and X-11 slabs (Figs. 60, 61) were subjected to *static loading* at the *high tensile stress* level on the diked surface. Tensile cracks were easily detected on the diked surfaces, having an average spacing of approximately 6 in. The results of both series indicated that there were significant differences in the rate of scaling of stressed and unstressed slabs. Both sets experienced considerable scaling, as shown in Figure 15. The results of both long and short sonic readings (Figs. 113, 114) confirmed the significant difference in durability of the X-10 stressed and unstressed slabs, with the stressed slab having consistently the lower relative dynamic modulus values.

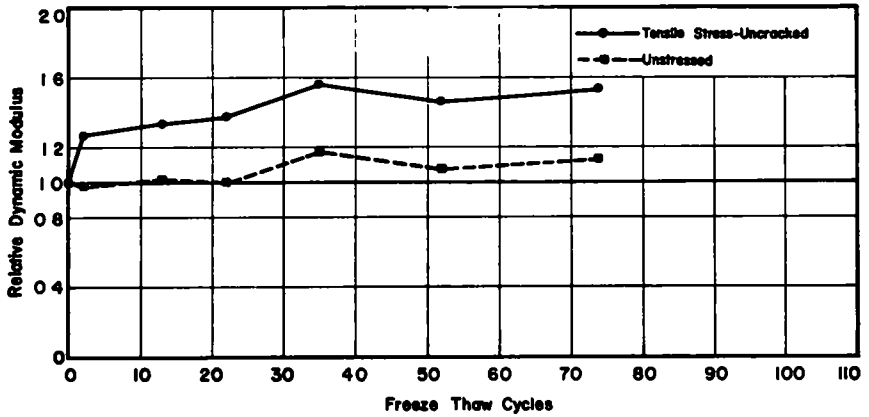

Figure 103. Influence of flexural stress on durability of sub-series X-5 slabs, long sonic readings.

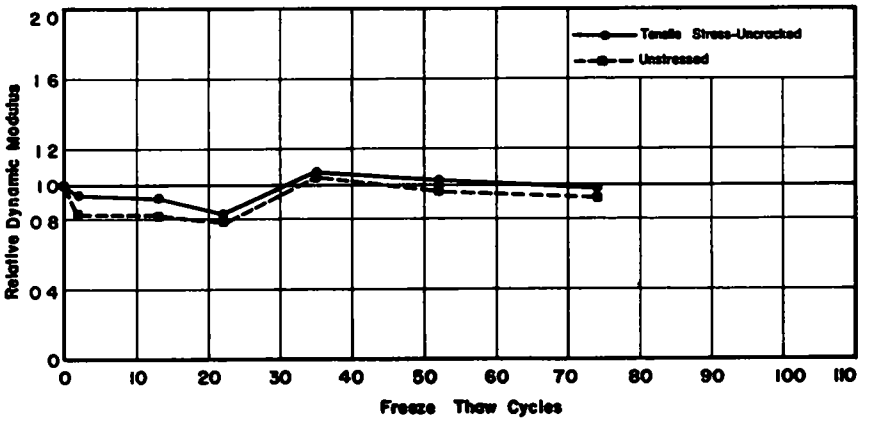

Figure 104. Influence of flexural stress on durability of sub-series X-5 slabs, short sonic readings.

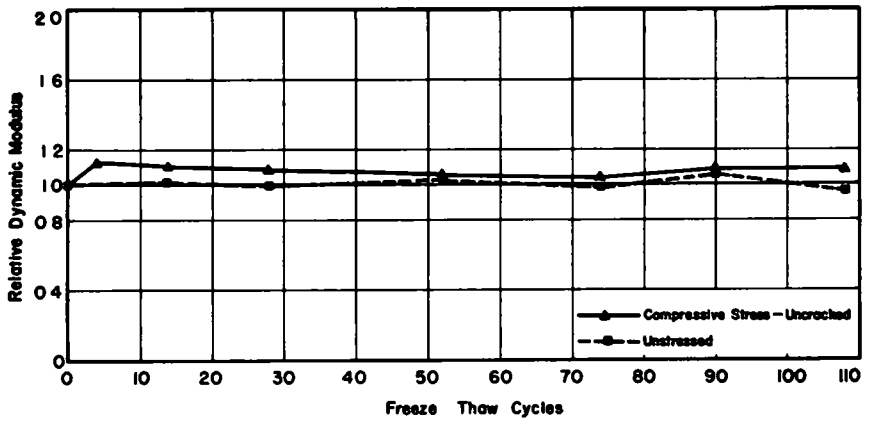

Figure 105. Influence of flexural stress on durability of sub-series X-6 slabs, long sonic readings.

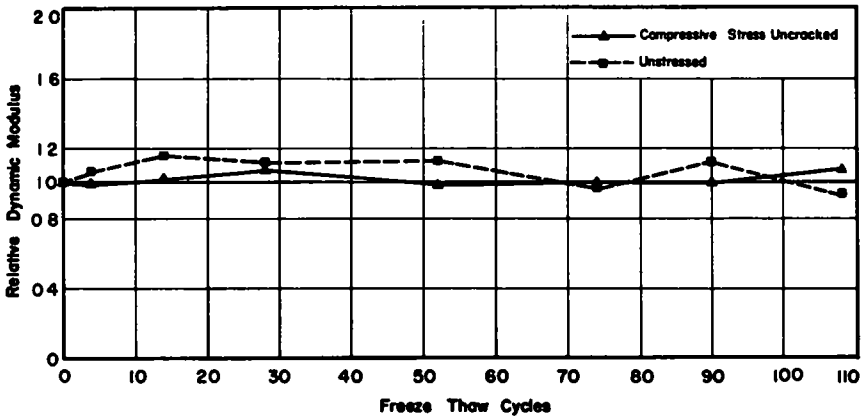

Figure 106. Influence of flexural stress on durability of sub-series X-6 slabs, short sonic readings.

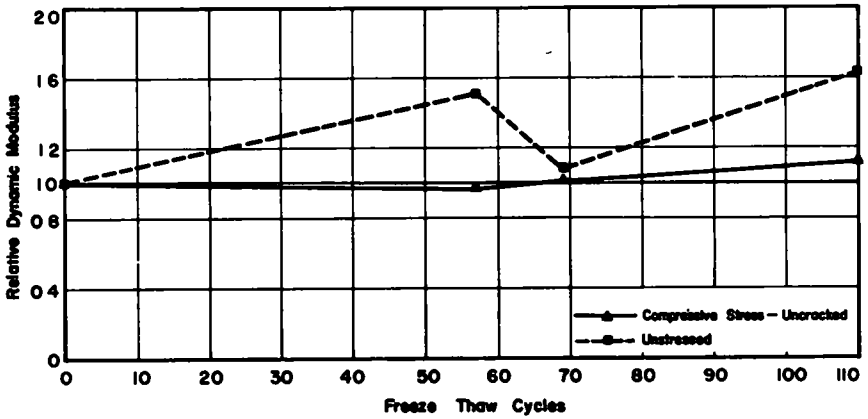

Figure 107. Influence of flexural stress on durability of sub-series X-7 slabs, long sonic readings.

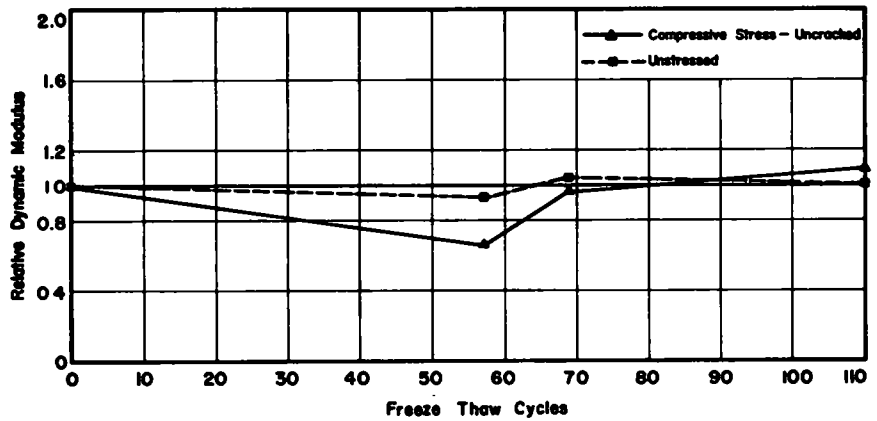

Figure 108. Influence of flexural stress on durability of sub-series X-7 slabs, short sonic readings.

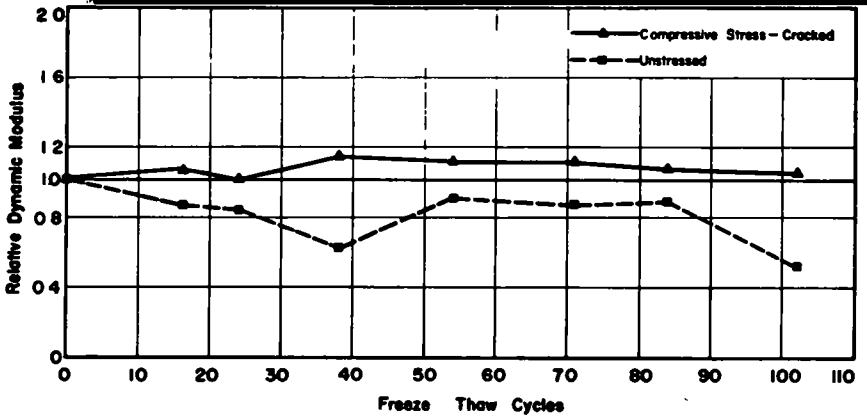

Figure 109. Influence of flexural stress on durability of sub-series X-8 slabs, long sonic readings.

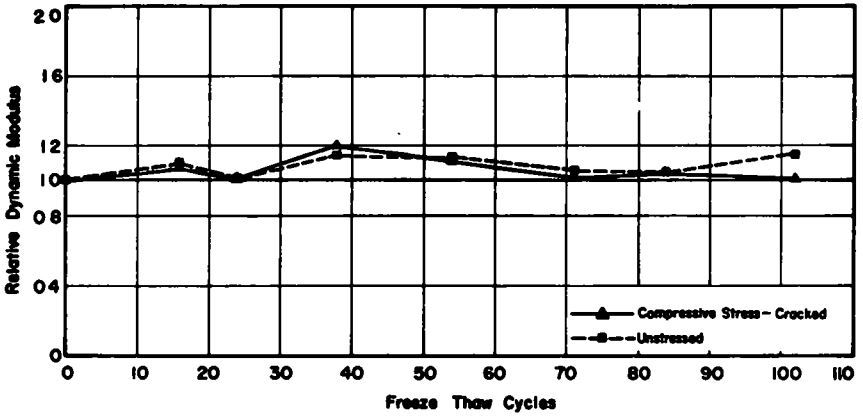

Figure 110. Influence of flexural stress on durability of sub-series X-8 slabs, short sonic readings

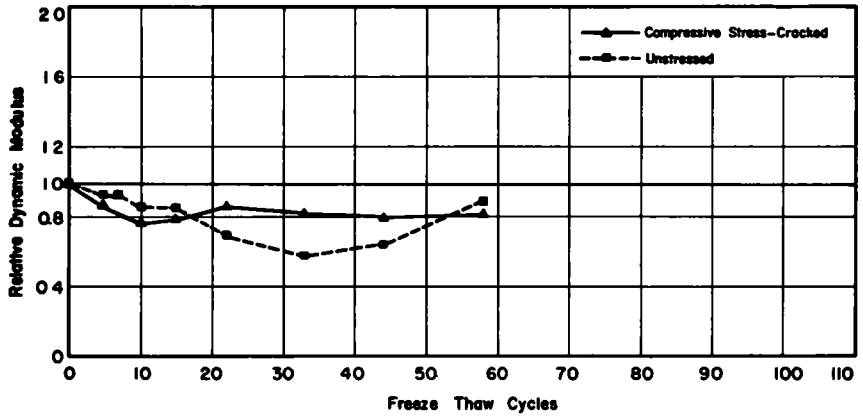

Figure 111. Influence of flexural stress on durability of sub-series X-9 slabs, long sonic readings.

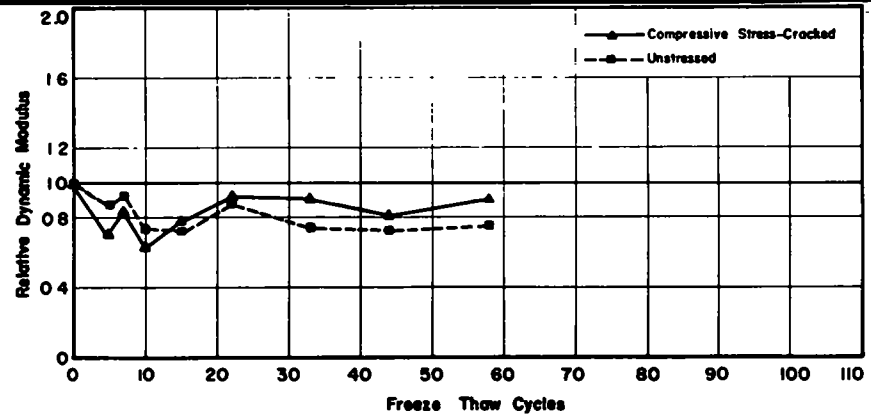

Figure 112. Influence of flexural stress on durability of sub-series X-9 slabs, short sonic readings.

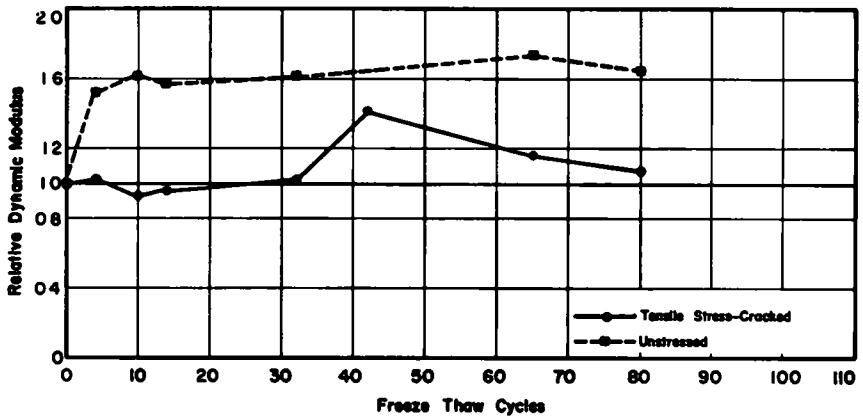

Figure 113. Influence of flexural stress on durability of sub-series X-10 slabs, long sonic readings.

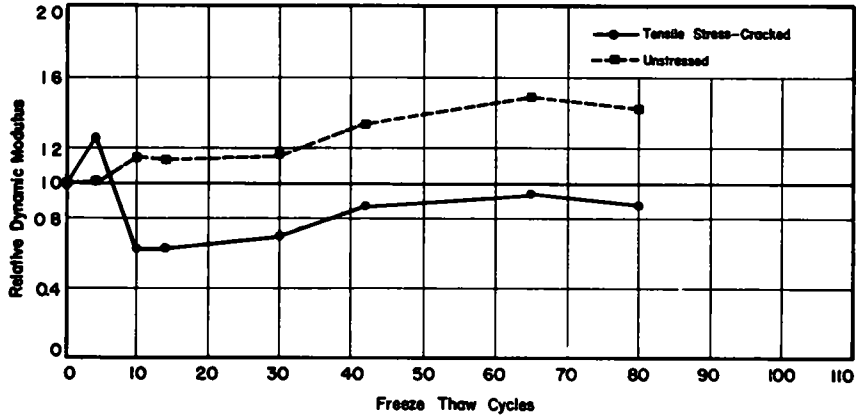

Figure 114. Influence of flexural stress on durability of sub-series X-10 slabs, short sonic readings.

Figures 62 and 64 consist of the results for sub-series X-12 and X-14, respectively. These specimens were subjected to *cyclic loading* at the *high tensile stress* level. The X-12 slab contained the amount of reinforcement used for low stress specimens. When subjected to the loading used for high stress, this slab was considerably more flexible than the X-14 specimen. As shown in Figures 16 and 17, sub-series X-14 experienced a moderate amount of scaling, whereas the X-12 specimens suffered little if any deterioration. There was no difference in behavior between stressed and unstressed slabs for sub-series X-14, and only a slight difference occurred in the case of the X-12 slabs, with the stressed slab experiencing a slightly higher degree of deterioration. The difference in slab flexibility had little apparent effect on scaling or severity of cracking, with average crack spacings of approximately 6 in. in both cases.

Figure 63 shows the results of sub-series X-13 slabs for the *low tensile stress* under *cyclic loading* conditions. No difference was seen between the stressed and unstressed slabs with respect to freeze-thaw durability. Both specimens reached a final scale rating of one. It should also be noted that these slabs were subjected to 35 wetting-drying cycles prior to freeze-thaw testing. This is discussed further in "Wetting and Drying," at the end of this chapter.

Sub-series X-15 and X-16 specimens (Figs. 65, 66) were subjected to *cyclic loading* at the *high compressive stress* level on the diked surfaces. The results for the X-15 slabs (Fig. 65) show that the stressed specimen deteriorated at a slightly faster rate than its unstressed companion. Sub-series X-16 was composed of slabs cast in two halves, using a different batch of ready-mixed concrete for each half. As shown in Figure 18, the two halves deteriorated at different rates; however, the average rate of slab deterioration plotted in Figure 64 indicated the same trend in relative rates of deterioration as was seen for the X-15 slabs. Under the cyclic loading the compression region of the construction joint remained sound, however, examination of the tension region showed that cracking had occurred along the joint. It should be noted that the observed increase in the rate of deterioration due to cyclic compressive stress was in direct opposition to the decrease in rate of deterioration of specimens subjected to static compression. This is discussed further in Chapter Five.

The results of the field slab study indicated that there was a slight amount of localized deterioration for the tensile slab and virtually no deterioration observed on the compression and unstressed slabs after three winters and 73 freeze-thaw cycles. Two cracks were observed in the tensile slab; however, no feathering or deterioration was present along the cracks. These slabs are shown in Figure 19.

Summary of Simulated Bridge Deck Study

The over-all effects of the various stressing conditions discussed in the preceding portions of this section for the simulated bridge deck study can be summarized as follows.

Under static loading at the low stress level there was a slight tendency for tensile stresses to accelerate the rate of deterioration. On the other hand, compressive stresses had little consistent effect. For static loadings at the high stress level, tensile stresses consistently produced a significant increase in deterioration, whereas compressive stress had little effect.

For cyclic loading conditions, at the low stress level there was no apparent difference in the rate of deterioration of the stressed and unstressed specimens. Cracks eventually appeared; however, at the end of testing they had an average width of 0.004 in. without signs of feathering. The cyclically loaded specimens subjected to high tensile stresses appeared to have no significant difference in rates of deterioration when compared with the unstressed companion specimens. Considerable feathering along the edges of the tensile cracks was observed; however, differences in slab flexibility had little effect on scaling or severity of cracking. The two cyclically loaded specimens with high compressive stress deteriorated at a slightly faster rate than their unstressed companion slabs. The construction joint present in the sub-series X-16 slab remained sound at the compression surface.

Uniaxial Stress

The average damage ratio curve for sub-series B-1, B-2, B-3, B-4, B-5, and B-6 (Fig. 96) summarizes the results of all uniaxial test specimens cast using natural river gravel. Noticeably cracked specimens were not included in this study. Figure 96 shows that little difference existed between the rates of deterioration of tension, compression, and unstressed specimens. The compression curve remained below the other curves until the end. The tension curve remained slightly above the other curves for the last half of the graph.

The results of the two uniaxial test series composed of crushed limestone coarse aggregate are summarized in Figure 97 for the B Series study, and in Figures 118, 122, and 126 for the A Series study.

The average damage ratio curves for sub-series B-7 through B-14 (Fig. 97) showed very little, if any, difference in the rates of deterioration of tensile, compressive, and unstressed specimens. For 60 percent of the graph the tension curve remained above the other two, but this difference was not of a sufficient magnitude to indicate that tensile stresses significantly accelerated the rate of deterioration.

The A Series study was conducted to reinforce the results observed during the B Series testing. This was believed to be desirable because of the findings of the surface stress evaluation study presented in Appendix A. The results of the three Series A uniaxial stress sub-series (Figs. 118, 122, 126) indicate little in the way of a trend with respect to stress effects. The three curves of sub-series A-1 (Fig. 118) consistently remained above a relative dynamic modulus of unity, thereby indicating that no deterioration had occurred. Durability of sub-series A-1 further verified by the reported absence of visible surface deterioration in all but one unstressed specimen. Figure 122 summarizes the results of sub-series A-2. Although the relative dynamic moduli for this sub-series were significantly below unity, no particular trend could be ascertained with respect to stress effects. The curves were highly inconsistent over the period of testing. None of the specimens of sub-series A-2 showed any

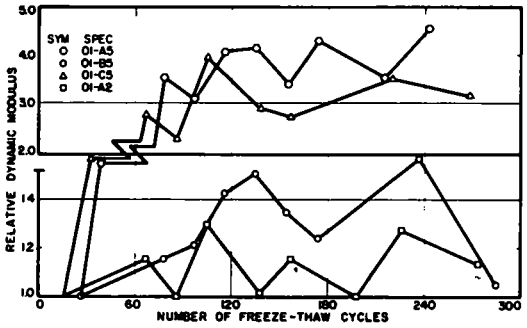

Figure 115. Effect of tensile stress on durability, sub-series A-1

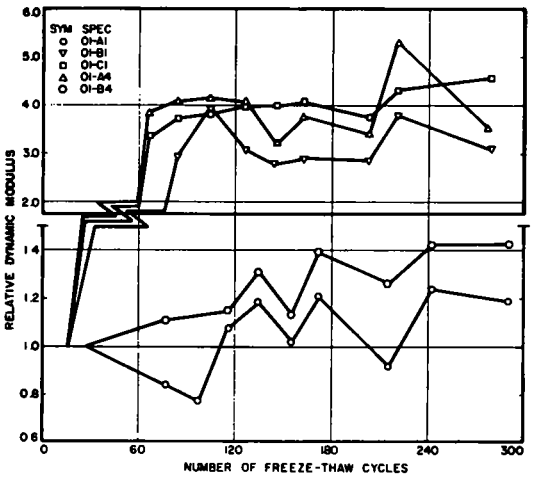

Figure 116. Effect of compressive stress on durability, sub-series A-1.

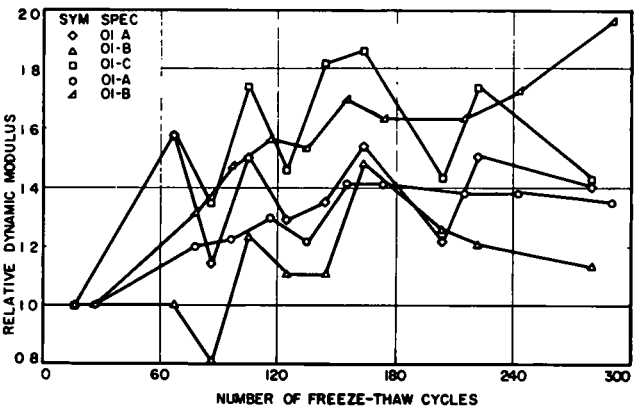

Figure 117. Durability of unstressed specimens, sub-series A-1.

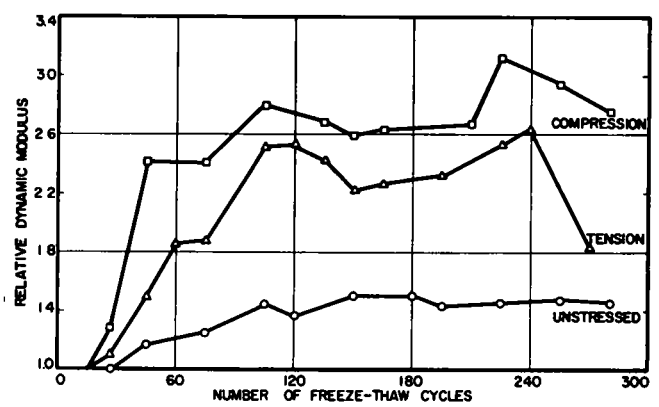

Figure 118. Average durability of sub-series A-1

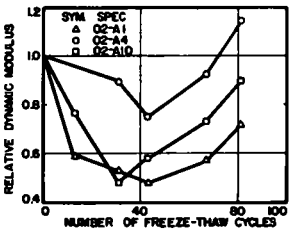

Figure 119 Effect of tensile stress on durability, sub-series A-2.

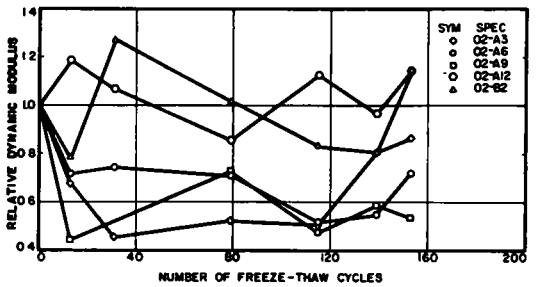

Figure 120 Effect of compressive stress on durability, sub-series A-2.

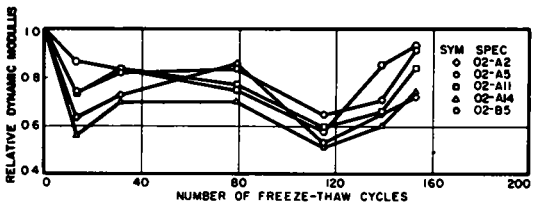

Figure 121. Durability of unstressed specimens, sub-series A-2

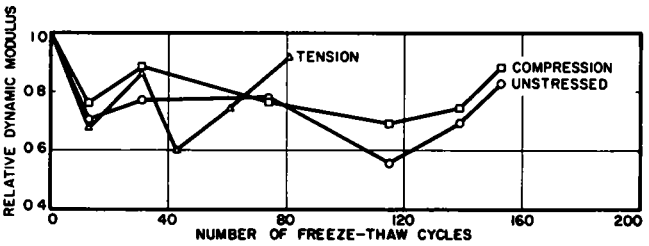

Figure 122. Average durability of sub-series A-2.

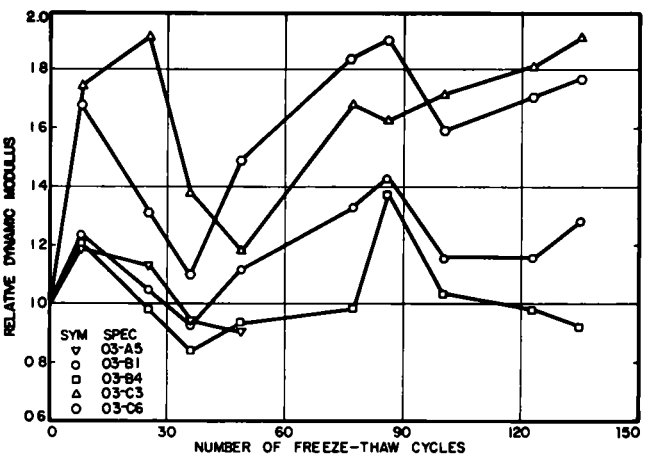

Figure 123 Effect of tensile stress on durability, sub-series A-3.

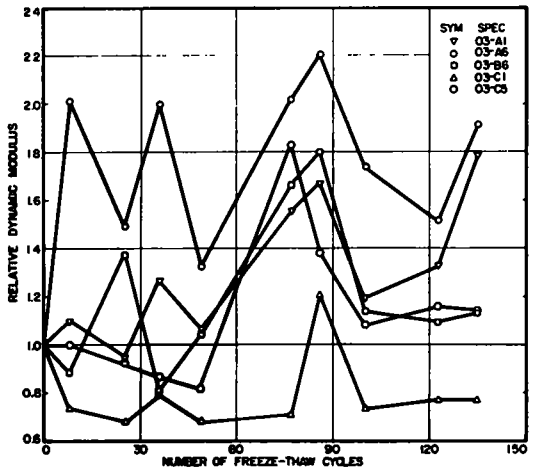

Figure 124. Effect of compressive stress on durability, sub-series A-3.

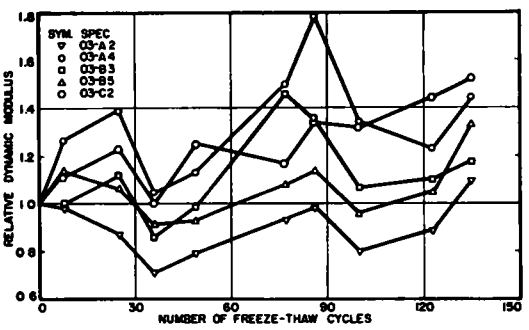

Figure 125. Durability of unstressed specimens, sub-series A-3.

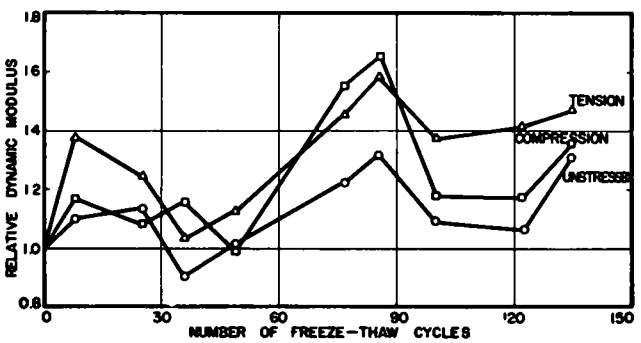

Figure 126. Average durability of sub-series A-3.

visible signs of surface deterioration. The tensile tests had to be discontinued prematurely because of frequent failures of the epoxy bond between the specimens and the load frames. The results of freeze-thaw testing of sub-series A-3 specimens (Fig. 126) also indicated no consistent trend with respect to the effect of stress on freeze-thaw durability, and the average curves remained above a relative dynamic modulus of unity. Surface scaling of a light nature was observed primarily on the finished surfaces. Tensioned and unstressed specimens experienced a higher degree of scaling than did the compression specimens.

The Series A results can be summarized as follows. For concretes containing crushed limestone aggregate and relatively high air contents, stress levels up to 25 percent of ultimate had little effect on freeze-thaw durability. The erratic sonic results could possibly be attributed to problems with the equipment which were prevalent throughout the course of this particular series of tests.

Figure 98 shows the average damage ratio curve for all B Series specimens. Some difference can be seen between the three curves representing tension, compression, and unstressed specimens; however, the three curves converged at the end-point. It can be concluded that for the stress levels investigated there was no significant effect of uniaxial static tensile or compressive stresses on freeze-thaw durability.

Biaxial Stress

The results of the biaxial stress study are shown in Figure 102. The plot indicates that static biaxial stresses produced by torsional loads significantly retard the rate of scaling of concrete cast using crushed limestone aggregates. The results of sub-series T-1 through T-5 fairly consistently indicated this result, but the number of ratings for T-3 and T-5 specimens was less than desirable.

Comparisons of Final Ratings

To determine the effect of stress on total cumulative deterioration, comparisons were made of the final scale ratings of the stressed and unstressed specimens and are summarized in Table 6. It can be seen that for all flexural tests, without regard to type of aggregates used, 64 percent of the static tensile specimens stressed to cracking received a higher final rating than their unstressed companions. Neither the uncracked tension or compression tests indicated a pronounced trend in behavior.

The only clear trend seen for the cyclic tests was with respect to flexural compression specimens. For the two sets of slabs tested, both showed a higher final rating for compression specimens than for those remaining unstressed.

The uncracked tension specimens of the static uniaxial stress study indicated a trend, with 64 percent having higher final ratings than the unstressed specimens. There was considerably less predominance in the behavior of uniaxial compression specimens given in Table 6.

If the type of stress (i.e., varying or uniform) can be considered to be less important than whether it is tensile or compressive, a combination of final ratings of both uniaxial and flexural series disclosed that 52 percent of the static tension tests had scale ratings higher than those of the unstressed specimens, whereas 40 percent of the compression sub-series had lower final ratings than their unstressed companions.

THERMAL LENGTH CHANGE

These tests were conducted for the purpose of obtaining experimental information concerning the inconsistencies in relative durability of the stressed study concretes.

The results of the four Series C thermal length change studies are shown in Figures 127 through 134. The symbols used in these figures are defined as follows:

L_o = original specimen length;
L = specimen length at the beginning of the cycle;
ΔL = thermal length change for the freezing portion of a single freeze-thaw cycle;
ΔL_o = difference between the original specimen length and its length at the lower temperature for a single cycle;
ΔT = temperature differential;
$\frac{\Delta L}{L \Delta T}$ = apparent thermal length change coefficient;
$\frac{\Delta L_o}{L_o \Delta T}$ = cumulative thermal length change coefficient; and
μin. = micro-inches (in. $\times 10^{-6}$).

Figures 127 and 128 show plots of the apparent thermal length change coefficients for sub-series C-3 and C-4 mortar, concrete, and no-fines specimens. Both of the mortars had air contents of 6 5 percent. During freeze-thaw testing of the X-10 (C-3) and X-12 (C-4) slabs, both concretes proved to be relatively durable, with the X-10 slab receiving a final rating of 3, and the X-12 slab receiving a rating of 1. The C-4 specimens were subjected to the more severe thermal cycle; this is probably why there is a greater difference in spacing of the three curves for C-4 specimens (Fig. 128) than there is for the corresponding C-3 specimens (Fig. 127).

From these data, the average differential strains were calculated for the two series. For sub-series C-3 the mortar-concrete differential was 200 μin./in. and the mortar-no-fines value was 350 μin /in , compared with corresponding values of 300 and 600 μin./in. for the C-4 specimens. No scaling was observed on any of the comparator specimens for these two series during the testing period.

The results of the sub-series C-5 axial tension tests for mortar specimens made using one part cement to one part sand by weight indicated an average ultimate tensile strength of 583 ± 7 psi for a maximum strain of 106 ± 3 μin./in. This corresponded to an average split cylinder tensile strength of 510 ± 27 psi. Both tests consisted of three specimens each.

Results from an earlier study using 1.3 mortar using the same apparatus resulted in average axial tensile strengths of 585 psi, with corresponding ultimate strains of 200 μin./in. (*28*). The significance of these results is discussed in Chapter Five.

The results of the study of thermal length change differentials for non-air-entrained mortars, sub-series C-1, and air-entrained mortars, sub-series C-2, are shown in Figures 129 through 134.

The only mortar showing much difference in apparent thermal length change coefficients for non-air-entrained mortar (Fig. 129) was the 1:4 mortar consisting of one part cement to four parts sand by weight. It was seen to show a significant reduction in thermal contractions after about 11 cycles. Figure 131, a plot of the so-called cumulative thermal length change coefficients, shows that the results in Figure 129 can be somewhat misleading. The plot of cumulative length changes indicates that the 1:4 mortar began its continuous expansion after a small number of cycles, which eventually resulted in failure. The same expansion tendency was seen for the 1:3 mortar in Figure 131 after 70 freeze-thaw cycles. The plots of data for the air-entrained mortars (Figs. 130, 132) do not show the same effect. Figure 130 shows very little difference in apparent thermal length change coefficients after the first 18 cycles, however, up to that point the 1:2 mortar showed a tendency for greater contraction, followed by the 1.3 mortars, with the 1:4 mortar exhibiting the least contraction. Figure 132 shows very little cumulative length change differential for the three mortars. It should be noted that Figures 130 and 132 were of necessity plotted to different vertical scales to be compatible with Figures 129 and 131, respectively.

The results of the sonic tests for sub-series C-1 and C-2 (Figs. 133, 134) show clearly the difference in structural integrity between the air-entrained and non-air-entrained mortars. The curve for 1:4 mortar in Figure 133 indicates that the set of specimens began to experience deterioration after approximately 13 cycles and continued to deteriorate, as shown by the downward slope of the curve to failure. The initiation of deterioration for the 1:3 non-air-entrained mortars did not begin until after approximately 67 freeze-thaw cycles The relative dynamics modulus of the 1.2 mortar remained well above the unity line, although by the end of the study it was beginning to drop. This series of curves clearly indicates the value of using rich mortars to provide durability of plain non-air-entrained concrete. With respect to reinforced concrete, however, the use of rich mortars can result in a greater tendency to form shrinkage cracks, thereby permitting corrodents to reach the reinforcing and eventually producing accelerated deterioration due to spalling.

The results of sonic testing of air-entrained mortars (Fig. 134) showed very little difference in average values for the three mortars. Except for a drop in moduli at approximately 10 cycles, the curves remained well above unity, thereby indicating that the mortars remained durable over the period of testing. No single curve showed any clear tendency to remain below the others.

REINFORCEMENT CORROSION

The results of the two phases of the reinforcement corrosion study are discussed separately. The first sub-section includes the results of the pressure study. This study (which did not involve corrosion as such) was used to investigate modes of failure of concrete that could result from reinforcement corrosion. The second sub-section discusses the results of the accelerated corrosion study.

Pressure Study

The hydraulic pressures needed to crack the concrete above the slotted pipes are given in Table 9. The three basic types of failures observed were as follows:

1. Trench type.—Failure consisting of curved surfaces extending upward from the pipe slot to the finished surface

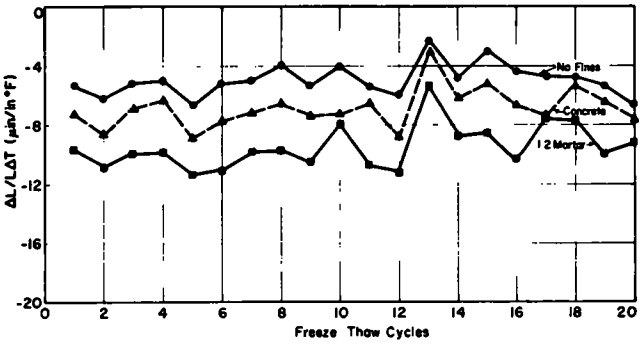

Figure 127. Thermal length change data, sub-series C-3 (X-10). Average of four specimens for temperatures of 64 F to −15 F.

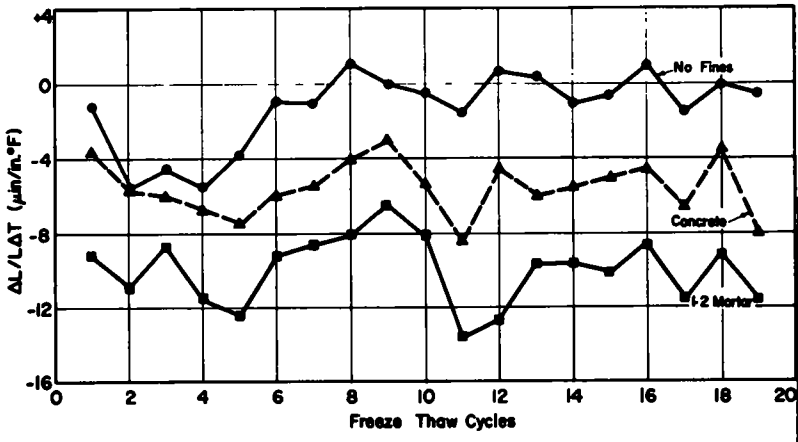

Figure 128. Thermal length change data, sub-series C-4(X-12). Average of three specimens for temperatures of 70 F to 0 F.

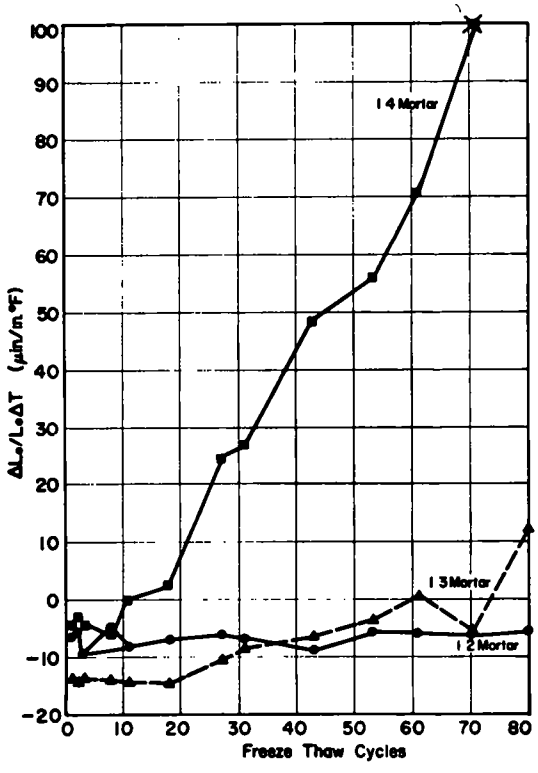

Figure 131 Thermal length change data, sub-series C-1, mortars. Average of three specimens for temperatures of 70 F to 20 F

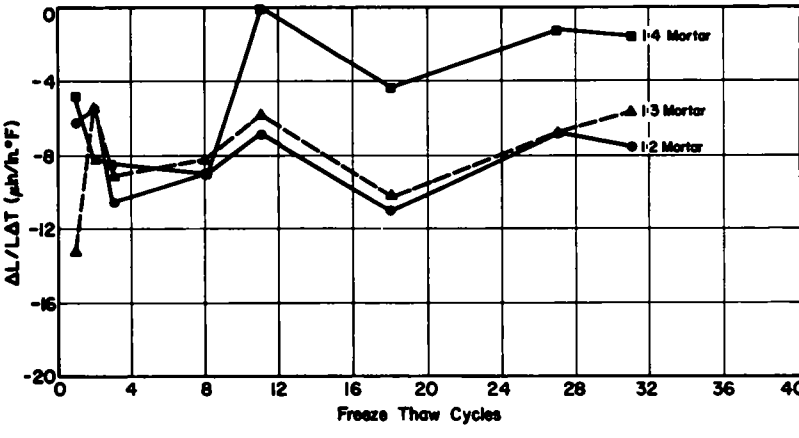

Figure 129 Thermal length change data, sub-series C-1, mortar Average of three specimens for temperatures of 70 F to 20 F.

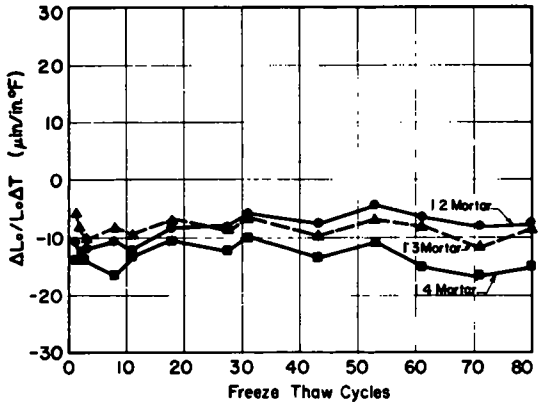

Figure 132. Thermal length change data, sub-series C-2, air-entrained mortars. Average of three specimens for temperatures of 70 F to 20 F

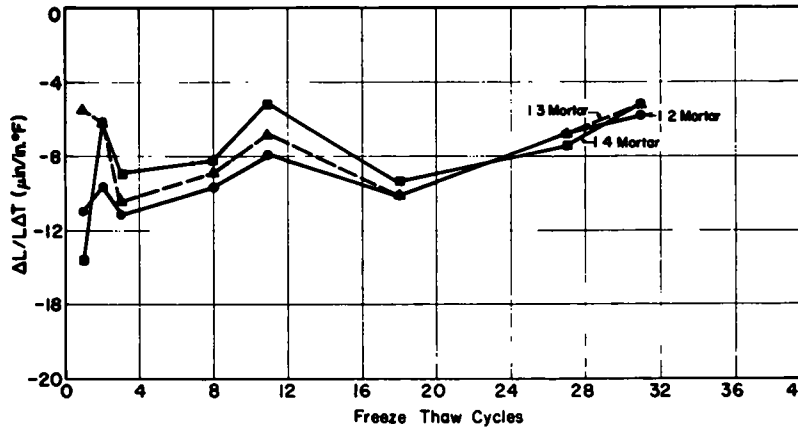

Figure 130 Thermal length change data, sub-series C-2, air-entrained mortar Average of three specimens for temperatures of 70 F to 20 F

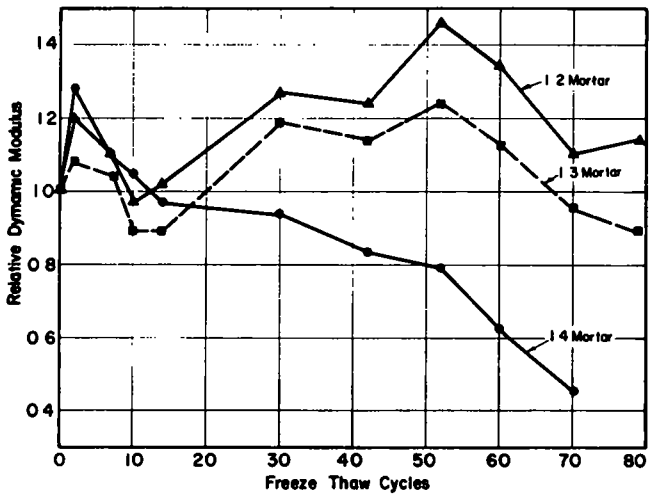

Figure 133. Sonic test data, sub-series C-1, mortars. Average of three specimens for temperatures of 70 F to 20 F

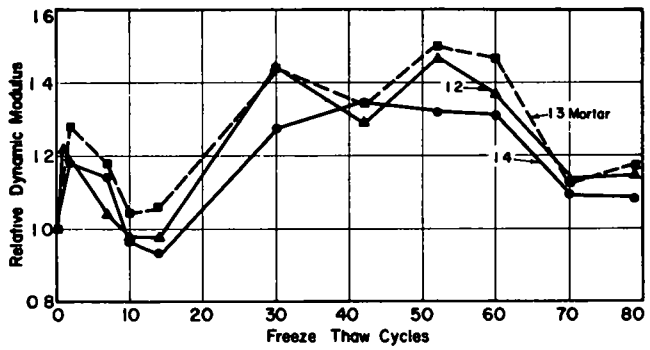

Figure 134. Sonic test data, sub-series C-2, air-entrained mortars Average of three specimens for temperatures of 70 F to 20 F.

of the slab. Generally, a vertical crack was formed directly above the pipe.

2. Horizontal cracking.—Consisting of a crack propagating along the tops of the pipes, forming a plane approximately parallel to the finished surface.

3. Vertical cracking.—Extending downward to the top of the pipe from the finished surface and extending downward from the bottom of the pipe, forming a vertical plane passing through the pipe center.

The specimens of sub-series E-1, E-2, and E-3 which were cast without lateral reinforcement failed primarily by vertical cracking. Only the specimens in these series having concrete covers of ¾ in. or less experienced the other types of failures; therefore, only these specimens and those from the remainder of the sub-series containing lateral reinforcing were included in the final analysis.

Variations of the three basic crack patterns were frequently observed. Often a trench type of failure would occur on one side of a pipe and a horizontal crack would run to the adjacent pipe on the other side (Fig. 135). The vertical crack shown between the pipes in this photograph is a saw cut that was made after testing. The trench-type failures occurred primarily over pipes having 1 in. of concrete cover or less. Specimens having concrete covers of 1¼ and 1½ in. failed for the most part by horizontal cracking. Many of the specimens with 1½ in. or more of cover failed by vertical cracking, even when lateral reinforcing was present, although the pressure necessary for either type of failure was approximately the same. It was observed that the series containing the 1½-in. maximum size aggregates failed more consistently by horizontal cracking than did those consisting of ¾-in. aggregate.

Figure 136 is a plot of the results for all specimens not previously excluded from the analysis. A regression line was determined for the data using the method of least squares (*29*). The 99.7 percent confidence lines were then determined and plotted as shown in Figure 136. The upper confidence line was then extrapolated to a pressure value of 4.7 ksi. This is the pressure required to stop the corrosion reaction. It was found that the amount of cover corresponding to this pressure was 4¼ in. Sub-series E-100 was then cast from the X-14 batch of ready-mixed concrete. Subsequent testing of these specimens disclosed that an average pressure of 2,180 psi caused a horizontal failure between the pipes. This pressure was less than half the value needed to inhibit corrosion. Although the strength of the X-14 concrete was below the average for the simulated bridge deck study, the mode of failure (i.e., by horizontal cracking) is an indication that the cracking pressure is primarily a function of pipe (or bar) spacing rather than cover thickness. Therefore, extrapolation as was used to obtain the 4¼-in. cover for the E-100 specimens should not be used for covers greater than 2 in.

Corrosion Study

The results of the corrosion study are given in Table 10. The weight losses and percentage crack expansions for various amounts of concrete cover and crack spacings show little in the way of a trend. Less crack expansion was recorded for the wide cracks for every depth of cover, except ½ in., than for the narrow cracks. The average weight loss due to corrosion also appeared to be greater for the narrow cracks. The three bars shown as having no concrete cover had one-third of their surface directly exposed to salt solution, which resulted in an average weight loss of only 3.0 grams.

AIR VOID DISTRIBUTION

Cores from unstressed slabs of sub-series X-6, X-7, X-9, and X-11 of the simulated bridge deck study were sliced at various depths, and the top of each slice was prepared for air void counting. The depths of the various readings were measured from marks made before slicing of the cores. The results of these air void counts are given in Table 11.

Probably the best measure of uniformity of air distribution is shown by paste air contents, because the paste contents of concrete will vary with depth. This is shown in Table 11 by comparing the paste contents of the various cores at the finished surface with those at particular depths.

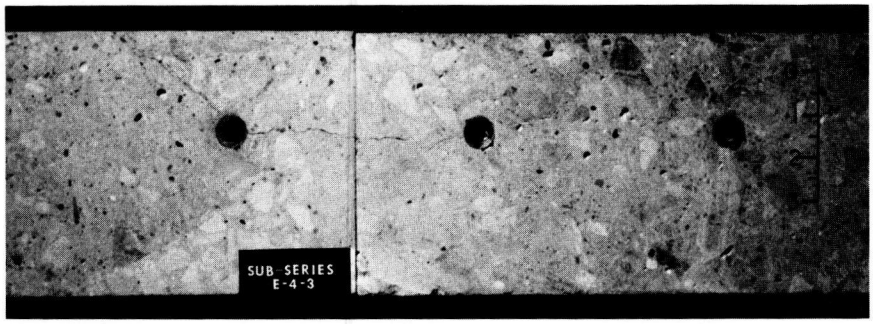

Figure 135. Pressure study specimen.

For each core the paste contents at lower depths decreased abruptly from the value for the finished surface.

Sub-series X-16 showed extremely high paste air contents for the 4.13- and 5.13-in. readings. There was apparently a high accumulation of air at the bottom of the slab. Because the slump of the concrete used in this slab was 5½ in., it is doubtful that the high readings would be due to entrapped air. The paste air content distribution was reasonably uniform for the other three cores; however, for all four cores the top surface paste air contents were consistently lower than the readings made at slightly over 1 in. below the finished surface. The X-7 core showed the most severe decrease of paste air content at the finished surface, and yet this was one of the most durable slabs of the simulated bridge deck study.

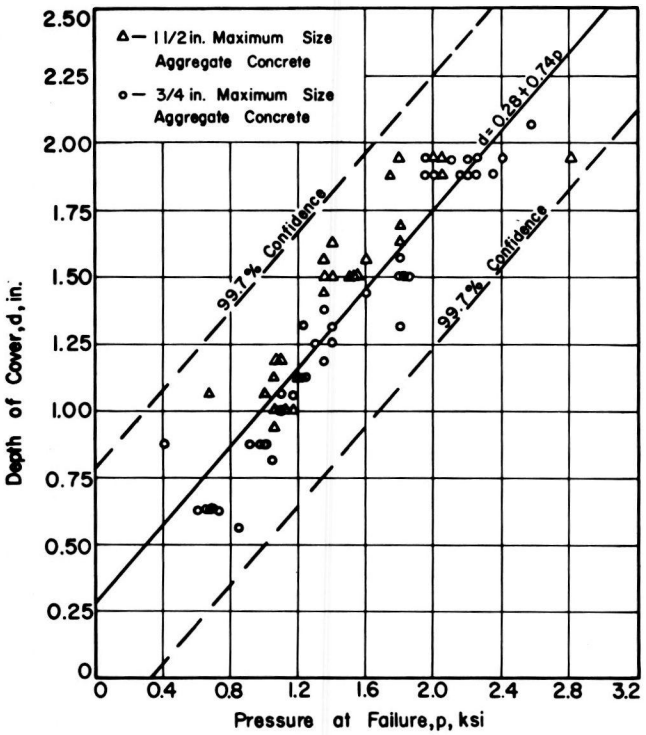

Figure 136. Combined results of pressure studies for concrete having lateral reinforcement.

WETTING AND DRYING

These studies were intended to determine if cyclic wetting and drying at various stages of freeze-thaw testing might have an adverse effect on concrete durability.

Figure 137 shows the average results for sub-series A-4. The beneficial effects of the cyclic air drying appear to be a continuation of the processes observed by Malisch (*6*). The rate of deterioration, as measured by percentage weight change, of the specimens subjected to continuous immersion was much greater than for the cyclically dried specimens. The weights of individual specimens are given in Table 12.

The results in Figure 138, however, show a different trend. The figure is divided into two sets of curves. The two curves for A-2V specimens represent the results of specimens treated the same as those in Figure 137 by having not been subjected to freezing and thawing prior to this test. The same results are seen for these two sets as was seen for the sub-series A-4 specimens, with the continuously immersed specimens, A-2VW, showing a much faster

TABLE 11

AIR VOID DISTRIBUTION DATA

Sub-series	Specimen Number	Surface Depth in.	Air Content %	Paste Content %	Per cent Air in Paste %	Spacing Factor in.
X-6	A	0.03	7.8	45.3	17.2	0.0077
	B	1.13	6.1	31.5	19.4	0.0072
	C	2.00	3.8	24.6	15.4	0.0060
	D	3.13	4.7	28.1	16.7	0.0061
	E	4.13	6.9	20.4	33.8	0.0057
	F	5.13	8.5	22.1	38.5	0.0051
X-7	A	0.09	2.9	40.3	7.2	0.0094
	B	1.19	3.6	32.0	11.3	0.0093
	C	2.00	3.0	24.6	12.2	0.0084
	D	2.94	2.2	25.2	8.7	0.0073
	E	4.00	2.7	25.9	10.4	0.0067
	F	4.94	1.8	21.9	8.2	0.0068
X-9	A	0.05	2.3	45.7	5.0	0.0130
	B	1.44	1.8	22.9	7.9	0.0092
	C	2.63	2.8	19.8	14.1	0.0298
	D	3.56	1.1	28.0	3.9	0.0150
	E	4.63	1.8	22.3	8.1	0.0150
X-11	A	0.04	4.6	45.6	10.1	0.0090
	B	1.13	3.7	23.6	15.7	0.0074
	C	2.07	4.3	21.9	19.6	0.0088
	D	3.19	3.7	29.4	12.6	0.0089
	E	4.13	3.6	25.6	14.1	0.0069

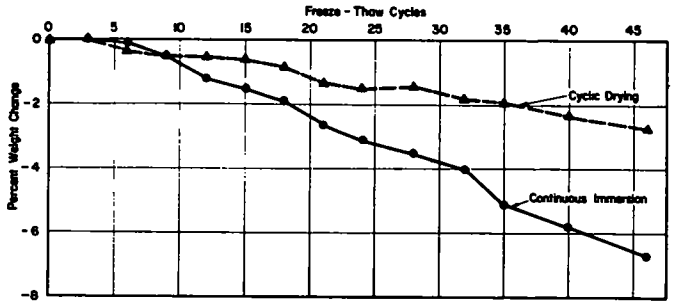

Figure 137. Effect of cyclic wetting and drying on freeze-thaw durability—sub-series A-4.

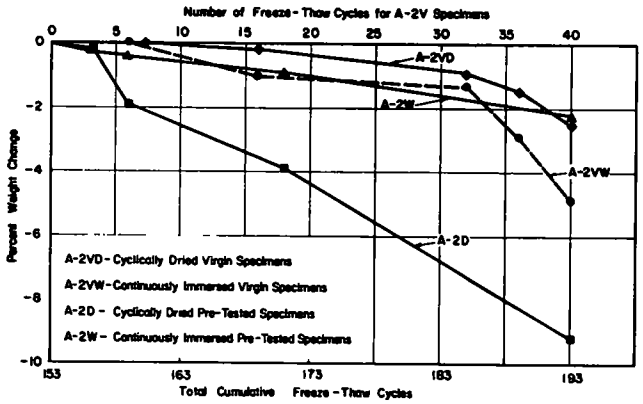

Figure 138. Effect of cyclic wetting and drying on freeze-thaw durability—sub-series A-2.

rate of deterioration than those subjected to periodic wetting and drying, specimens A-2VD. The remaining two curves were for specimens subjected to 153 freeze-thaw cycles prior to the wetting-drying study. The results of these two groups were the reverse of those seen for the A-2V specimens. It is thus evident that the cyclically dried specimens deteriorated at a significantly greater rate than those remaining continuously immersed. Although no observable damage was done to these specimens during their initial relatively mild freeze-thaw testing, they had apparently reached a condition such that cyclic wetting and drying, coupled with additional cycles of freezing and thawing, accelerated the rate of deterioration. The individual specimen weights are given in Table 13.

The remainder of the cyclic wetting and drying studies were conducted using sub-series X-13 and X-14 slabs.

The photographs of the sub-series X-13 slabs (Fig. 16) show that the 35 cycles of wetting and drying experienced prior to freeze-thaw testing did not adversely affect the freeze-thaw durability of either the stressed or unstressed specimen.

Slightly different conclusions can be made concerning the effect of the 30 cycles of wetting and drying after freeze-thaw testing of the 8-ft X-13 and X-14 slabs. The slab from sub-series X-14 had been severely cracked during freeze-thaw testing, whereas the X-13 slab contained fine cracks having an average width of 0.004 in. It was observed that toward the end of the wetting-drying period the X-13 slab began to experience scaling of a thin layer of surface mortar. Up to this time this slab had remained free of scaling. The more severely cracked X-14 slab did not experience any scaling during the period of the wetting-drying test. At the end of the 30 cycles, the concrete was removed from above the reinforcing bars in the region of the cracks. As shown in Figure 139, only a small amount of corrosion was observed on the surfaces of the bars. The locations of intersections of the bars with cracks could be traced easily by discoloration of the steel reinforcing of the X-14 slab and are indicated in the figures by small signs placed along the crack lines. In Figure 139a the region of bar discoloration was not as pronounced as for the X-14 slab (Fig. 139b) and it was distributed over larger sections of the bars. This was probably because the X-13 slab had earlier been subjected to 35 wetting-drying cycles while being cyclically loaded. A surprisingly small amount of corrosion was found on the bars of either slab.

TABLE 12

SUB-SERIES A-4 CYCLIC WETTING AND DRYING STUDY RESULTS

Number of Freeze-Thaw Cycles	Continuously Immersed		Cyclic Wetting and Drying		
	A-4-2	A-4-6	A-4-4	A-4-7	A-4-8
0	12 20	12 29	12 01	12 02	11 99
3	12 20	12 29	12 01	12 03	11 98
6	12 20	12 28	12.00	11 98	11 96
9	12 14	12 24	11.95	11 98	11.93
12	12 04	12 16	11 94	11 97	11 93
15	11 99	12 13	11 94	11.95	11 93
18	11 95	12 08	11 91	11 95	11 90
21	11 88	11 98	11 84	11 87	11 83
24	11 79	11 95	11 82	11 86	11 82
28	11 70	11 93	11.84	11 86	11 82
32	11 67	11 84	11 78	11 82	11 79
35	11 55	11 69	11 74	11 85	11 72
40	11 42	11 66	11 68	11 84	11 66
46	11 32	11 54	11 66	11.76	11 64

Specimens' SSD weight in lb.

TABLE 13

SUB-SERIES A-2 CYCLIC WETTING AND DRYING STUDY RESULTS

Number of Freeze-Thaw Cycles	Continuously Immersed				Cyclic Wetting and Drying		
	A2-1W	A2-2W	A2-3W	A2-VW*	A2-1D	A2-2D	A2-VD*
0	12 16	11 80	12 17	11 92	12 45	12 24	12 13
3	12 14	11 79	12 15		12 42	12 22	
6	12 11	11 74	12 13	11 92	12 20	12 02	12 13
16				11 80			12 10
18	12 08	11 64	12 09		11 96	11 77	
32				11 76			12 02
36				11 57			11 96
40	11 90	11 45	11 98	11 34	11 55	10 87	11 83

*The V denotes specimens not previously subjected to freeze-thaw cycles
Specimens' SSD weight in lb.

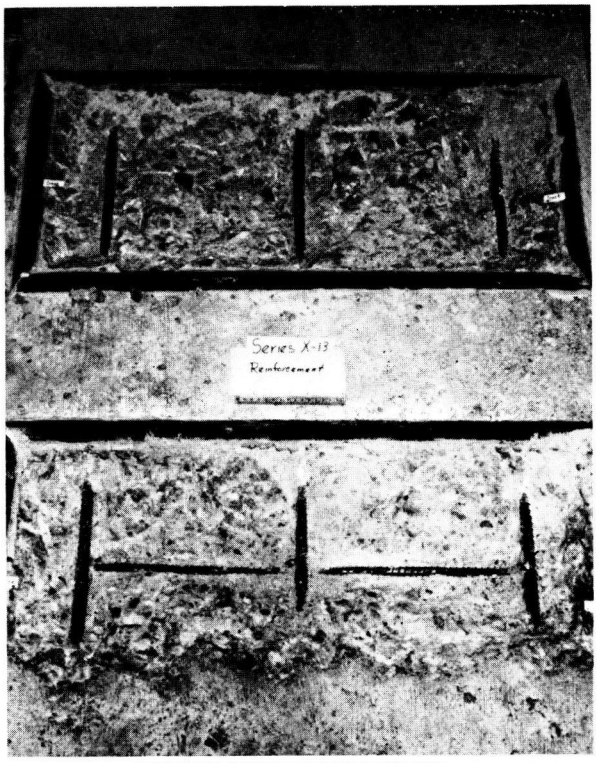

a. Sub-Series X-13

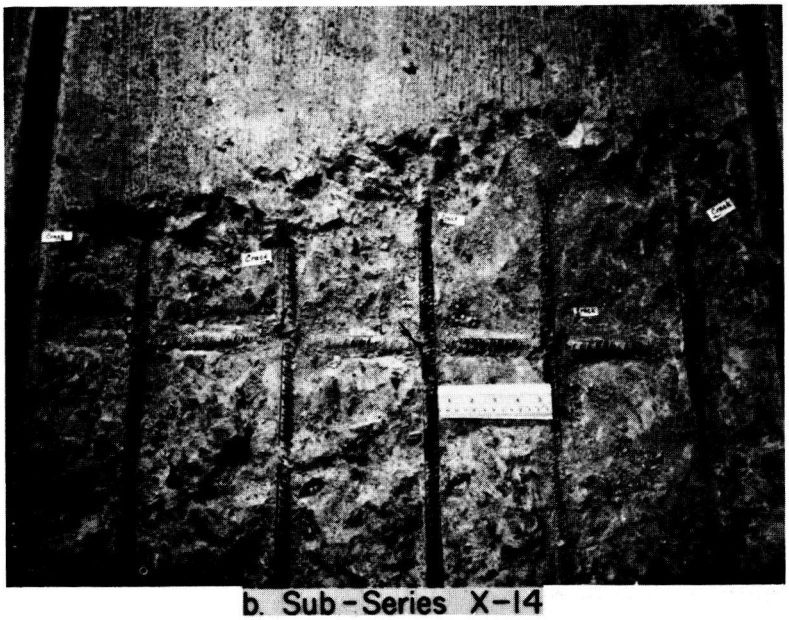

b. Sub-Series X-14

Figure 139. Reinforcement corrosion after cyclic wetting and drying.

CHAPTER FIVE

INTERPRETATION OF RESULTS

Several hypotheses have been proposed to explain deterioration which occurs during freezing and thawing of concretes exposed to deicing solutions. These hypotheses can be classified into the following categories:

1. Crystal growth.
2. Chemical reactions.
3. Hydraulic and related pressures.
4. Differential expansion and contraction.

The first two of these have been virtually eliminated as major causes through the results of research; however, several mechanisms remain under the last two categories that still offer reasonable explanations of the phenomena. Unfortunately, it is virtually impossible to explain all occurrences of deterioration due to freezing and thawing in the presence of deicers with a single mechanism. For this reason, after evaluating the data resulting from this study, together with additional laboratory and field survey data, two mechanisms of bridge deck deterioration for air-entrained concrete made from approved ingredients have been formulated. These two mechanisms are explained in this chapter and the results leading to their formulation are discussed.

INCOMPATIBILITY MECHANISM

There is a tendency during compacting and finishing operations to force coarse aggregate particles down, leaving a layer of mortar at the top surface of the concrete. This layer is usually ⅛ to ¼ in. thick, and conceivably could be thicker, depending on the quality of the concrete. Beneath the surface mortar is a material consisting of coarse aggregate and mortar. Because, in a properly designed concrete, the coarse aggregates should be as closely packed as possible and should have a gradation that provides slightly smaller particles to fill the spaces between the next larger sizes, the behavior of the underlying material will be characterized by the properties of the coarse aggregate, with only sufficient mortar to coat the coarse aggregates and fill the smaller voids. The remainder of this section discusses the behavior of concrete, based on the thesis that it is composed of a bi-layered system.

Visual inspection of the finished surfaces of the specimens in both the stressed surface study and the simulated bridge deck study after the normal two-week air-drying period showed that a pattern of surface cracking (Fig. 140) was present. This cracking can possibly be explained by examining the results given in Table 11. For all four of the cores represented the surface paste contents were considerably higher than the values for the remainder of the sections. The high paste content of the surface mortar could result in cracking because of differential shrinkage. The cracks were extremely fine and were revealed only after wetting the surface. However, microscopic examination of the cross section failed to reveal any penetration of these "cracks" below the surface.

The thermal length change study produced considerable information concerning possible thermal volume change characteristics of the mortar and coarse aggregate layers. The results of the tests conducted using sub-series C-3 were probably more representative of length change differentials developing in concrete during freeze-thaw testing of X Series specimens as well as of freezing and thaw-

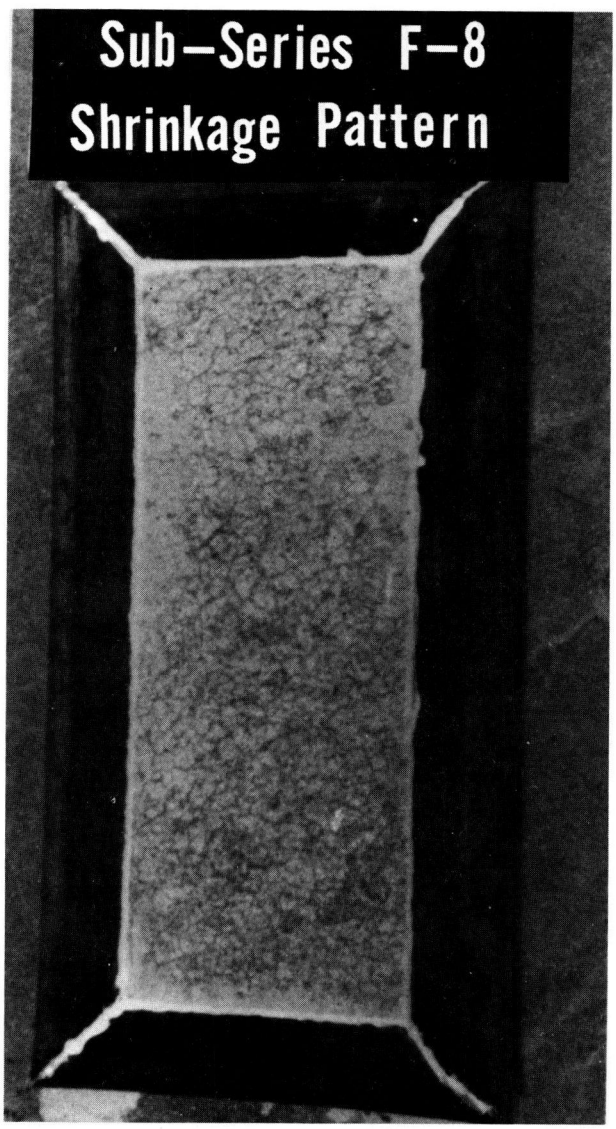

Figure 140. Finished surface crack pattern of moistened concrete.

ing under natural outdoor conditions. These specimens were allowed to remain for several hours at both the low and high temperature levels before comparator readings were made. This practice eliminates possible hygrothermal volume change effects (*27*, p. 12) which were probably responsible for the significantly greater length change differentials measured for the sub-series C-4 specimens. These results also demonstrate the need for exercising care in deciding on concrete durability based on the results of laboratory freeze-thaw testing using severe temperature cycles.

The two concretes used in casting sub-series C-3 and C-4 specimens were relatively durable, as shown by the results of the corresponding Series X tests. The cement-to-sand ratio of the mortar isolated from the X-10 concrete was found to be 1:1.8 by weight. The results of the sub-series C-5 direct tension test of 1.1 mortar indicated that the specimens failed at an average strain of 106 μin./in. Previous direct tension tests for 1:3 mortars indicated an average maximum strain of 200 μin./in. Thus, a reasonable value for the maximum strain for the C Series mortars would be 200 μin./in This value corresponded to the thermal strain differentials measured for the C-3 mortar and concrete specimens. Because the materials used in making these specimens were identical to those of the sub-series X-10, mortar and coarse aggregate layers, the differential strains measured correspond to the values needed to cause vertical cracking in the mortar layer. Because a cracking pattern already exists on the finished surface due to shrinkage effects, it is possible that thermal volume change differentials would assist in the propagation of these cracks through the surface mortar layer. When the cracks reach the coarse aggregate layer, the larger particles could act to "arrest" the vertical crack propagation and, with the help of the freezing and thawing of solution in the vertical cracks and voids, lead to cracking along a horizontal plane between the layers. [See Lott and Kesler (*31*) for a discussion of how aggregates function as crack arrestors.] The length of time needed to develop scaling would depend on the severity of shrinkage cracking and magnitude of the differential strain level.

The strain differential determined between the mortar and no-fines specimens represents the most extreme ultimate differential possible. This would occur when the coarse aggregate in the concrete had been compacted to the point that the limestone particles were in physical contact with each other. It can be seen that the resulting differential strains are almost twice the mortar-concrete differentials for both sub-series.

For differential strain levels below the fracture value, deterioration might not appear until after the number of freeze-thaw cycles necessary to produce fatigue failure had occurred. This would be aided by expansive forces produced during freezing of solution in the cracks and voids. Examples of concrete having a prolonged durable period prior to eventual scaling are shown in Figure 141. Sub-series B-12 and B-14 remained durable through 100 freeze-thaw cycles; however, during subsequent testing, specimens from both sub-series experienced a sudden scaling of the mortar layer.

The scaling of the sub-series X-13 slab during cycles of wetting and drying, as well as observations reported from both the field and the laboratory by Ryell (*32*), could have resulted from thermal cycling at a high temperature range accompanied by excessive rates of drying.

The presence of the types of salt concentration gradients shown in Figure 142 could also have a significant effect on thermal volume change characteristics which, depending on the magnitude of the concentration, could either increase or decrease thermal strain differentials between the layers.

There is the possible alternative that the thermal strain differentials between the two layers could remain low enough so that concrete would remain durable indefinitely. It is therefore important to examine the basic factors involved in the development of thermal incompatibilities.

The results in Table 11 indicate that the paste air content of the surface mortar was consistently lower than the values at greater depths in the concrete. It appears that for even a minimal amount of finishing, as was done on the X Series slabs, the paste air contents were reduced at the surface. Therefore, when the effects of excessive manipulations and additions of water during finishing are being considered, it appears that concretes having relatively high pressure air readings could be lacking sufficient entrained air at the surface to reduce differential strains between mortar and coarse aggregate layers.

Significant variations in the composition of the sand (Fig. 20) could also result in concrete having reasonably consistent air contents which would exhibit different degrees of durability This possibility was confirmed by Callan (*26*) who reported that

> . . concrete containing limestone coarse aggregates has shown a high resistance to laboratory freezing and thawing when sand manufactured from the limestone was used as the fine aggregate; on the other hand, combinations of the same coarse aggregates with natural sands as fine aggregates have low resistance in many cases.

He attributed this lack of durability to "differences in thermal expansion of the coarse aggregate and mortar."

In attempting to explain the great differences in durability of the various Series X concretes, every aspect of the material was examined. The supplier of the ready-mixed concrete indicated that he periodically observed erratic behavior of the electronic sensor used to determine the moisture content of the sand. It was found that these periods of erratic behavior corresponded to times when the excavator at the sand borrow pits was moved to a new location. It is possible that changes in basic composition of sand from this single source could be the cause of the drastic differences in durability observed during the simulated bridge deck study.

Based on the incompatibility mechanism, the effect of stress on durability can now be explained. Compressive stress of a static nature would have the effect of prestressing the mortar layer of the concrete so that it would be more difficult to produce cracking during freezing and thawing and would thereby lead to possible improvement in concrete durability. If, however, the strain differential is of

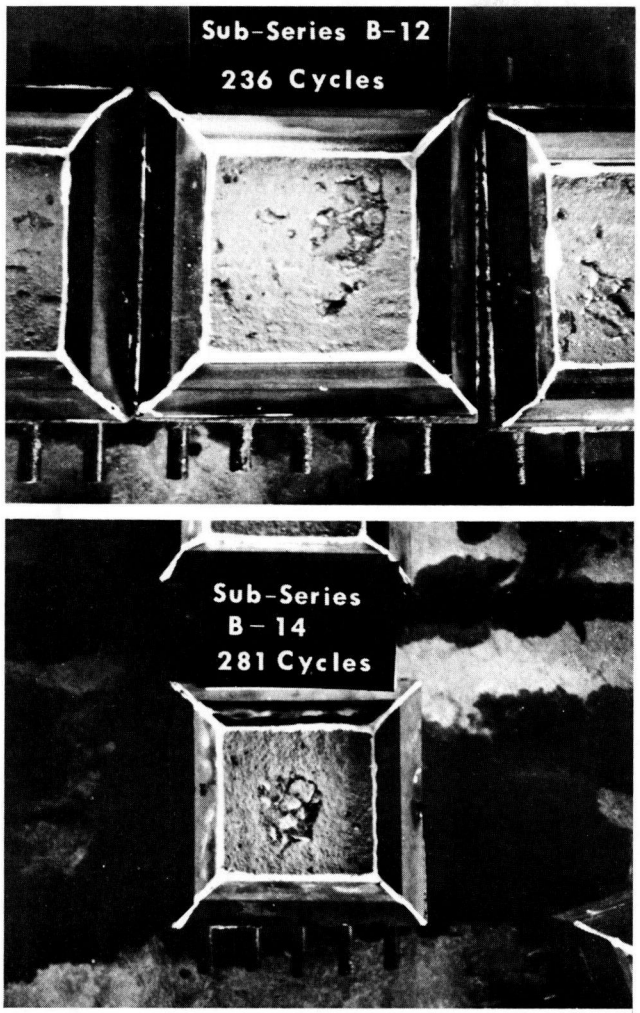

Figure 141. Weakened plane formation resulting from freeze-thaw testing in the presence of deicers.

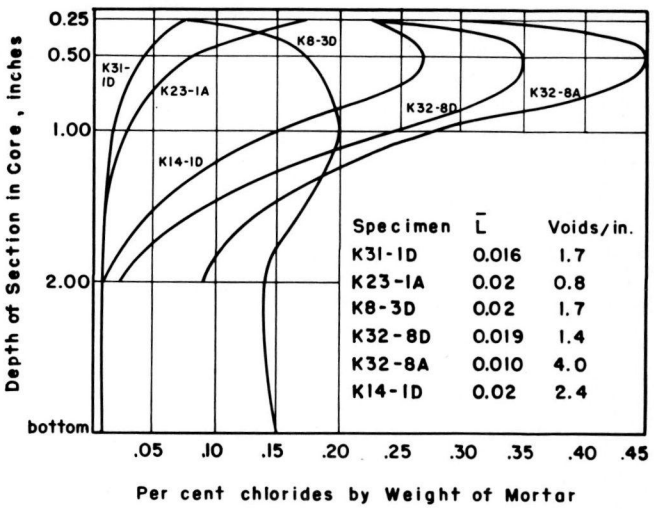

Figure 142. Measurement of salt concentration of cores from spalled and unspalled decks (11, 12).

sufficient magnitude to cause reversal, the initial compressive stress probably would not retard scaling. Static tensile stresses would tend to produce a detrimental condition by opening cracks and causing cracking to start at lower differential strains than for the unstressed case. Cyclic loading, however, would not necessarily result in the same effects as were seen in the static states.

It should be emphasized that the incompatability mechanism is intended to describe only the behavior of air-entrained concretes. The extreme differences in behavior of air-entrained and non-air-entrained concretes can be seen by comparing the results shown in Figures 131 and 132. The non-air-entrained mortars (Fig. 131) experienced a completely different effect during freezing and thawing, which resulted in expansions leading to deterioration. The pressure theories discussed in Chapter One adequately describe the mechanism of deterioration of these mortars. The air-entrained mortars (Fig. 132) remained in the contraction region. It is also interesting to note that during the first 12 cycles (Fig. 130), which is the period during which the greater portion of the Series X scaling occurred, the richer mortars experienced the greater contractions. This raises the question of the possibility that some optimum cement content might produce the greatest durability.

STRUCTURAL CRACKING MECHANISM

The second basic mechanism of deterioration of air-entrained concrete made from durable ingredients involves cracking of bridge deck slabs. Observations of numerous bridge decks in Illinois and the results of two of the published cooperative bridge deck surveys (*11, 13*) indicated that a predominant number of bridge decks have been cracked in the transverse direction. However, when the direction of critical stressing induced by traffic was analyzed (*33*) it was shown that the critical stresses would tend to produce cracking in the longitudinal direction. The stresses acting along transverse planes would be secondary in nature. Therefore, the transverse cracks are probably the result of either volume changes of the concrete, structural displacements other than those caused by live loads, or consolidation occurring while the concrete is in a plastic condition. It was found during the pressure study that vertical cracks directly above the reinforcing (Fig. 22a) were not difficult to produce in the laboratory for concrete covers of less than 1½ in. There is no doubt, as seen by first-hand observations, that, once formed, many of these cracks are repeatedly opened and closed by traffic action.

Observations of repairs along several major Chicago, Ill., freeways revealed an apparent relationship between bridge deck deterioration and transverse cracking. The examination of numerous sawed sections from which deteriorated concrete had been removed revealed a unique condition. The salt solution present on the bridge deck had penetrated through the ever-present transverse cracks to the level of the upper reinforcement. It was also noted that discoloration was present at the top of the reinforcement directly beneath these transverse cracks, indicating that corrosion had developed. This corrosion differed considerably from

that seen on removal of concrete from the 8-ft X-13 and X-14 slabs. For these two slabs the corrosion was found around the entire perimeter of the bars, whereas in the field observations the corrosion was confined primarily to the top surfaces. Also, because the cracks formed during the cyclic loading of X Series specimens corresponded to longitudinal cracks in a bridge deck, they did not occur along the upper (transverse) reinforcement. The observed field corrosion was more typical of that found during laboratory testing of corrosion study specimens having preformed cracks directly above the bars. The corrosion of reinforcement in the field produced cracking of the concrete along a horizontal plane at the top of the bar, which propagated toward the outer surface along roughly a parabolic path (Fig. 143). When reinforcement was spaced 1 ft on centers, these cracks eventually reached the finished surface of the slab and produced a trench-like failure; however, when the reinforcing was spaced 6 in. apart the tendency was for these cracks to connect with other cracks from adjacent bars and thus form a "weakened plane." When tapped with a metal tool, an area where this type of cracking had occurred would have a characteristic hollow sound. As corrosion of reinforcing and subsequent formation of concrete laminations occurred, little change was seen in the width of the original transverse cracks (Fig. 143). The finished surface of the concrete in which this type of deterioration occurred appeared to be free from flaking or surface scaling. It should be pointed out that this phenomenon had been observed on numerous occasions for shallow cover, but the cover measured on the Chicago freeways was approximately 2 in. in many areas. It should also be emphasized that these disruptions were not isolated cases but appeared on numerous structures throughout the freeway system.

Comparisons of the field observations with results of the pressure study indicated that the failures produced during the laboratory study closely approximated those observed in the field. The pressure study specimens were designed to simulate the pressures produced by corrosion at the tops of the transverse bars and, because the same types of failures resulted, it is reasonable to assume that the prescribed mechanism is valid.

Figure 143. Bridge deck deterioration resulting from reinforcement corrosion at transverse cracks.

CHAPTER SIX

CONCLUSIONS AND APPLICATIONS

Bridge deck deterioration not attributable to obvious violations of either materials or construction specifications can be divided into two classes:

1. The scaling of surface mortar.
2. Spalling of concrete due to corrosion of transverse reinforcement.

Stress will have a certain influence on both of these types of deterioration. In these tests static tensile stresses somewhat accelerated the rate of scaling, whereas static compressive and biaxial stresses slightly retarded the development of scaling. In contrast to cyclic tensile stresses which showed little influence, cyclic compressive stresses had an accelerating effect on the rate of scaling. Scaling can definitely result from freezing and thawing. On the other hand, stress affects spalling by providing the mechanical action for initiating and feathering cracks, and for feeding saline solution down to the level of the reinforcement. Once the salt solution gains access to the reinforcement the optimum conditions for the corrosion reaction consist of cyclic wetting and drying at the higher temperatures without the need of additional salt solution. The attempts to develop an accelerated corrosion study proved unsatisfactory; therefore, the laboratory studies could not be extended for the necessary time period required to observe spalling. The cracking of more highly stressed slabs was extensive, and mechanical action resulted in considerable feathering.

The most important conclusion from the results of this study is that *although stress appears to influence somewhat the rate of development of surface scaling, it is not a primary factor. The physical characteristics of the surface mortar compared with those of the coarse aggregate layer of the concrete appear to be the most important factor.* Concrete having a tendency to scale cannot be altered by superimposing a particular stress condition so that scaling can be entirely prevented. Conversely, concrete with no tendency to scale cannot be stressed to the point that scaling will occur.

Corrosion of reinforcement at transverse cracks and subsequent spalling of concrete appears to be the most serious problem with respect to durability of bridge decks. From all observations, transverse cracking of bridge decks is a common occurrence. These transverse cracks seem to result primarily from effects not related to vehicle loading, such as shrinkage and consolidation of plastic concrete. The time needed to develop spalling for bridge decks already having transverse cracking will depend on the frequency of deicer application, traffic density, and the depth of concrete cover. There is little doubt that spalling eventually will occur in regions where deicers are frequently used. It is also doubtful that this type of deterioration could be prevented by increasing the cover above the reinforcement, but this might delay its eventual development. An excessively high cement factor in bridge deck concrete would have little apparent remedial effect and could conceivably produce greater amounts of cracking because of increased shrinkage. Prevention of deterioration associated with transverse cracking can possibly be achieved through the use of some procedure, such as revibration, or by using corrosion-resistant reinforcement.

CHAPTER SEVEN

RECOMMENDATIONS FOR FURTHER STUDY

SURFACE SCALING

There is need for additional information concerning the influence of the basic composition of air-entrained concrete on freeze-thaw durability. If the physical characteristics of the sand prove to be a primary factor, it may be possible to prescribe a particular air content that would minimize the thermal length change differentials that may develop. The relative richness of mortars should be given a closer look to determine if it might also be a significant factor with respect to scaling of air-entrained concrete.

A study should be made to determine the significance of the observations made during batching of ready-mixed concrete concerning the ability of an electronic moisture sensor

to detect radical differences in the basic composition of sand. It is a possibility that, using some type of electrical resistance probe, natural sand borrow pits could be logged, and the regions containing excessively high amounts of undesirable materials could be rejected. A basic understanding of this phenomenon is needed.

SPALLING DUE TO REINFORCEMENT CORROSION

As far as can be determined, no laboratory investigation has successfully reproduced concrete spalling caused by corrosion of reinforcement. There is need for such a study to determine factors significantly affecting concrete spalling. The paramount problem is to devise a realistic method for accelerating reinforcement corrosion. A study could then be conducted using equipment similar to the environmental test unit described in this report, equipped with radiant heaters directly above the concrete finished surfaces. Using this apparatus, specimens under cyclic loading could be subjected to cycles of successive wetting, freezing, thawing, and drying. This type of test would be more likely to produce the desired reinforcement corrosion and would permit a study of the effects of such factors as crack width and reinforcement depth; it would also permit a study of the effectiveness of possible methods for preventing spalling, such as revibration of retarded concrete to re-close cracks, chemical methods of sealing of cracks, or the use of corrosion-resistant reinforcement.

Consideration should also be given to the possibility of prestressing bridge decks in the longitudinal direction, or the use of either chopped wire fibers or expansive cements as possible methods for minimizing or preventing the detrimental effects of transverse cracks.

REFERENCES

1. Britton, H. B., "The Problem of Bridge Deck Deterioration." *Roads and Streets,* Vol. 103, No. 5, pp. 92, 95-96 (May 1960).
2. Reagel, F. V., "Effects of De-Icing Chemicals on Structures." *HRB Bull. 323* (1962) pp. 1-2.
3. Spellman, D. L., and W. H. Ames, "Factors Affecting Durability of Concrete Surfaces." *Hwy. Res. Record No. 195* (1967) pp. 41-55.
4. Malisch, W. R., et al., *Physical Factors Influencing Resistance of Concrete to Deicing Agents. NCHRP Report 27* (1966) 41 pp.
5. Wuerpel, C. E., "Laboratory Studies of Concrete Containing Air-Entraining Admixtures." *Proc. Amer. Conc. Inst.,* Vol. 42, p. 345 (1946).
6. Malisch, W. R., "The Effect of Air Drying Upon the Freezing and Thawing Resistance of Concrete." Ph.D. Thesis, Univ. of Ill. (Aug. 1966) 62 pp.
7. Powers, T. C., "A Working Hypothesis for Further Studies of Frost Resistance of Concrete." *Proc. Amer. Conc. Inst.,* Vol. 41, pp. 245-272 (1945).
8. Kennedy, T. W., "Mechanisms of Concrete Scaling." Ph.D. Thesis, Univ. of Ill. (1965).
9. "Durability of Bridge Deck Concrete." Phase I of *Durability Studies of Structural and Paving Concretes,* Penn. State Univ. College of Eng. (Jan. 1965) 154 pp.
10. Hughes, R. D., and J. W. Scott, *Concrete Bridge Decks: Deterioration and Repair, Protective Coatings and Admixtures.* KYHR 64-2, -3, and -4; HRP 1 (1) Ky. Dept. of Highways Div. of Res. (June 1966) 246 pp.
11. *Durability of Concrete Bridge Decks.* A Cooperative Study, Report 1, Portland Cement Assn., State Highway Comm. of Kansas, and BPR (1965) 130 pp.
12. *Durability of Concrete Bridge Decks.* A Cooperative Study, Report 2, Portland Cement Assn., Mich. State Highway Dept., and BPR (1965) 94 pp.
13. *Durability of Concrete Bridge Decks.* A Cooperative Study, Report 3, Portland Cement Assn., Calif. Div. of Highways, and BPR (1967) 128 pp.
14. "Progress Report of Committee on Curing of Concrete Pavement Slabs." *Proc. HRB,* Vol. 10 (Dec. 1930) p. 370.
15. Adams, Andrew, "Durability of Concrete in Maine Bridges Built Since 1947." *Hwy. Res. Correlation Service, Circular 411,* Maine State Highway Comm., pp. 1-8 (Feb. 1960).
16. Lindsay, J. D., "A Survey of Air-Entrained Structures in Illinois." *HRB Bull. 323* (1962) pp. 12-14.
17. Faul, A. F., and T. E. McElherne, "Survey Technique and Iowa Experience." *HRB Bull. 323* (1962) pp. 19-22.
18. Aten, C. E., "Visual Examination of Structural Damage in Wisconsin." *HRB Bull. 323* (1962) pp. 15-18.
19. Cordon, W. A., "Freezing and Thawing of Concrete: Mechanism and Control." *Monograph No. 3,* Amer. Conc. Inst. (1966).
20. Kennedy, T. B., "Tensile Crack Exposure Tests of Stressed Reinforced Concrete Beams." *Proc. Amer. Conc. Inst.,* Vol. 52, pp. 1049-1063 (1955-56).
21. Rieb, S. L., "Preparation and Durability Testing of Pretensioned Prestressed Concrete." *J. Prestressed Conc. Inst.,* Vol. 4, No. 3, pp. 102-126 (Dec. 1959).

22. GUTZWILLER, M. J., and F. E. MUSLEH, "Freezing and Thawing Effects of Prestressed Concrete." *J. Struc. Div.*, ASCE, Vol. 86, St. 10, pp. 109-124 (Oct. 1960).
23. MOSKVIN, V. M , and A. M. PODVALNYI, "Concerning the Frost Resistance of Concrete in a Stressed State." *Beton i Zhelezobeton*, Vol. 2, pp. 58-64 (1962).
24. Moss, M. E , *Prestressed Concrete Durability and Corrosion.* Mont. State Highway Dept , BPR, and Mont. State Univ (1966) 217 pp
25. ROSHORE, E. C , "Durability and Behavior of Prestressed Concrete Beams." *Tech. Report No. 6-570,* Post-tensioned Conc. Investig Progress to July 1966, Report 2, U.S. Army Waterways Exper. Sta. (Mar 1967) 14 pp.
26. CALLAN, E. J., "Thermal Expansion of Aggregates and Concrete Durability." *Proc., Amer. Conc. Inst.*, Vol 48, pp. 485-499 (Feb. 1952).
27. POWERS, T C., "The Physical Structure and Engineering Properties of Concrete." *Portland Cement Assn. Res. Bull. No. 90* (July 1958) 28 pp
28 RYDER, J. T., "A Direct Tensile Test for Cement Mortar and Paste." *Seventh Student Symposium on Engineering Mechanics,* Dept of Theoretical and Applied Mechanics, Univ. of Ill. (June 1967).
29. SPIEGEL, M. R., "Statistics." *Schaums Outline Series,* Schaum Publ. Co., N Y. (1961).
30. TREMPER, B., J. L. BEATON, and R. F. STRATFULL, "Causes and Repair of Deterioration to a California Bridge Due to Corrosion of Reinforcing Steel in a Marine Environment—Part II: Fundamental Factors Causing Corrosion." *HRB Bull. 182* (1958) pp. 18-41.
31. LOTT, J. L., and C. E. KESLER, "Crack Propagation in Plain Concrete." *Report No. 648,* Dept. of Theoretical and Applied Mechanics, Univ. of Ill. (Aug. 1964).
32. RYELL, J., "An Unusual Case of Surface Deterioration on a Concrete Bridge Deck." *Proc. Amer. Conc. Inst ,* Vol. 62, p. 421 (1965).
33. REJALI, M. H M., "Distribution of Transverse Moments on Concrete Bridge Decks." Master's Thesis, Univ of Ill. (1966).
34. BROMS, B. B , "Stress Distribution in Reinforced Concrete Members with Tension Cracks." *Proc. Amer. Conc. Inst ,* Vol 62, pp. 1095-1107 (1965).

APPENDIX A

SURFACE STRESS EVALUATION—STRESSED SURFACE STUDY

To determine if the load frames used for the various stressed surface specimens produced the desired stress conditions, a series was cast from the same concrete and using the same casting and curing procedures that were used for sub-series T-5. Series A specimens were not included in this study.

The ½-in bolts used in the axially loaded specimens of the B Series consisted of AISI-SAE 4340 high-strength steel for compression specimens and AISI-SAE M-1020 mild steel for tension specimens

The reinforcing used in both flexural and torsional specimens (F and T Series) was Number 2 intermediate grade deformed bars conforming to ASTM Designations A 15-64 and A 305-64.

Prior to casting, the reinforcement was prepared by grinding areas until they were smooth. Electrical resistance gauges were then attached to these areas of the reinforcing and to the ½-in. bolts at the locations shown in Figures A-2, A-4, A-6, and A-7. These gauges were all subsequently waterproofed with melted tar.

Following curing, the finished surfaces of the concrete were smoothed and electrical resistance strain gauges were attached at the locations shown in Figures A-1, A-3, A-5, A-6, and A-7.

The specimens were placed into their respective frames and loaded using a torque wrench in the manner followed for the various stressed surface specimens. The resulting strains were recorded for their respective loads.

The results of this study can be seen in Figures A-1 through A-7. All gauges were placed at either the longitudinal mid-point or one-third point locations, as shown in the figures. Because specimens were loaded by means of a torque wrench, the results are shown as plots of load torque versus corresponding strain values. The torques used to stress the various stressed surface specimens are noted on the curves.

Figures A-1 and A-2 show results of the B Series uniaxial tensile study. The strains recorded by gauges attached to the concrete (Fig. A-1) indicate that, for torques of from 275 to 300 in-lb, the concrete was subjected to a stress reversal. Prior to this level the strain increased in proportion to the torque; however, when tensile cracking was initiated, a sudden redistribution of stress occurred which resulted in the steel assuming additional tensile force, as

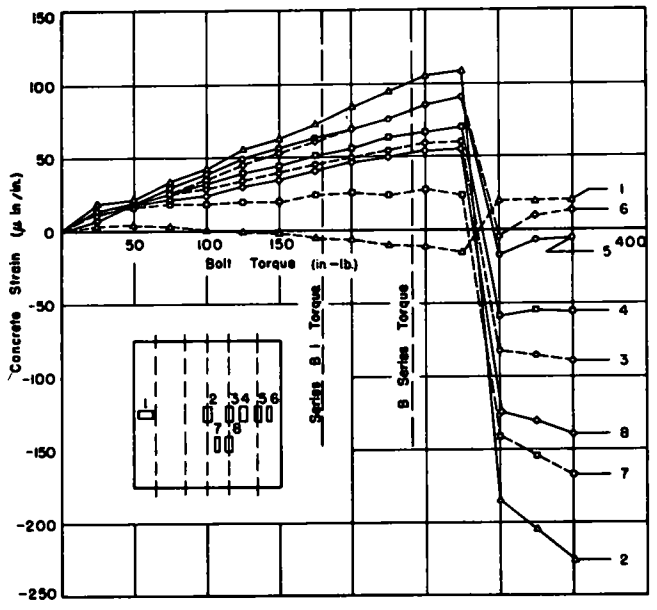

Figure A-1. Strain gauge analysis results and gauge locations for the concrete of B Series tension specimens.

indicated by the rapid increase in steel strain shown in Figure A-1. The concrete was then subjected to compressive stresses at the finished surface. Although these results appeared to be unique, similar observations had been made by Broms, who previously had described the cause as a redistribution of stresses during cracking of a tension member (*34*). As noted on the figures, all of the B Series uniaxially stressed specimens (except those of sub-series B-1) were subjected to a tensile stress in the proximity of that necessary for stress reversal. As can be seen by strength variations between B series mixes, it is possible that although cracks were not visible many of the tensile specimens may have been cracked, which, in turn, would mean that a portion of the diked surface could have been in compression rather than in tension.

The results of the compression strain gauge study of the uniaxially stressed specimens were less spectacular and much more desirable than the tension results. The strains recorded at various locations on the concrete surface yielded fairly consistent values over the cross section, and the strains recorded in the direction normal to the plane of principal stress were reasonably low. Therefore, it is safe to assume that the axially loaded compression specimens were subjected to the desired stress condition.

The strain readings recorded for the torsion test apparatus in the two principal stress directions indicated that the desired stress condition was achieved, as shown in Figure A-5. It should be noted that the strains for gauges number 1 and 2 were positive, whereas those for gauge number 3 were negative. The strains were plotted as absolute values in order to compare magnitudes, which ideally should be the same.

The data for flexural specimens are shown in Figures A-6 and A-7. The specimens subjected to tension on top revealed that cracking of the particular concrete used in this study occurred in the range of torque applied to all flexural tension specimens. In contrast to the uniform tensile study, these specimens were not subjected to a stress reversal after cracking occurred.

The results of the strain gauge study of flexural loading producing compression on the diked surface indicated that the desired stressing condition was produced.

It can be concluded from the surface stress evaluation that the results of freeze-thaw testing of the B Series axially

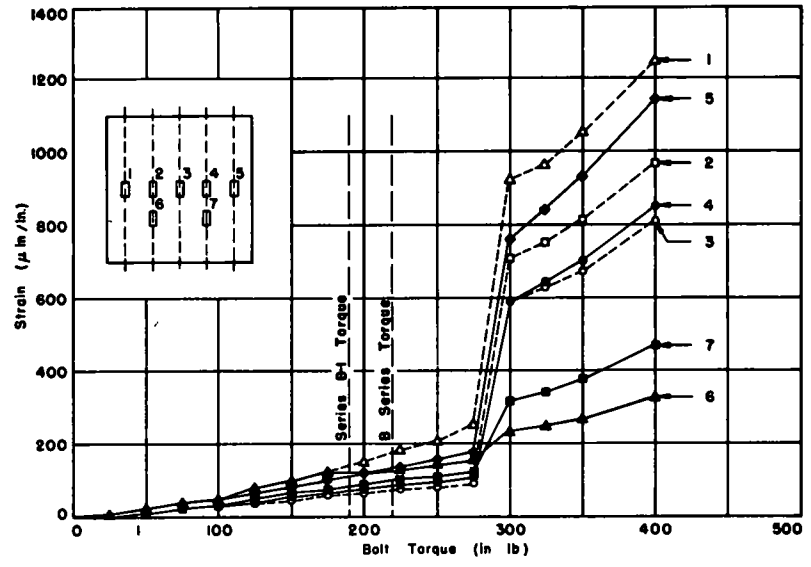

Figure A-2. Strain gauge analysis results and gauge locations for the reinforcing of B Series tension specimens.

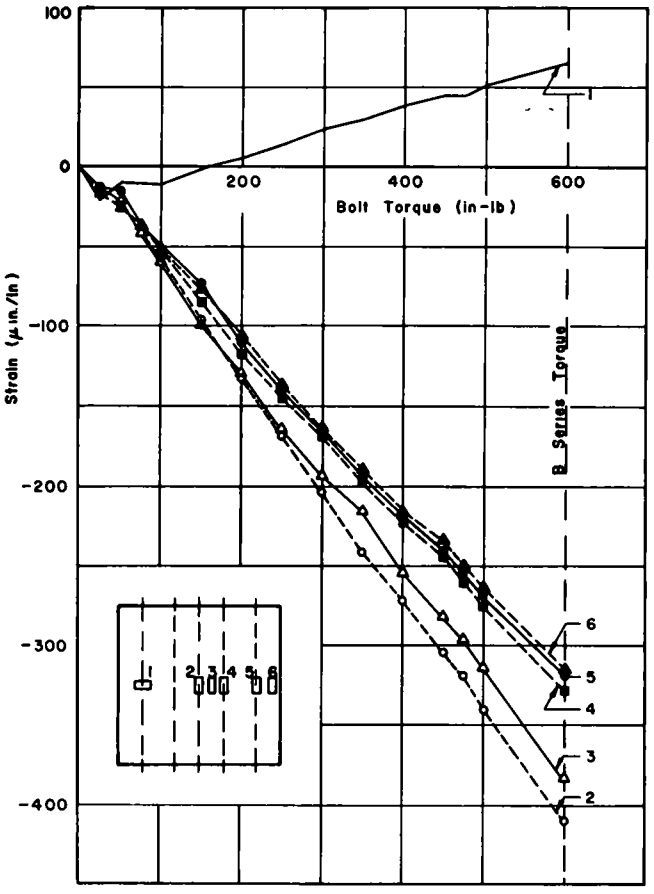

Figure A-3. Strain gauge analysis results and gauge locations for the concrete of B Series compression specimens.

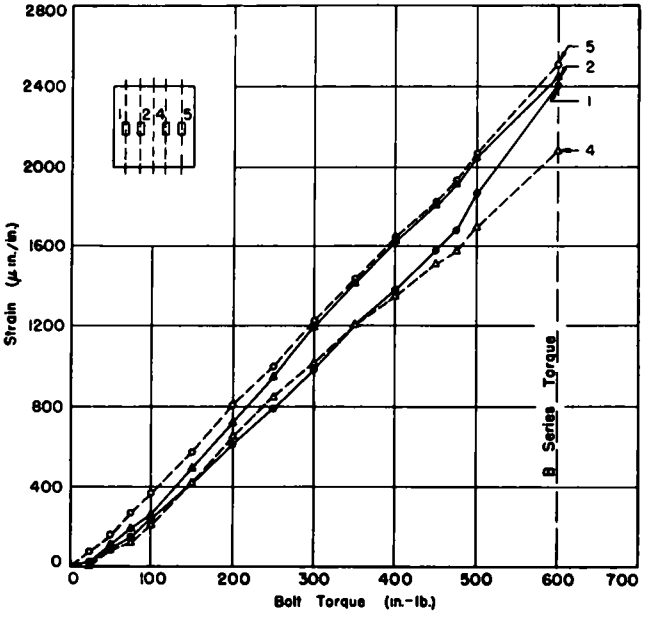

Figure A-4. Strain gauge analysis results and gauge locations for reinforcing of B Series compression specimens.

stressed specimens in tension should not be considered conclusive as to the effect this particular stress condition might have on freeze-thaw durability. Also, the flexurally stressed specimens having tension on the top surface should not be considered to show any absolute measure of differences between cracked and uncracked tension conditions, because small cracks possibly could have escaped detection in the case of the specimens assumed to have been uncracked.

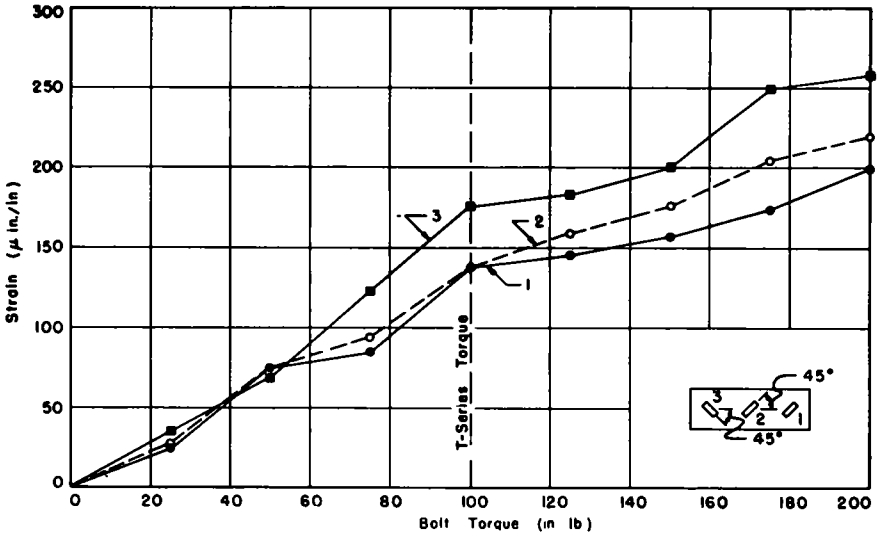

Figure A-5. Strain gauge analysis results and gauge locations for concrete of T Series torsion specimens.

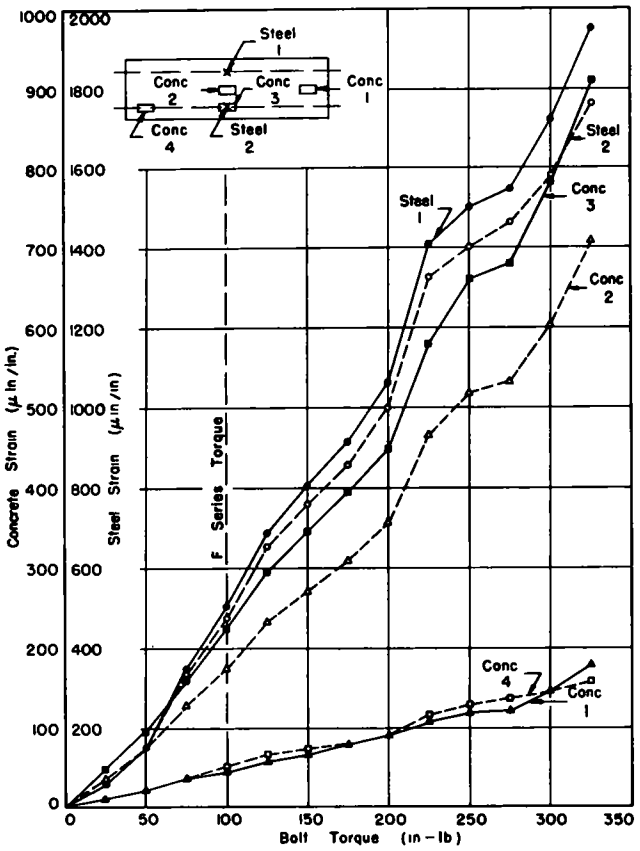

Figure A-6. Strain gauge analysis results and gauge locations for concrete and steel of F Series flexural specimens having compression on top

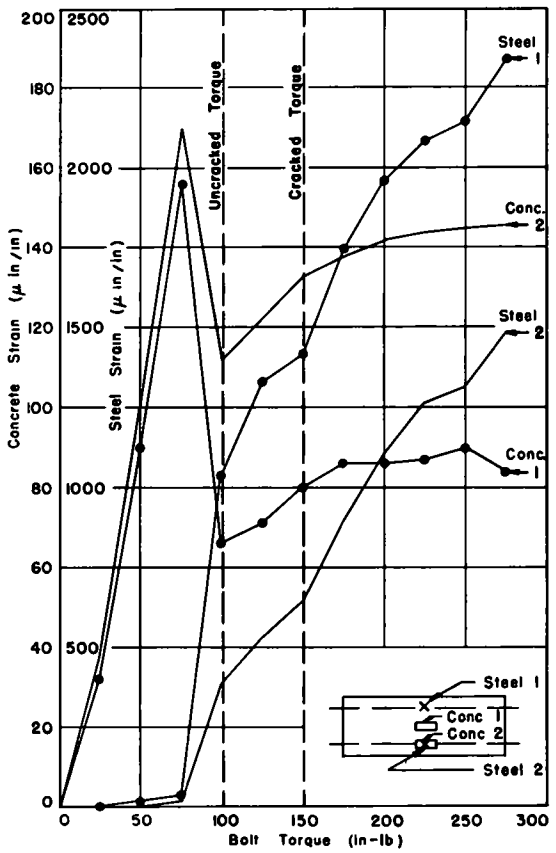

Figure A-7. Strain gauge analysis results and gauge locations for concrete and steel of F Series flexural specimens having tension on top.

Published reports of the

NATIONAL COOPERATIVE HIGHWAY RESEARCH PROGRAM

are available from:

Highway Research Board
National Academy of Sciences
2101 Constitution Avenue
Washington, D.C. 20418

Rep. No. *Title*

—* A Critical Review of Literature Treating Methods of Identifying Aggregates Subject to Destructive Volume Change When Frozen in Concrete and a Proposed Program of Research—Intermediate Report (Proj. 4-3(2)), 81 p., $1.80

1 Evaluation of Methods of Replacement of Deteriorated Concrete in Structures (Proj. 6-8), 56 p., $2.80

2 An Introduction to Guidelines for Satellite Studies of Pavement Performance (Proj. 1-1), 19 p., $1.80

2A Guidelines for Satellite Studies of Pavement Performance, 85 p.+9 figs., 26 tables, 4 app., $3.00

3 Improved Criteria for Traffic Signals at Individual Intersections—Interim Report (Proj. 3-5), 36 p., $1.60

4 Non-Chemical Methods of Snow and Ice Control on Highway Structures (Proj. 6-2), 74 p., $3.20

5 Effects of Different Methods of Stockpiling Aggregates—Interim Report (Proj. 10-3), 48 p., $2.00

6 Means of Locating and Communicating with Disabled Vehicles—Interim Report (Proj. 3-4), 56 p. $3.20

7 Comparison of Different Methods of Measuring Pavement Condition—Interim Report (Proj. 1-2), 29 p., $1.80

8 Synthetic Aggregates for Highway Construction (Proj. 4-4), 13 p., $1.00

9 Traffic Surveillance and Means of Communicating with Drivers—Interim Report (Proj. 3-2), 28 p., $1.60

10 Theoretical Analysis of Structural Behavior of Road Test Flexible Pavements (Proj. 1-4), 31 p., $2.80

11 Effect of Control Devices on Traffic Operations—Interim Report (Proj. 3-6), 107 p., $5.80

12 Identification of Aggregates Causing Poor Concrete Performance When Frozen—Interim Report (Proj. 4-3(1)), 47 p., $3.00

13 Running Cost of Motor Vehicles as Affected by Highway Design—Interim Report (Proj. 2-5), 43 p., $2.80

14 Density and Moisture Content Measurements by Nuclear Methods—Interim Report (Proj. 10-5), 32 p., $3.00

15 Identification of Concrete Aggregates Exhibiting Frost Susceptibility—Interim Report (Proj. 4-3(2)), 66 p., $4.00

16 Protective Coatings to Prevent Deterioration of Concrete by Deicing Chemicals (Proj. 6-3), 21 p., $1.60

17 Development of Guidelines for Practical and Realistic Construction Specifications (Proj. 10-1), 109 p., $6.00

18 Community Consequences of Highway Improvement (Proj. 2-2), 37 p., $2.80

19 Economical and Effective Deicing Agents for Use on Highway Structures (Proj. 6-1), 19 p., $1.20

20 Economic Study of Roadway Lighting (Proj. 5-4), 77 p., $3.20

21 Detecting Variations in Load-Carrying Capacity of Flexible Pavements (Proj. 1-5), 30 p., $1.40

22 Factors Influencing Flexible Pavement Performance (Proj. 1-3(2)), 69 p., $2.60

23 Methods for Reducing Corrosion of Reinforcing Steel (Proj. 6-4), 22 p., $1.40

24 Urban Travel Patterns for Airports, Shopping Centers, and Industrial Plants (Proj. 7-1), 116 p., $5.20

25 Potential Uses of Sonic and Ultrasonic Devices in Highway Construction (Proj. 10-7), 48 p., $2.00

26 Development of Uniform Procedures for Establishing Construction Equipment Rental Rates (Proj. 13-1), 33 p., $1.60

27 Physical Factors Influencing Resistance of Concrete to Deicing Agents (Proj. 6-5), 41 p., $2.00

28 Surveillance Methods and Ways and Means of Communicating with Drivers (Proj. 3-2), 66 p., $2.60

29 Digital-Computer-Controlled Traffic Signal System for a Small City (Proj. 3-2), 82 p., $4.00

30 Extension of AASHO Road Test Performance Concepts (Proj. 1-4(2)), 33 p., $1.60

31 A Review of Transportation Aspects of Land-Use Control (Proj. 8-5), 41 p., $2.00

32 Improved Criteria for Traffic Signals at Individual Intersections (Proj. 3-5), 134 p., $5.00

33 Values of Time Savings of Commercial Vehicles (Proj. 2-4), 74 p., $3.60

34 Evaluation of Construction Control Procedures—Interim Report (Proj. 10-2), 117 p., $5.00

35 Prediction of Flexible Pavement Deflections from Laboratory Repeated-Load Tests (Proj. 1-3(3)), 117 p., $5.00

36 Highway Guardrails—A Review of Current Practice (Proj. 15-1), 33 p., $1.60

37 Tentative Skid-Resistance Requirements for Main Rural Highways (Proj. 1-7), 80 p., $3.60

38 Evaluation of Pavement Joint and Crack Sealing Materials and Practices (Proj. 9-3), 40 p., $2.00

39 Factors Involved in the Design of Asphaltic Pavement Surfaces (Proj. 1-8), 112 p., $5.00

40 Means of Locating Disabled or Stopped Vehicles (Proj. 3-4(1)), 40 p., $2.00

41 Effect of Control Devices on Traffic Operations (Proj. 3-6), 83 p., $3.60

42 Interstate Highway Maintenance Requirements and Unit Maintenance Expenditure Index (Proj. 14-1), 144 p., $5.60

43 Density and Moisture Content Measurements by Nuclear Methods (Proj. 10-5), 38 p., $2.00

44 Traffic Attraction of Rural Outdoor Recreational Areas (Proj. 7-2), 28 p., $1.40

45 Development of Improved Pavement Marking Materials—Laboratory Phase (Proj. 5-5), 24 p., $1.40

46 Effects of Different Methods of Stockpiling and Handling Aggregates (Proj. 10-3), 102 p., $4.60

47 Accident Rates as Related to Design Elements of Rural Highways (Proj. 2-3), 173 p., $6.40

48 Factors and Trends in Trip Lengths (Proj. 7-4), 70 p., $3.20

49 National Survey of Transportation Attitudes and Behavior—Phase I Summary Report (Proj. 20-4), 71 p., $3.20

* Highway Research Board Special Report 80.

Rep. No.	Title
50	Factors Influencing Safety at Highway-Rail Grade Crossings (Proj. 3-8), 113 p., $5.20
51	Sensing and Communication Between Vehicles (Proj. 3-3), 105 p., $5.00
52	Measurement of Pavement Thickness by Rapid and Nondestructive Methods (Proj. 10-6), 82 p., $3.80
53	Multiple Use of Lands Within Highway Rights-of-Way (Proj. 7-6), 68 p., $3.20
54	Location, Selection, and Maintenance of Highway Guardrails and Median Barriers (Proj. 15-1(2)), 63 p., $2.60
55	Research Needs in Highway Transportation (Proj. 20-2), 66 p., $2.80
56	Scenic Easements—Legal, Administrative, and Valuation Problems and Procedures (Proj. 11-3), 174 p., $6.40
57	Factors Influencing Modal Trip Assignment (Proj. 8-2), 78 p., $3.20
58	Comparative Analysis of Traffic Assignment Techniques with Actual Highway Use (Proj. 7-5), 85 p., $3.60
59	Standard Measurements for Satellite Road Test Program (Proj. 1-6), 78 p., $3.20
60	Effects of Illumination on Operating Characteristics of Freeways (Proj. 5-2) 148 p., $6.00
61	Evaluation of Studded Tires—Performance Data and Pavement Wear Measurement (Proj. 1-9), 66 p., $3.00
62	Urban Travel Patterns for Hospitals, Universities, Office Buildings, and Capitols (Proj. 7-1), 144 p., $5.60
63	Economics of Design Standards for Low-Volume Rural Roads (Proj. 2-6), 93 p., $4.00
64	Motorists' Needs and Services on Interstate Highways (Proj. 7-7), 88 p, $3 60
65	One-Cycle Slow-Freeze Test for Evaluating Aggregate Performance in Frozen Concrete (Proj 4-3(1)), 21 p., $1.40
66	Identification of Frost-Susceptible Particles in Concrete Aggregates (Proj. 4-3(2)), 62 p., $2.80
67	Relation of Asphalt Rheological Properties to Pavement Durability (Proj. 9-1), 45 p., $2.20
68	Application of Vehicle Operating Characteristics to Geometric Design and Traffic Operations (Proj. 3-10), 38 p., $2.00
69	Evaluation of Construction Control Procedures—Aggregate Gradation Variations and Effects (Proj. 10-2A), 58 p., $2.80
70	Social and Economic Factors Affecting Intercity Travel (Proj. 8-1), 68 p., $3.00
71	Analytical Study of Weighing Methods for Highway Vehicles in Motion (Proj. 7-3), 63 p., $2.80
72	Theory and Practice in Inverse Condemnation for Five Representative States (Proj. 11-2), 44 p., $2.20
73	Improved Criteria for Traffic Signal Systems on Urban Arterials (Proj. 3-5/1), 55 p., $2.80
74	Protective Coatings for Highway Structural Steel (Proj. 4-6), 64 p., $2 80
75	Effect of Highway Landscape Development on Nearby Property (Proj 2-9), 82 p. $3 60
76	Detecting Seasonal Changes in Load-Carrying Capabilities of Flexible Pavements (Proj. 1-5(2)), 37 p., $2.00
77	Development of Design Criteria for Safer Luminaire Supports (Proj. 15-6), 82 p., $3.80
78	Highway Noise—Measurement, Simulation, and Mixed Reactions (Proj. 3-7), 78 p., $3.20
79	Development of Improved Methods for Reduction of Traffic Accidents (Proj. 17-1), 163 p., $6.40
80	Oversize-Overweight Permit Operation on State Highways (Proj. 2-10), 120 p., $5.20
81	Moving Behavior and Residential Choice—A National Survey (Proj. 8-6), 129 p., $5.60
82	National Survey of Transportation Attitudes and Behavior—Phase II Analysis Report (Proj. 20-4), 89 p., $4.00
83	Distribution of Wheel Loads on Highway Bridges (Proj. 12-2), 56 p., $2.80
84	Analysis and Projection of Research on Traffic Surveillance, Communication, and Control (Proj. 3-9), 48 p., $2.40
85	Development of Formed-in-Place Wet Reflective Markers (Proj. 5-5), 28 p., $1.80
86	Tentative Service Requirements for Bridge Rail Systems (Proj. 12-8), 62 p., $3.20
87	Rules of Discovery and Disclosure in Highway Condemnation Proceedings (Proj. 11-1(5)), 28 p., $2.00
88	Recognition of Benefits to Remainder Property in Highway Valuation Cases (Proj 11-1(2)), 24 p., $2.00
89	Factors, Trends, and Guidelines Related to Trip Length (Proj. 7-4), 59 p., $3.20
90	Protection of Steel in Prestressed Concrete Bridges (Proj. 12-5), 86 p., $4.00
91	Effects of Deicing Salts on Water Quality and Biota —Literature Review and Recommended Research (Proj. 16-1), 70 p., $3 20
92	Valuation and Condemnation of Special Purpose Properties (Proj. 11-1(6)), 47 p., $2.60
93	Guidelines for Medial and Marginal Access Control on Major Roadways (Proj. 3-13), 147 p., $6.20
94	Valuation and Condemnation Problems Involving Trade Fixtures (Proj. 11-1(9)), 22 p., $1.80
95	Highway Fog (Proj. 5-6), 48 p., $2.40
96	Strategies for the Evaluation of Alternative Transportation Plans (Proj. 8-4), 111 p., $5.40
97	Analysis of Structural Behavior of AASHO Road Test Rigid Pavements (Proj. 1-4(1)A), 35 p., $2.60
98	Tests for Evaluating Degradation of Base Course Aggregates (Proj. 4-2), 98 p. $5.00
99	Visual Requirements in Night Driving (Proj. 5-3), 38 p., $2.60
100	Research Needs Relating to Performance of Aggregates in Highway Construction (Proj. 4-8), 68 p., $3.40
101	Effect of Stress on Freeze-Thaw Durability of Concrete Bridge Decks (Proj. 6-9), 70 p., $3.60

Synthesis of Highway Practice

1	Traffic Control for Freeway Maintenance (Proj. 20-5, Topic 1), 47 p., $2.20
2	Bridge Approach Design and Construction Practices (Proj. 20-5, Topic 2), 30 p., $2.00
3	Traffic-Safe and Hydraulically Efficient Drainage Practice (Proj. 20-5, Topic 4), 38 p., $2.20
4	Concrete Bridge Deck Durability (Proj 20-5, Topic 3), 28 p., $2.20

THE NATIONAL ACADEMY OF SCIENCES is a private, honorary organization of more than 700 scientists and engineers elected on the basis of outstanding contributions to knowledge. Established by a Congressional Act of Incorporation signed by President Abraham Lincoln on March 3, 1863, and supported by private and public funds, the Academy works to further science and its use for the general welfare by bringing together the most qualified individuals to deal with scientific and technological problems of broad significance.

Under the terms of its Congressional charter, the Academy is also called upon to act as an official—yet independent—adviser to the Federal Government in any matter of science and technology. This provision accounts for the close ties that have always existed between the Academy and the Government, although the Academy is not a governmental agency and its activities are not limited to those on behalf of the Government.

THE NATIONAL ACADEMY OF ENGINEERING was established on December 5, 1964. On that date the Council of the National Academy of Sciences, under the authority of its Act of Incorporation, adopted Articles of Organization bringing the National Academy of Engineering into being, independent and autonomous in its organization and the election of its members, and closely coordinated with the National Academy of Sciences in its advisory activities. The two Academies join in the furtherance of science and engineering and share the responsibility of advising the Federal Government, upon request, on any subject of science or technology.

THE NATIONAL RESEARCH COUNCIL was organized as an agency of the National Academy of Sciences in 1916, at the request of President Wilson, to enable the broad community of U. S. scientists and engineers to associate their efforts with the limited membership of the Academy in service to science and the nation. Its members, who receive their appointments from the President of the National Academy of Sciences, are drawn from academic, industrial and government organizations throughout the country. The National Research Council serves both Academies in the discharge of their responsibilities.

Supported by private and public contributions, grants, and contracts, and voluntary contributions of time and effort by several thousand of the nation's leading scientists and engineers, the Academies and their Research Council thus work to serve the national interest, to foster the sound development of science and engineering, and to promote their effective application for the benefit of society.

THE DIVISION OF ENGINEERING is one of the eight major Divisions into which the National Research Council is organized for the conduct of its work. Its membership includes representatives of the nation's leading technical societies as well as a number of members-at-large. Its Chairman is appointed by the Council of the Academy of Sciences upon nomination by the Council of the Academy of Engineering.

THE HIGHWAY RESEARCH BOARD, organized November 11, 1920, as an agency of the Division of Engineering, is a cooperative organization of the highway technologists of America operating under the auspices of the National Research Council and with the support of the several highway departments, the Bureau of Public Roads, and many other organizations interested in the development of transportation. The purpose of the Board is to advance knowledge concerning the nature and performance of transportation systems, through the stimulation of research and dissemination of information derived therefrom.

HIGHWAY RESEARCH BOARD
NATIONAL ACADEMY OF SCIENCES—NATIONAL RESEARCH COUNCIL
2101 Constitution Avenue Washington, D. C. 20418

ADDRESS CORRECTION REQUESTED